

Robotic Tools for Improving the Quality of Bone Drilling

by

Ashkan Pourkand

Submitted in Partial Fulfillment
of the Requirements for the Degree of
Master of Science in Mechanical Engineering
with Specialization in Mechatronics Systems and Robotics
Department of Mechanical Engineering

New Mexico Institute of Mining and Technology
Socorro, New Mexico
August, 2016

ProQuest Number: 10163682

All rights reserved

INFORMATION TO ALL USERS

The quality of this reproduction is dependent upon the quality of the copy submitted.

In the unlikely event that the author did not send a complete manuscript and there are missing pages, these will be noted. Also, if material had to be removed, a note will indicate the deletion.



ProQuest 10163682

Published by ProQuest LLC (2016). Copyright of the Dissertation is held by the Author.

All rights reserved.

This work is protected against unauthorized copying under Title 17, United States Code
Microform Edition © ProQuest LLC.

ProQuest LLC.
789 East Eisenhower Parkway
P.O. Box 1346
Ann Arbor, MI 48106 - 1346

ABSTRACT

Training residents for orthopedic surgery can be challenging due to the variety of parameters involved in critical tasks. This project presents a method for skill assessment of surgical drilling. The parameters measured, which include arm and tool kinematics, applied force, tool and bone vibration, and drill RPM, were measured using a combination of force, acceleration, and optical tracking sensors. High correlations were found between different combinations of penetration distance, applied force, drill toggle, drill orientation, and drill RPM. As a whole, the differences between experienced and novice surgeons measured in these trials were not statistically significant. However, when looking at certain performance criteria individually, "expert" surgeons tended to outperform their "novice" counterparts. As the second part of the study, we explored the feasibility of using a predictive model of axial force during simulated orthopaedic drilling. Synthetic bone samples were used with a robotic device to simultaneously record force, position, and velocity trajectories. A nonlinear function relating force to axial position and velocity was used to fit the data. The models obtained for various bone types fit the well, and are relatively distinct, one from another. This suggests that a predictive model can be used and is able to capture relevant variations in the thickness and hardness of cortical and cancellous bone. The device used to capture this data may also be utilized for augmented haptics, allowing the simulation of anatomic variability in bone while providing necessary force/torque levels.

Keywords: Bone drilling; Skill assessment; Augmented haptics; Orthopaedics; Virtual reality

ACKNOWLEDGMENTS

I wish to express my profound and sincere gratitude to many individuals. This thesis would not have been completed without their contribution.

First and most, I would like to give my special thanks to my research advisor, professor David Grow, for his patience, motivation, and immense knowledge. David has supported me not only by providing a research assistantship over this two years, but also academically and emotionally through the rough road to finish this thesis. He taught me Robotics from the beginning and the art of design. Aside from academic help and advice, I would like to give special thanks to him and his lovely family, Mary, Josh, Essie and Calvin for their invaluable support in these two years.

I wish to greatly acknowledge Dr. Salas and Dr. Mercer who have inspired me a lot during this research. Their help and generosity to answer my questions during this study have always been a great asset to me.

My deepest gratitude goes to my family for their love and support in my life especially in these two years. Mohsen, Parveneh, and Donya have always been a great motivation for me in all aspects of life, and I am indebted to them for their care and love.

This thesis was typeset with \LaTeX ¹ by the author.

¹The \LaTeX document preparation system was developed by Leslie Lamport as a special version of Donald Knuth's \TeX program for computer typesetting. \TeX is a trademark of the American Mathematical Society. The \LaTeX macro package for the New Mexico Institute of Mining and Technology thesis format was written for the Tech Computer Center by John W. Shipman.

CONTENTS

LIST OF TABLES	vi
LIST OF FIGURES	vii
1. INTRODUCTION AND BACKGROUND	1
1.1 Motivation	1
1.2 Background and previous work	1
1.2.1 Quantifying and Improving Surgical Results in Orthopaedics	1
1.2.1.1 Improving the tools in the operation room	2
1.2.1.2 Improving the training methods by quantifying the results	3
1.2.2 Development of Robotic Tools for Orthopaedics Surgical Skill Training	5
1.2.2.1 Haptics	5
1.2.2.2 Augmented Haptics	6
1.2.2.3 Surgical Simulators	6
1.3 Organization of the Thesis	6
2. ASSESSMENT OF ORTHOPAEDIC SURGICAL SKILL	7
2.1 Introduction	7
2.2 Methods	8
2.2.1 Human Subjects	8
2.2.2 Task design	8
2.2.3 Experimental Setup	11
2.2.4 Data post processing	13
2.2.5 Post hoc analysis of bone specimens	15
2.3 Results	18
2.3.1 Pre and Post Survey	19
2.4 Conclusions	19

3. DESIGN OF AN AUGMENTED HAPTICS DEVICE FOR ORTHOPAEDIC SURGICAL SKILLS TRAINING	21
3.1 Introduction	21
3.2 Methods	22
3.2.1 Hardware Design and Calibration	23
3.2.2 Bone Drilling Mechanical Model	25
3.3 Results	27
3.3.1 Force Modeling	27
3.3.2 Test Evaluation	37
3.4 Conclusions	38
4. CONCLUSIONS AND RECOMMENDATIONS	40
4.1 Summary	40
4.1.1 Skill Assessment	40
4.1.2 Augmented Haptics	40
4.2 Future Work	41
4.2.1 Skill Assessment	41
4.2.2 Augmented Haptics	42
Appendices	43
A. SURVEYING RESULT FROM NOVICE PARTICIPANTS	43
B. MATLAB CODES AND FUNCTIONS	52
B.1 Skill assessment project	52
B.1.1 Main file 1	52
B.1.2 Costume correlation function 1	52
B.1.3 Costume correlation function 2	53
B.1.4 Data fitter function	75
B.1.5 Row data adder function	76
B.1.6 General analyzer function	76
B.1.7 Low pass filter function 1	77
B.1.8 Main file 2	77
B.1.9 File loader (Customized Matlab generated code)	79
B.1.10 List loader	80
B.1.11 Low pass filter function 2	81
B.1.12 Labview opener	82

B.1.13	Nan available correlation function	82
B.1.14	Omni data cutter	84
B.1.15	Plot generator function	85
B.1.16	RPM function 1	85
B.1.17	RPM function 2	86
B.1.18	General SYNC function	86
B.2	Augmented haptic project	87
B.2.1	General code for type A	87
B.2.2	Force filter function	87
B.2.3	Location filter function	88
B.2.4	Labview opener	88
B.2.5	File opener	89
B.2.6	Calculator	89
B.2.7	Error calculator	90
C.	C++ CODES AND FUNCTIONS	92
C.1	Augmented Haptic	92
D.	IRB APPLICATION	98
	REFERENCES	104

LIST OF TABLES

2.1 Summary of quantified measured parameters 9

2.2 Mean and standard deviation of values measured pre-test. 10

2.3 Mean and standard deviation of values measured post-test. 10

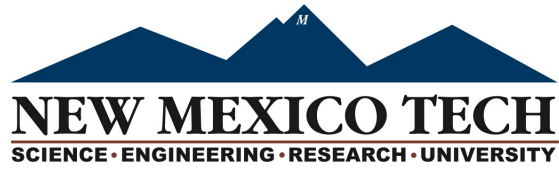
3.1 Model (surface) parameters, where the units of each term are such that when multiplied by the corresponding position-, velocity-, or offset-based parameter (e.g. x) the result is in Newtons. Note that the kinematic equations were derived using inches as the length unit to match design and manufacturing around imperial units. . . 28

LIST OF FIGURES

1.1	A robotic system to detect and prevent over-penetration is shown[1].	2
1.2	Optical methods to register the robotic arm for bone drilling[2]. . .	3
1.3	(a): Using electro magnetic sensor to track the hand's motion[3]. (b): Using gyroscope to track the hand's motion[4].	4
1.4	Comparing the movement of two hands for experts (left hand, left-up, right hand, right-up) vs. novice (left hand, left-down, right hand, right-down) [5].	5
2.1	Definitions of the measured parameters in the post-test.	11
2.2	Shown here is the experimental setup used in the assessment trials. A surgical drill is instrumented with optical markers, accelerometer, and RPM sensor. The synthetic bone is attached to a fixture which is also used to measure applied force and to which an additional accelerometer is attached. Additional motion capture markers are applied to the participant to track arm and, indirectly, torso movement. Finally, the conventions for drill orientation (roll, pitch and yaw) are defined with respect to the drill body.	12
2.3	(a) Stryker system 5 drill, (b) PCB-352C03 accelerometer, (c) Reed switch, (d) Motion-tracking system's markers.	12
2.4	(a) Futek load sensor, (b) NIcDAQ data logger, (c) Flex 13 Optitrack camera, (d) high current usb hub.	13
2.5	To find the upper-body position first, (a) motive recorded the location and orientation of the upper and lower arm. (b) In the post-processing procedure, with least square method, the location of the elbows and shoulders were estimated.	14
2.6	The drill-tip's path calculated from the location and orientation of the drill with forward kinematic (blue path). The low-pass-filtered path of the drill-bit's location(red path)	14
2.7	The pullout test setup to measure the maximum strength of the standard screws inside each hole.	15
2.8	Various types of failure of the bone in the pullout test	16
2.9	The general flow chart of data from various channels and devices, stamped with the CPU time for each device.	17

2.10	A visualization of how various parameters were found to co-vary is given by color-mapping correction coefficients. Correlations on color map toward blue include negative correlations. Axes are defined by variable in table 3.1. Plot (a) is the result from the test before the SOWTA training and plot (b) is the result from the test after the SOWTA training.	18
2.11	Plot of the ranked data for average (a) force, (b) mean roll of the drill, (c) maximum penetration of the drill and, (d) final minor axis of the drilled hole vs the hole number. For each plot we checked the id number of the winner and see if it was an expert or a novice.	19
3.1	(a) Phantom Premium 1.5HF mounted to the Stryker System 5 drill via a customized gimbal. Yaw and pitch angle are captured using an Arduino Mega and two Avago HEDM-5500 encoders. (b) The forward-kinematics for the modified device use the length and angle definitions shown. The joint angles $\{q_1, q_2, \dots, q_5\}$ of device are defined with the device in the home configuration.	23
3.2	(a) 3D model of the gimbal. (b) The schematic of the drill	24
3.3	To validate the Jacobian matrix, the output force of the device was measured by a Shimpo force gage, relative to the commanded value at various configurations.	25
3.4	Cross-sections of two types of synthetic bone were used for the purpose of modeling each with differing thickness of cortical and cancellous (trabecular) bone. (a) Hard bone with cancellous , (b) hard bone without cancellous , (c) softbone with cancellous and, (d) softbone without cancellous	25
3.5	Test setup for measuring the force during the drilling.	26
3.6	Plot of the force model with respect to the measured data sets (multiple trials) are shown for the sample comprised of hard bone with a cancellous region (Sample A), RMSE 8%. The model is shown to fit the data well; however, it is critical to note that the model extends well beyond the domain actually sampled. This is also true for the models shown in the immediately following figures.	28
3.7	Plot of the force model with respect to the measured data sets (multiple trials) are shown for the sample comprised of hard bone without a cancellous region (Sample B), RMSE 9%.	29
3.8	Plot of the force model with respect to the measured data sets (multiple trials) are shown for the sample comprised of soft bone with a cancellous region(Sample C), RMSE 11%.	29
3.9	Plot of the force model with respect to the measured data sets (multiple trials) are shown for the sample comprised of soft bone without a cancellous region (Sample D), RMSE 13%.	30

3.10	Comparison of the four force models, each resulting from one of the bone samples tested, also shown in figures 3.6 - 3.9.	31
3.11	Comparing the four force models with respect to the measured data sets are shown for the sample comprised of hard bone with a cancellous region (Sample A)	32
3.12	Comparing the four force models with respect to the measured data sets are shown for the sample comprised of hard bone without a cancellous region (Sample B)	32
3.13	Comparing the four force models with respect to the measured data sets are shown for the sample comprised of soft bone with a cancellous region (Sample C)	33
3.14	Comparing the four force models with respect to the measured data sets are shown for the sample comprised of soft bone without a cancellous region (Sample D)	33
3.15	Plot of the average force model with respect to the measured data sets (all trials) are shown for the sample comprised of hard bone with a cancellous region (Sample A)	34
3.16	Plot of the average force model with respect to the measured data sets (all trials) are shown for the sample comprised of hard bone without a cancellous region (Sample B)	34
3.17	Plot of the average force model with respect to the measured data sets (all trials) are shown for the sample comprised of soft bone with a cancellous region (Sample C)	35
3.18	Plot of the average force model with respect to the measured data sets (all trials) are shown for the sample comprised of soft bone without a cancellous region (Sample D)	35
3.19	The modified haptic device (right) is shown with the force-gage-embedded bone fixture (bottom) and data acquisition system (right). In order to obtain the kinematic parameters (x, \dot{x}), the raw encoder values were read using a custom C++ script and then fed into the inverse kinematic equations we derived. The force sensor was driven by and read using an National Instruments data acquisition system.	36
3.20	The test setup to check the modified Jacobian. By putting the robot on a force sensor in a vertically slider table, during the evaluation test, the applied force from the robot was continuously measured and compared with the calculated force.	37
3.21	The applied force in validation study.	38



This thesis is accepted on behalf of the faculty
of the Institute by the following committee:

David Grow
Academic Advisor

David Grow
Research Advisor

Alva Keith Miller
Committee Member

Cristina Salas
Committee Member

I release this document to New Mexico Institute of Mining and Technology

Ashkan Pourkand
Student Signature

07/08/2016
Date

CHAPTER 1

INTRODUCTION AND BACKGROUND

1.1 Motivation

Standard tools from the field of robotics may allow significant advances in surgical-skill assessment, training, and related procedures. In 2009, the Patient Safety Committee of the American Academy of Orthopaedic Surgeons released results of a member survey, which was used to identify common errors in orthopaedic surgery [3]. Results of this study showed that the orthopaedic surgeons were directly involved in 60% of the total errors. Seventy eight percent of errors occurred in the hospital, with 54% occurring in the operating room. The hand and/or fingers and the knee (35% for each) were the most frequent sites of surgical error. As of July 2013, prompted by the quality initiative set forth by the Patient Protection and Affordable Care Act, the American Board of Orthopaedic Surgeons (ABOS) and the Residency Review Committee (RRC) for Orthopaedic Surgery have mandated formal motor skills training outside of the OR [1, 6] Figure 1.1. The ABOS and RRC believe that this training will enhance resident's acquisition of basic surgical skills. Currently, no criteria has been established for hands-on training of surgical residents on common procedures used in each orthopaedic surgery subspecialty rotation. Since the inception of the ABOS requirement, some surgical skills simulation has been implemented by residency programs in the form of fracture skills courses [6, 2, 7]. Unfortunately, limited data exist on the effectiveness of these courses. Prior work in surgical skill evaluation using sophisticated robotic training tools includes the work specifically where data obtained through the actual surgical robot [8, 9] or by video during the surgery [5] is subsequently analyzed. This study used various robotic tools to improve the quality of training in different fields.

1.2 Background and previous work

1.2.1 Quantifying and Improving Surgical Results in Orthopaedics

Although modern teaching skills mentioned above are important aspects of surgical training, quantified assessment has not played a significant role in it. Orthopaedic surgical residents were traditionally taught in operating rooms were

they observe surgical tasks. Currently, skill laboratories are also being used to teach and test residents. These skill laboratories not only improve the confidence of the residents significantly but also improve the results in orthopaedic surgery [10]. In general, research in this field follows two main goals: improving the tools in the operation room (OR) and improving training methods by quantifying results.

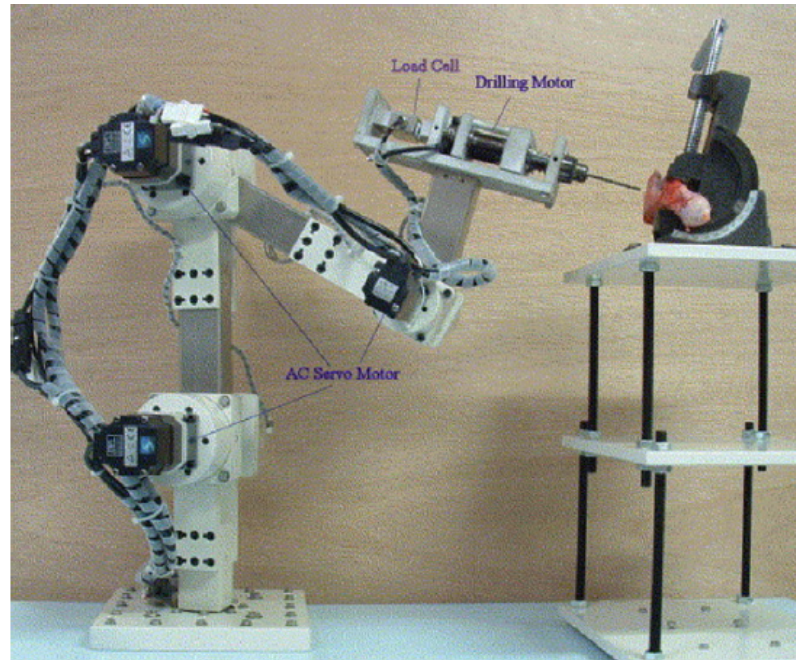


Figure 1.1: A robotic system to detect and prevent over-penetration is shown[1].

1.2.1.1 Improving the tools in the operation room

In last three decades, a wide variety of approaches have been applied to help surgeons in the OR ranging from developing simple tools like drill guides to sophisticated, robotic tools. Although autonomous drilling robots might have high precision, using these robots in ORs is not yet possible due to safety factors [1]. These robots can monitor many critical parameters during the task, but variations in shapes and properties of human organs also limits the automations capacities [11].

Numerous skills are critical to orthopaedic repair. Over-penetration is one of the biggest challenges in orthopaedic drilling. To detect the over-penetration, multiple studies with different algorithms were conducted [1, 12], and different automated robots used some of the results in the mentioned studies to predict this action. Some of these studies were general and some others were for specific operations, such as spine surgery, Figure 1.2 [2]. Although most of these robots

monitor the revolution per minute (RPM) or the axial force, in some cases they apply image processing to find the location of the drill bit [6, 13, 14].

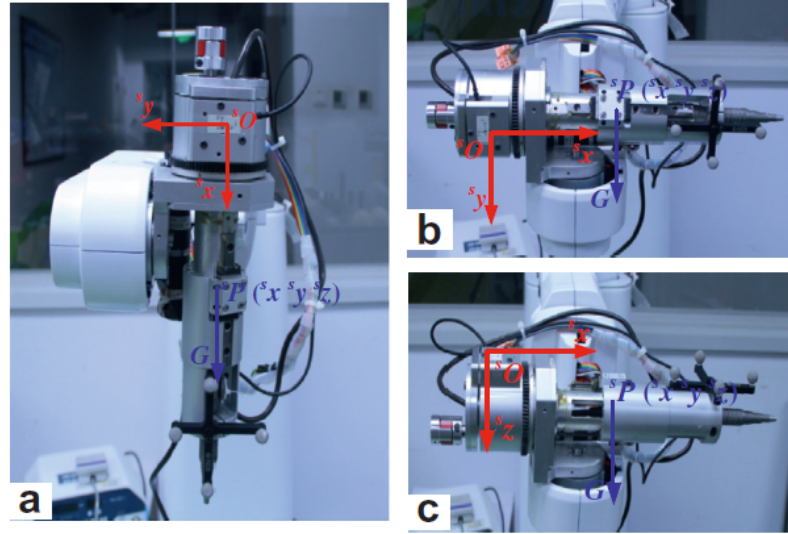


Figure 1.2: Optical methods to register the robotic arm for bone drilling[2].

Temperature is another critical parameter in bone drilling receiving significant attention from scientists [15]. Overheating can cause serious, and in some cases permanent, damage to the bone and tissues structure in the vicinity. Distinct experimental and theoretical approaches were applied to find the temperature of the bone during drilling. In general, experimental studies related to bone drilling show better results than numerical studies [16, 17, 18, 19, 20]. Automated robots used most of these results and methods to perform a better task.

Optimization of drilling has a significant role in bone drilling studies [19]. Unlike temperature and over-penetration, numerical and theoretical approaches to optimization have not yielded consistent results [7]. Neural Network and Fuzzy logic have shown the best results compared to others[9]. Drill bit geometry, bone type, RPM, temperature, and down ward force are the most important parameters of the optimization[7, 8, 9, 21, 19]. Combining the results of the optimization studies with safety studies is another challenge that the automated robots have to consider. The most optimized performance is not always the safest one. In general, robotic tools in the OR must follow various algorithms to be able to keep the task safe and optimized.

1.2.1.2 Improving the training methods by quantifying the results

Perhaps the most obvious approach to improving bone drilling in the operating room is to improve training methods for orthopaedic residents. One of

the main requirements in a precision training method is quantifying the test. To create the quantified scale and test, results from safety and optimization studies were combined with the skill assessment and monitoring approaches[22]. Comparing experts with novice surgeons is an effective way to design a quantified scale, Figure 1.3[3, 5]. For example, a quantified scale has been made by following the motion of the hand during the laparoscopic surgery and comparing certified and non-certified surgeons[4]. Robb RA, developed a virtual reality system for endoscopy. As a skill assessment, they developed specific clinical protocols that compared virtual endoscopy with real endoscopy [23].

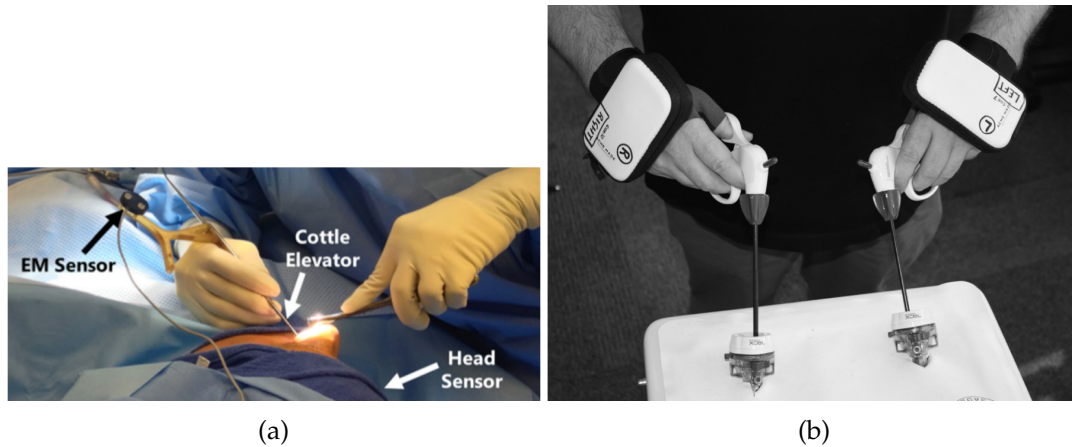


Figure 1.3: (a): Using electro magnetic sensor to track the hand's motion[3]. (b): Using gyroscope to track the hand's motion[4].

There have been multiple studies to simulate the surgical tasks without preliminary output. Later, Lee et al. made another simulator for laproscopic surgery with a quantified skill assessment approach [24]. In 2004, Eversbusch and Grantcharov found the learning curves for a simulated colonoscopy via a randomized trial algorithm [25]. Recently, Sezek et al. conducted research in training, simulation, and reducing complications in Urology. The study showed e-learning and observation of a procedure have a significant effect on the learning curve in reducing the learning time and improved the learning peak[26]. Uemura et al. showed that, the number of operations performed by a surgeon do not necessarily improve the skill of the surgeon, Figure 1.4 [5]. Reznick applied educational psychology methods to optimize the of teaching residents [3].

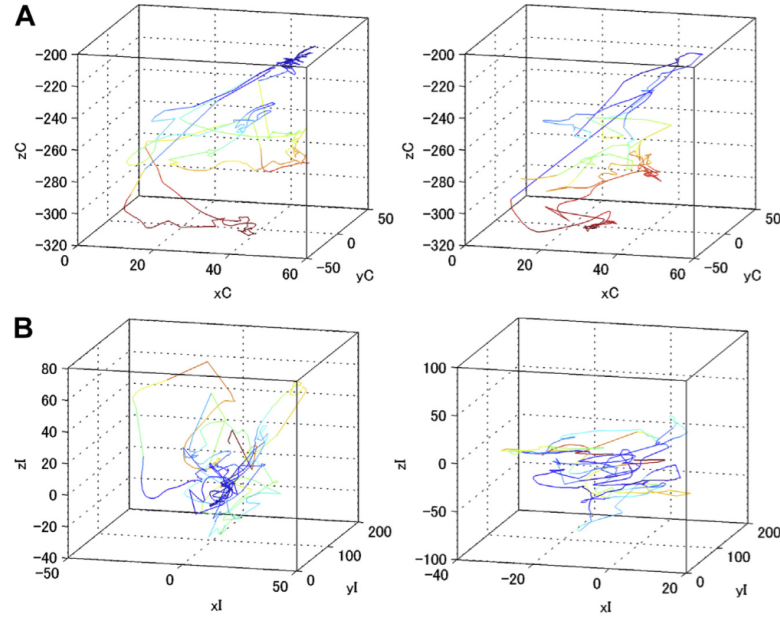


Figure 1.4: Comparing the movement of two hands for experts (left hand, left-up, right hand, right-up) vs. novice (left hand, left-down, right hand, right-down) [5].

Finally, tools can and are being designed with safety features to add additional safety measures to the procedure. In one case hand-held drills with an interruption mechanism were used to avoid over-penetration [27]. This study showed the design was effective, but additional work is required to allay safety concerns. Designing a safe device can be a significant challenge given the uncertainty in human behavior.

1.2.2 Development of Robotic Tools for Orthopaedics Surgical Skill Training

1.2.2.1 Haptics

Haptic technology is designed to interact with the human touch sense. Quickly, this technology was incorporated into virtual reality (VR) and training simulators. It also can play a significant role in teleoperation systems such as those used for explosive ordinance disposal or telesurgery [28, 29]. These robots can be classified into two major categories admittance and impedance types. Impedance type robots are most common in commercial haptic robots. Impedance robots are designed to be back-drivable by minimal friction and inertia. Admittance type robots can generate more force feedback but due to their high friction and inertia, they are not back-drivable[30].

1.2.2.2 Augmented Haptics

Although haptic robots are popular in VRs and training simulators, occasionally, they suffer from lack of fidelity with respect to graphical and haptic elements. The use of augmented haptics can largely address this problem. In 2014, Steyn et al. developed an augmented-reality environment for a wheeled mobility system [31]. One of the main usage of haptic robots is in tele-operations. Maddahi et al., conducted a study to reduce the error of manipulator robots, by combining the haptic environment with a robotic assisted-line tracker[32].

Augmented reality environments (AEs) do not always include haptics. For example, Hallet et al. combined the graphical VR with the real environment in the operation room (OR) to decrease the risk of error during the trans-thoracic (minimally invasive) liver resection[33]. In contrast, there have been similar studies where haptics were included in the AE to great effect, such as haptic systems with an augmented observer approach for high-impedance haptic system, and laser projection with surface recognition for laparoscopic surgery [34, 35, 36].

1.2.2.3 Surgical Simulators

Using robots to improve training methods is not a new idea. Simulators have been used in different studies to train surgeons. For simulators to be realistic, a precision mechanical model is required[37, 19, 38, 39, 40]. Some of these models were derived from other studies in safety and optimization fields. Some of these models are flexible[41] while others are fixed, but with feedback for learning purposes[42]. Even with a precision mechanical model, most of the haptic devices are not strong enough to simulate the exact feeling of the bone drilling[43]. Instead, the focus of the simulators are on graphics, sound, and feedback[44, 45, 42]. The efficiencies of the feedback from these studies are sometimes unreliable, due to the lack of accurate force feedback in the simulators[11, 43, 41, 42]. Despite these limitations residents with simulator training were shown to perform better in surgical tasks and had higher self-confidence[46, 47, 48].

1.3 Organization of the Thesis

The chapters that follow are organized into three major parts, which each showcase how tools from the field of robotics can be applied to current clinical needs: surgical-skill assessment (chapter 2), augmented haptics for bone drilling simulators (chapter 3). Finally, the fourth chapter contains the conclusion and the future recommendations.

CHAPTER 2

ASSESSMENT OF ORTHOPAEDIC SURGICAL SKILL

2.1 Introduction

Orthopaedic training is a hands-on, motor skills-demanding surgical specialty. Historically, much of the technical learning occurs in the operating room (OR). This is an effective method of training for simple fractures or low-risk cases. For more complicated operations or high-risk situations (spinal surgery, potential for vascular or nerve impingement, etc.), using the OR as an introduction to surgical techniques can introduce unnecessary risk. Instead the motor skills tasks can be simulated in the lab prior to performing the tasks in the OR. This model has been utilized in the endoscopic training of general surgeons.

As was mentioned in chapter one, a standardized method of training outside of the operating room has not been developed. Modules delineating the tasks deemed important by the ABOS have been provided as guidance in this endeavor and are publicly available (www.ABOS.org). Since the inception of the ABOS requirement, some surgical skills simulation and structured resident evaluation have been implemented by residency programs [49, 50, 51, 52]. A study by Egol et al. used a written examination known as the objective structured assessment of technical skill (OSATS) to assess the improvement of residents after a hands-on skills course and found that it was a valuable training source [51]. This assessment is characterized by having an experienced surgeon evaluate a task and rate the participant based on whether the task was: A. done correctly, B. partially done, or C. not done/done incorrectly. A recent study by Hohn et al. qualitatively and quantitatively evaluated outcomes of a surgical drilling course through measures evaluating the ability to hit an intended target[52]. A more sophisticated assessment of surgical skill has been reported by Karam et al. [49] This group implemented a one month surgical skills training experience for year-1 residents in their orthopaedic program. Assessment was derived by a combined qualitative evaluation through OSATS and quantitative evaluation using a motion capture system. Using high resolution cameras and retroreflective markers placed on the hands of the surgeon, the researchers captured data on the number of discrete hand motions used to perform the desired task and the distance that each hand traveled to perform said task.

In the context of orthopaedic drilling, successful task performance relates to creating a hole at the correct location with the correct orientation without the

use of excessive force, heating, over-penetration, toggle, or skiving with the drill to maximize efficiency and prevent harm.[40, 53, 54] The interdependency of task-related parameters is significant. For instance, the relationship between drill kinematics to force and heating are governed by drill bit type, drill RPM, bone parameters, feed rate, etc[55, 56, 57]. Building off work done by Karam et al. , the primary goal of the work presented in this chapter is to quantitatively assess orthopaedic drilling performance. This assessment was conducted at an American Board of Orthopaedic Surgery-approved surgical skills training course.

2.2 Methods

2.2.1 Human Subjects

This study was approved by the institutional review boards at both NMT (New Mexico Institute of Mining and Technology) (IRB #2014-10-004) and UNM (University of New Mexico) (HRRC #15-087) universities . Subjects were recruited during the 2015 Surgical Skills Training Course held by the Southwest Orthopaedic Trauma Association (SWOTA) for Year 1 orthopaedic residents in Phoenix, AZ. This is an ABOS residency surgical skills training course with participation from orthopaedic surgery residents from New Mexico, Arizona, Colorado, Texas, and Utah. In all, 22 residents and 7 attending surgeons were included (9 female, 20 male, with ages ranging from 36 to 62 years, height range from 5'1" to 6'2" feet).

2.2.2 Task design

Prior to the start of the course, we asked each resident to perform a single task: drill holes through both cortices of a mechanically equivalent synthetic bone following a pre-defined trajectory. Following the fourth day of the training period, we asked each participant to repeat the task. In addition, surveys were administered before and after the surgical skills course. In order to characterize performance parameters and their relation to clinically-relevant outcomes, a wide variety of parameters (as defined in Table 2.1 and Figure 2.1) were collected. The values obtained are listed in Tables 2.2 and 2.3.

Table 2.1: Summary of quantified measured parameters

	Parameter	Notes
1	Hole Loc	Which of four locations drilled on bone
2	L_T	
3	L_1	
4	L_2	
5	Subj Num	Year in residency, where applicable
6	Years	
7	Sex	
8	Height	
9	Holes	Estimated total number of holes drilled in bone
10	Days Since	Days since most last bone drilling
11	Program Q1	Does residency program have cadaveric training
12	Program Q2	Does residency program have dedicated skills training
13	PVC	Have they practiced with PVC bone analogs
14	OR Exp	Have they extensive OR experience
15	Ave RPM	Over-penetration distance
16	Max Pen	
17	Ave Force	
18	Max Force	
19	Std Force	Bone-fixtue-mounted accelerometer (std)
20	Bone Vibr	
21	Drill Vibr	
22	Drill toggle	
23	Ave Roll - $\hat{\theta}_R$	Drill-body-mounted accelerometer (std)
24	Ave Pitch - $\hat{\theta}_P$	
25	Ave Yaw - $\hat{\theta}_Y$	

Table 2.2: Mean and standard deviation of values measured pre-test.

<i>param.</i>	L_T	<i>drill toggle</i>	v_{min}	<i>sho. angle</i>	L_O	<i>targ. error</i>	L_1	L_2	$\hat{\theta}_R$	$\hat{\theta}_P$	$\hat{\theta}_Y$	<i>drill vibr.</i>	<i>bone vibr.</i>	years	RPM	Force
mean	52.4	2.480	.0018	81.3	.523	.191	.124	.0978	53.3	55.1	58.8	.0295	.0052	2.38	1877	91
std	4.13	.74	.0074	30.7	.181	.142	.110	.0047	.0026	.0101	.0091	3.13	.0029	1.56	4733	164
units	deg	in/s	in/s	deg	in	in	in	in	deg	deg	deg	in/s ²	in/s ²	yrs	RPM	N

Table 2.3: Mean and standard deviation of values measured post-test.

<i>param.</i>	L_T	<i>drill toggle</i>	v_{min}	<i>sho. angle</i>	L_O	<i>targ. error</i>	L_1	L_2	$\hat{\theta}_R$	$\hat{\theta}_P$	$\hat{\theta}_Y$	<i>drill vibr.</i>	<i>bone vibr.</i>	years	RPM	Force
mean	59.1	3.751	.0017	61.8	.495	.175	.134	.0978	51.7	53.6	52.5	.0351	.0083	2.38	1765	88.7
std	11.49	0.99	.0061	12.8	.172	.166	.122	.0047	.0031	.0084	.0072	3.13	.0025	1.56	2675	122
units	deg	in/s	in/s	deg	in	in	in	in	deg	deg	deg	in/s ²	in/s ²	yrs	RPM	N

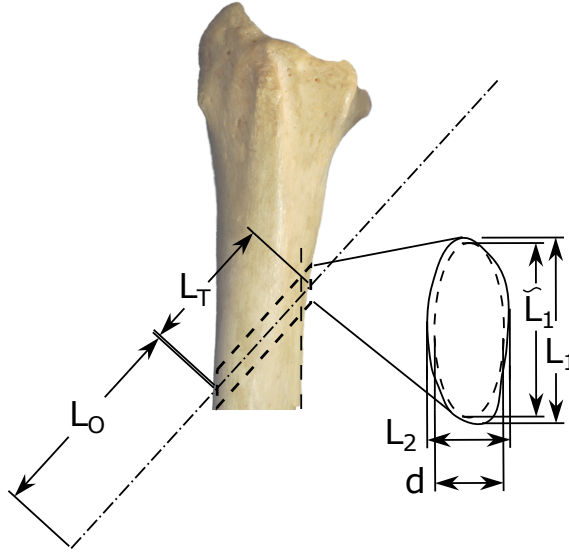


Figure 2.1: Definitions of the measured parameters in the post-test.

2.2.3 Experimental Setup

The parameters described in tables 2.2 and 2.3 were measured using a combination of motion-tracking, force, and acceleration measurements, and measurements taken subsequently from the bones used in the study Figure 2.2.

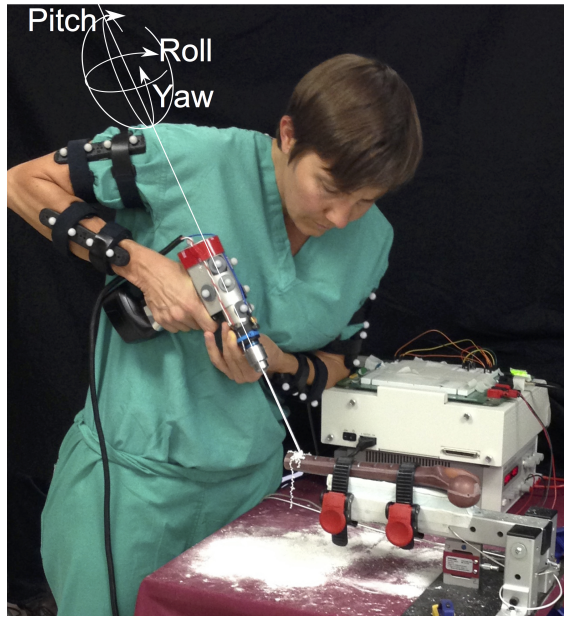


Figure 2.2: Shown here is the experimental setup used in the assessment trials. A surgical drill is instrumented with optical markers, accelerometer, and RPM sensor. The synthetic bone is attached to a fixture which is also used to measure applied force and to which an additional accelerometer is attached. Additional motion capture markers are applied to the participant to track arm and, indirectly, torso movement. Finally, the conventions for drill orientation (roll, pitch and yaw) are defined with respect to the drill body.

A Stryker System 5 rotary handpiece was adapted with sensors to measure acceleration (PCB-352C03) and rotational speed (reed switch) and motion-tracking markers for tool position and orientation. The vibration of the drill was logged via a datalogger, (Figures 2.3 and 2.4).

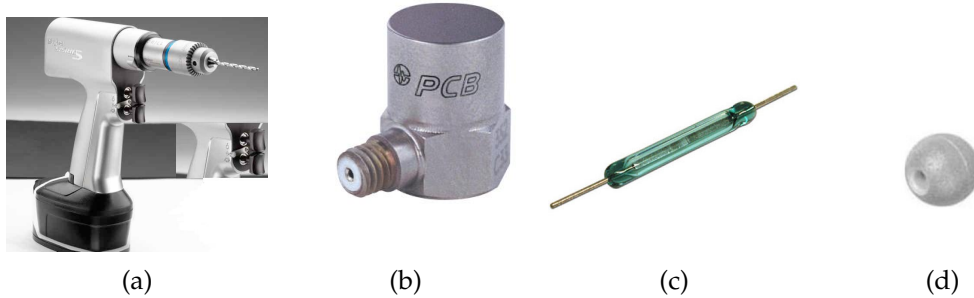


Figure 2.3: (a) Stryker system 5 drill, (b) PCB-352C03 accelerometer, (c) Reed switch, (d) Motion-tracking system's markers.

A fixture was designed to hold the bone specimen (Figure 2.2). It contained another accelerometer of the same type and a force sensor to measure load generated during drilling (Futek LSB302). Data from these sensors was measured using a modular DAQ system (NI cDAQ) at a sampling frequency of 10 kHz. In addition to this, the arms of subjects were fit with motion-tracking markers to monitor arm kinematics. In particular, marker sets were oriented on the upper and lower arm using the greater tuberosity, lateral epicondyle, and ulnar styloid process as anatomical landmarks. The locations of all markers were measured using two Optitrack motion capture systems (one setup used eight Flex 13 cameras, the other used six Prime 13 cameras; two stations) with a capture frequency of 20Hz.

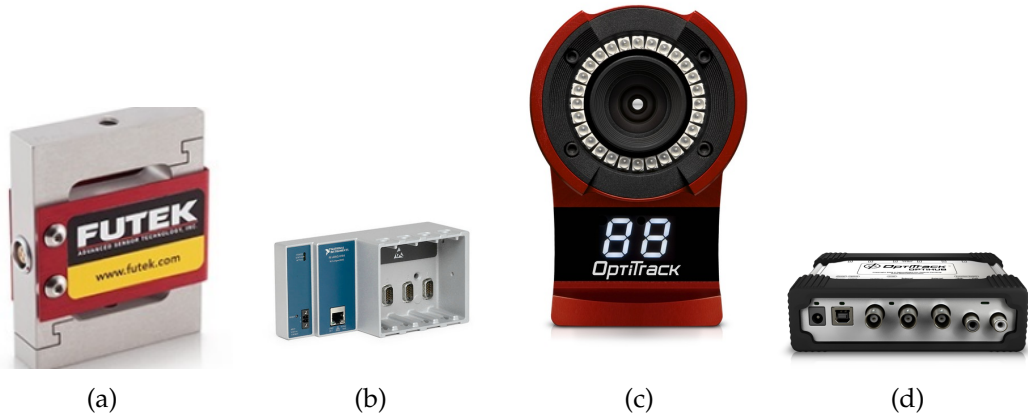


Figure 2.4: (a) Futek load sensor, (b) NIcDAQ data logger, (c) Flex 13 Optitrack camera, (d) high current usb hub.

Pre- and post-surveys were also administered to allow correlation between personal characteristics and training to measured drilling performance. Each subject was asked to drill five holes on the marked locations on a single bone mounted to a custom fixture as shown in Figure 2.2 (right). The marked locations produced drill trajectories of approximately 0 (normal to bone surface), +/- 25, and +/- 45.

2.2.4 Data post processing

The force, acceleration, and reed switch data was post-processed with low-pass filtering, as necessary, before mean, max, and standard deviation values were determined. Motive Body software provided with the Optitrack system recorded the location and orientation of the drill ($\theta_R, \theta_P, \theta_Y$) and the rigid-body kinematics of the arms. The arm rigid bodies were used to calculate elbow and shoulder angles. The elbow center was determined by making a best fit of the upper- and lower-arm vectors obtained from the respective rigid bodies. The

shoulder centers were then determined by moving in the known direction a distance determined by Dempsters anthropomorphic table. Subsequently, trunk rotation relative to the orientation of the bone axis was determined. Finally, the authors developed forward-kinematic equations to relate the drill-body location and orientation to drill-tip location. The force and drill trajectories were time correlated to the motion-tracking data and manually clipped, using force data as the key indicator, Figures 2.5 and 2.6.

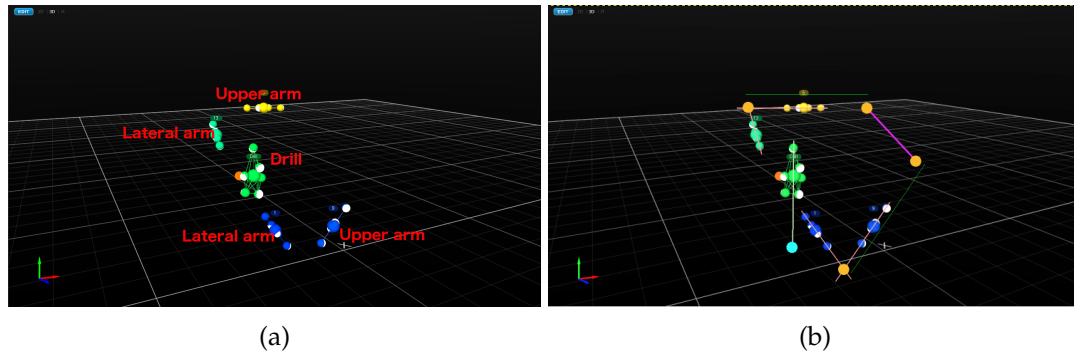


Figure 2.5: To find the upper-body position first, (a) motive recorded the location and orientation of the upper and lower arm. (b) In the post-processing procedure, with least square method, the location of the elbows and shoulders were estimated.

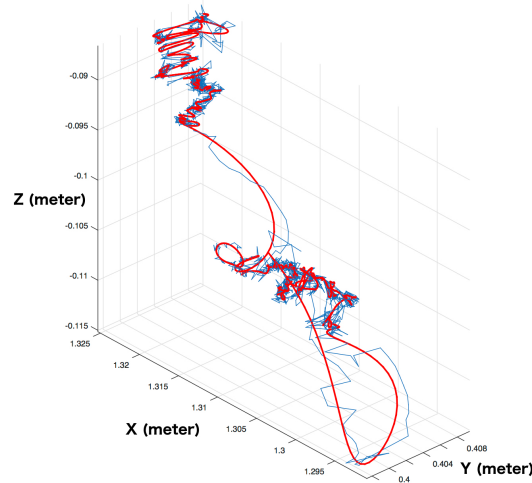


Figure 2.6: The drill-tip's path calculated from the location and orientation of the drill with forward kinematic (blue path). The low-pass-filtered path of the drill-bit's location (red path)

2.2.5 Post hoc analysis of bone specimens

The integrity and accuracy of drilled holes was measured directly in the laboratory after the conclusion of SWOTA. Digital calipers were used to measure the accuracy (L_E in Tables 2.2 and 2.3) of the holes, as well as the major (L_1) and minor (L_2) axis lengths, Figure 2.1. The pull-out strength was measured by installing 3.5 mm cancellous bone screws into the mechanically equivalent synthetic bones (Sawbones, Pacific Research Laboratories, Vashon Island, WA; Figure 2.7). Specimens were mounted to a modified angle vise that allowed positioning the screws in line with the test actuator, Figure 2.8. The bones were cyclically loaded using an MTS 858 Mini Bionix II loading system using a protocol described in Ezechieli et al. [58] Briefly, the protocol is as follows:

1. Screw pre-tensioned with a constant load of 60 N for 60 s
2. Adding 30 s of dwell
3. Followed by 500 cycles between 60 N and 250 N at 0.75 Hz
4. Force was ramped down to zero
5. Followed by a 30 s break
6. A pull-out test was subsequently carried out at 1 mm/s to failure

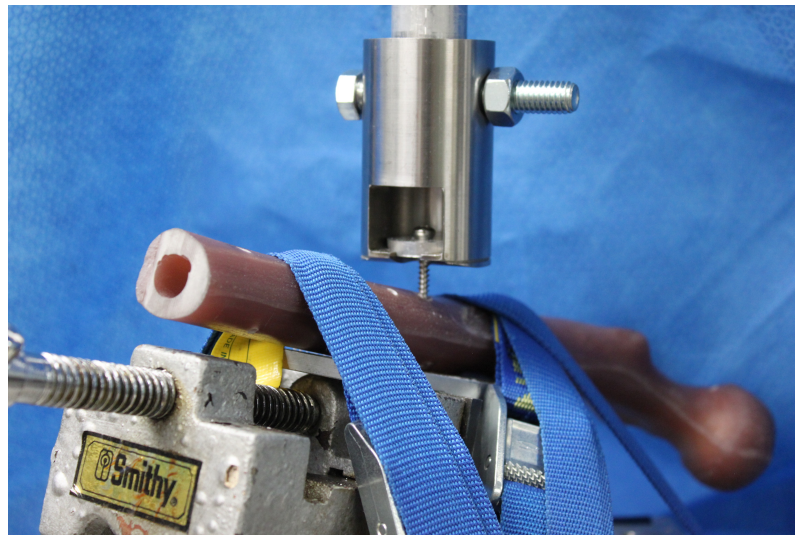


Figure 2.7: The pullout test setup to measure the maximum strength of the standard screws inside each hole.

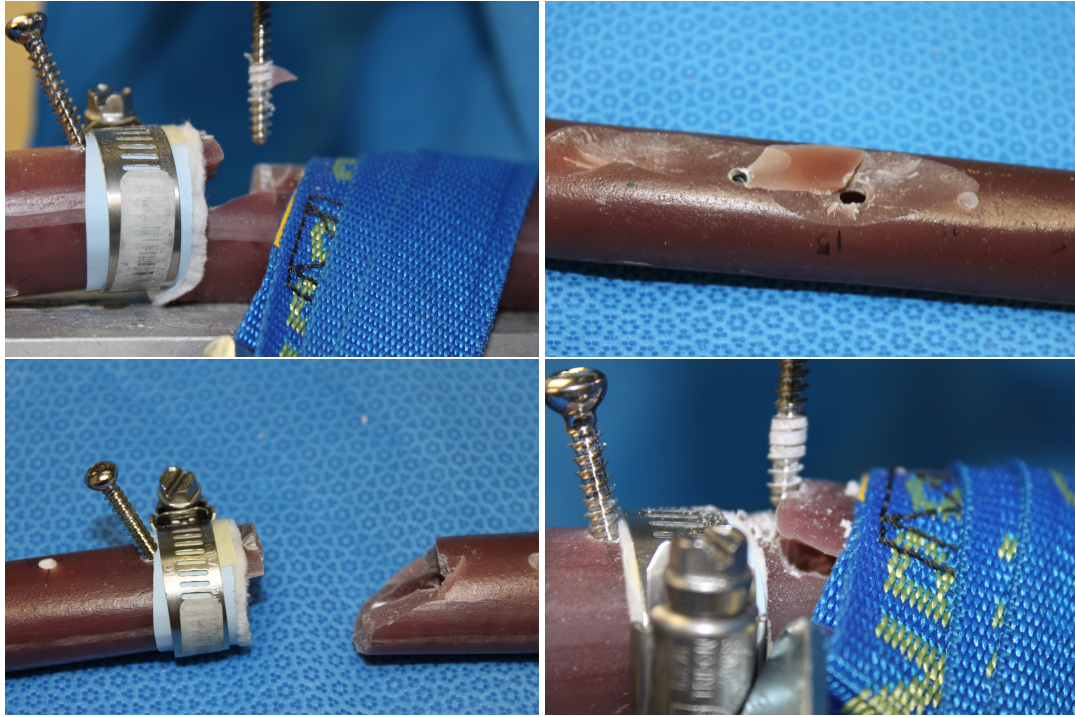


Figure 2.8: Various types of failure of the bone in the pullout test

Figure 2.9 shows the general flow of the data in one chart. The data from each part of the setup, marked with a time stamp from the CPU, and then the time stamp used to synchronize and clip all of the data.

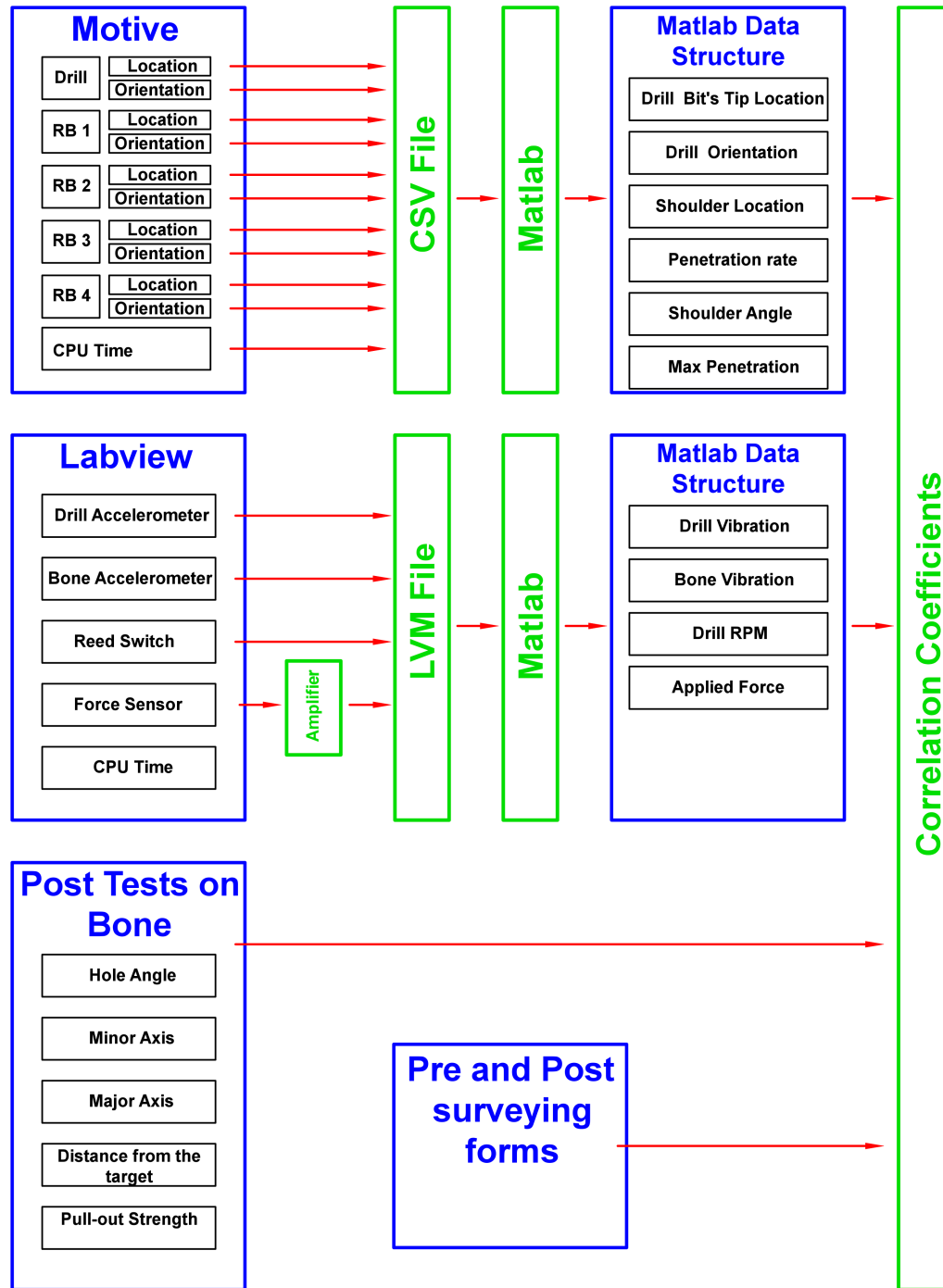


Figure 2.9: The general flow chart of data from various channels and devices, stamped with the CPU time for each device.

2.3 Results

The assessment data were obtained through a combination of post-processing data obtained by the motion-tracking system, force sensor, accelerometers, reed switch, and subsequent measurements made on the bones used in the study, as summarized in Tables 2.2 and 2.3. To assess the interdependency of the measured parameters, a covariance matrix for all variables was generated (Figure 2.10). Non-trivial (e.g. sex with height) correlations whose magnitude exceeded 0.5 were (correlation values listed taken from post data set):

- Maximum penetration distance with force (SD, 0.72)
- Maximum penetration distance with force (max, 0.73)
- Maximum penetration distance with force (mean, 0.91)
- Drill toggle with drill roll angle (mean, 0.70)
- Drill RPM with force (mean, 0.53)

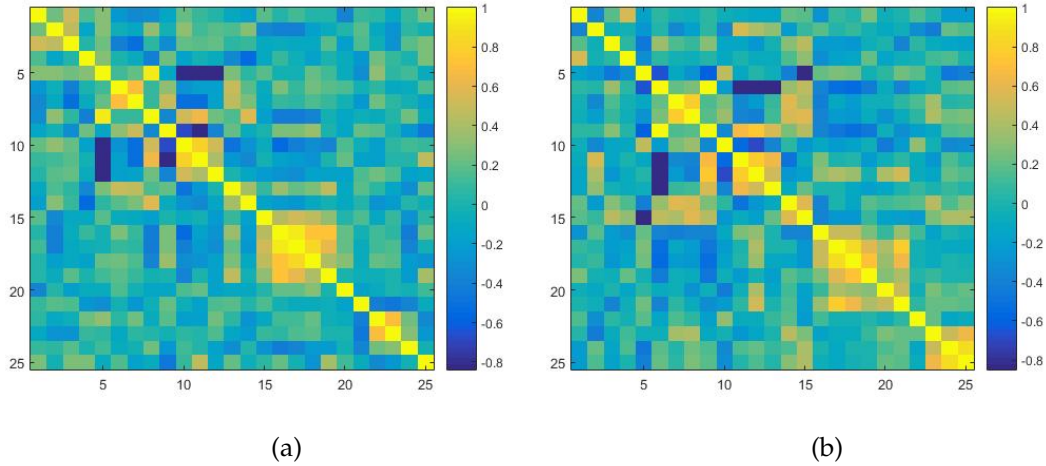


Figure 2.10: A visualization of how various parameters were found to co-vary is given by color-mapping correlation coefficients. Correlations on color map toward blue include negative correlations. Axes are defined by variable in table 3.1. Plot (a) is the result from the test before the SOWTA training and plot (b) is the result from the test after the SOWTA training.

To have a better understanding of the data, the result of each parameter plotted separately respect to the user id. The best performance for the majority of parameters belonged to experts. Figure 2.11.

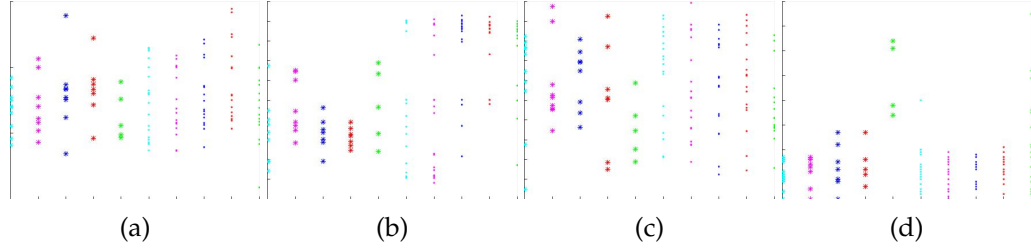


Figure 2.11: Plot of the ranked data for average (a) force, (b) mean roll of the drill, (c) maximum penetration of the drill and, (d) final minor axis of the drilled hole vs the hole number. For each plot we checked the id number of the winner and see if it was an expert or a novice.

2.3.1 Pre and Post Survey

Full summery results are included in the Appendix A. Key parameters are included in Tables 2.2 and 2.3. The participant's feedbacks will be consider in the future studies.

2.4 Conclusions

This study used various sensors to measure the parameters addressed by the trainers as the most critical factors in bone drilling. To find the effects that these parameters have on each other, the measured parameters were expressed as scalars and their covariances were calculated. Some immediately evident results include that the covariance matrices are not drastically different before and after the training, nor are the parameters themselves as can be seen by comparing Tables 2.2 and 2.3. This may not be a surprising result given that the training which occurred over the intervening time covered many skills, with no particular emphasis on drilling. The data suggests that when taken as a group, the experienced surgeons tested here did not, on average, outperform the residents collectively. However, when looking at clinically relevant parameters independently, an interesting pattern does seem to provide some insight into the effects of additional experience. The very best performers out of the total 29 participants, when looking at one performance aspect at a time, came from the experienced surgeon subset with respect to: maintaining steady force (highest minimum before exiting the distal cortex), minimizing over-penetration, minimizing both the major and minor axis diameters, minimizing toggle and drill vibration. Additionally, an experience surgeon was nearly (second) best in terms of accurately targeting the mark on the distal cortex and (third) best in terms of the force before failure during subsequent screw pull-out testing.

No parameters related to arm or torso kinematics were found to vary in a patterned manner with respect to other parameters. This may be due to the varying height and dominate handedness of participants as well as the observation that surgeons were quite unique in their chosen stance.

Limitations of this study include the fact that three residents had to leave the event early and could not be retested, that the pool of experienced surgeons was small and perhaps not representative (some had moved into specializations that did not involve significant amounts of bone drilling), and that a significant fraction of the motion-tracking data had to be excluded due to occlusions which resulted from the manner in which surgeons chose to position themselves during the task. Additionally, many surgeons commented in the post-survey that either the bones felt too hard or that the drill bit felt dull. This is perhaps not surprising given that the synthetic bones used in this trial were composite bone models, rather than the compressed foam-type that is more commonly used for training. Planned future work includes major revisions to the instrumentation to reduce post-processing time and expanding the study to include a larger participant pool. We expect that this will further elucidate the differences between novice and experienced orthopaedic surgeons. Ultimately, we hope to translate the outcomes into improved surgical training methodologies.

CHAPTER 3

DESIGN OF AN AUGMENTED HAPTICS DEVICE FOR ORTHOPAEDIC SURGICAL SKILLS TRAINING

3.1 Introduction

Orthopaedic surgery requires a wide range of technical skills that are mainly acquired through an apprenticeship model. Recently the American Board of Orthopaedic Surgery agreed to increase skills training requirements for orthopaedic surgical residents [59]. Specific skills can be practiced on cadavers, synthetic materials, and animals. However, these materials can be prohibitively expensive [60]. Furthermore, none of these training methods constitutes a perfect analog to live surgery on humans. Even the simple task of drilling a hole in the bone prior to fixation requires that the surgeon simultaneously: (1) avoid skivvyng (slipping) off the bone when beginning a hole, especially when oblique, (2) maintain a desired orientation vs. toggling, (3) drill rapidly to avoid overheating the bone [49], (4) anticipate the changes in the mechanical properties of the bone related to its non-uniform profile [50], (5) drill through the entire width of the bone for a bicortical screw placement, and yet (6) avoid over-penetration. These aspects are greatly complicated by the wide range of bone geometry and material properties that relate to age, sex, and disease state. The focus of this work is training orthopaedic residents in the placement of bicortical screws. These screws are meant to span the entire width of the bone, engaging on both cortices.

Significant recent work has explored the use of virtual environments (VEs) and robotic tools to simulate various surgical tasks, including those relevant to orthopaedic surgery [51, 40, 52, 61, 54, 23, 62, 47]. For those VEs where a manipulation task is involved, haptic elements are often incorporated. One of the first VEs for orthopedic surgery was developed by Dar Tsai et al . [55]. These simulations have been generally received with cautious optimism, despite significant limitations that often exist in fidelity [52]. For instance Fang et al . received feedback suggesting that their VE did not allow surgeons to know the strength of the drilling bone or the distance between the drill-tip and the target location on the temporal bone [57]. In fact, studies have shown that axial forces range widely from task to task, but can easily exceed 200 N [63]. Moreover, once the drill has penetrated some distance into the bone, torque feedback is evident and critical to maintaining a desired trajectory, estimating hole depth, and monitoring bone properties. As such, those VEs that have previously relied on haptic feedback are

intentionally limited to procedures that required low force and/or no torque [52].

Augmented Environments (AEs) have been used for a wide range of purposes [58, 49, 58], including related tasks such as the feeling of skin when inserting a needle into the body [51]. Likewise for bone drilling, the combined use of a physical synthetic bone for realistic torque and axial force magnitudes with additional force from a custom haptic interface seems promising. Critically, the ability to arbitrarily affect net force enables the simulation of anatomic variability of bone. Moreover, if this method is shown to perform well, it might be extended to allow the use of low-cost (e.g. PVC pipe) materials, which are currently used in locations where funding is particularly limited.

A large fraction of the previous research in augmented haptics utilizes real and virtual elements dealt with separately. For instance, forces on one hand would come from interaction with a real object while forces on other hand would come from interaction with a virtual environment by means of haptic technology. Here we focus on applications where a the task is best suited to physical coincidence of virtual and real aspects – both in terms of contact/force and visual elements. As one example, Kurita et al. combined an elastic gel with force feedback to render visco-elastic behavior [64]. Similarly, Kuchenbecker et al. superposed high-frequency force transients during impact with physical objects [65]. Jeon et al. made an augmented-haptic model for breast cancer palpation, combining a silicone breast model with a virtual tumor [66]. In another application, a virtual sphere was rendered coincident to a rubber ball in order to compensate for actuator saturation during deep penetration [32].

The specific task of modeling cutting/drilling bone has been pursued previously, including first-principles approaches [52, 63]. For a given drill bit, and where rotational speed material properties are constant, the model in [52] predicts an axial force that scales linearly with feedrate. Yanping et al. used the damping model for simulating bone sawing [40]. Tsai et al. used an exclusive model for the haptic interaction orthopedic simulator built upon the feed rate and torque of the drill [66]. Lee et al. modeled the drilling of the bone with respect to the rpm and feed rate [50]. In some studies force is modeled linearly with respect to feed rate [67].

3.2 Methods

This study attempts to combine positive aspects of synthetic bones with virtual reality as an augmented reality environment. Residents will have different perception from the applied force feedback from the haptic environment while drilling in the same bone. This difference in feeling trains residents to drill in various bones with different densities. Therefore the rendered force is based on the difference of the force in the various cross-sections of synthetic bones.

3.2.1 Hardware Design and Calibration

To characterize the mechanics of drilling into long bone, a system of simultaneously recording kinematics and force was required. A Phantom Premium (high force model, Geomagic, Rock Hill, SC) already capable of measuring gimbal location, was modified to connect to a surgical drill while capturing pitch and yaw angles (Figure 3.1).

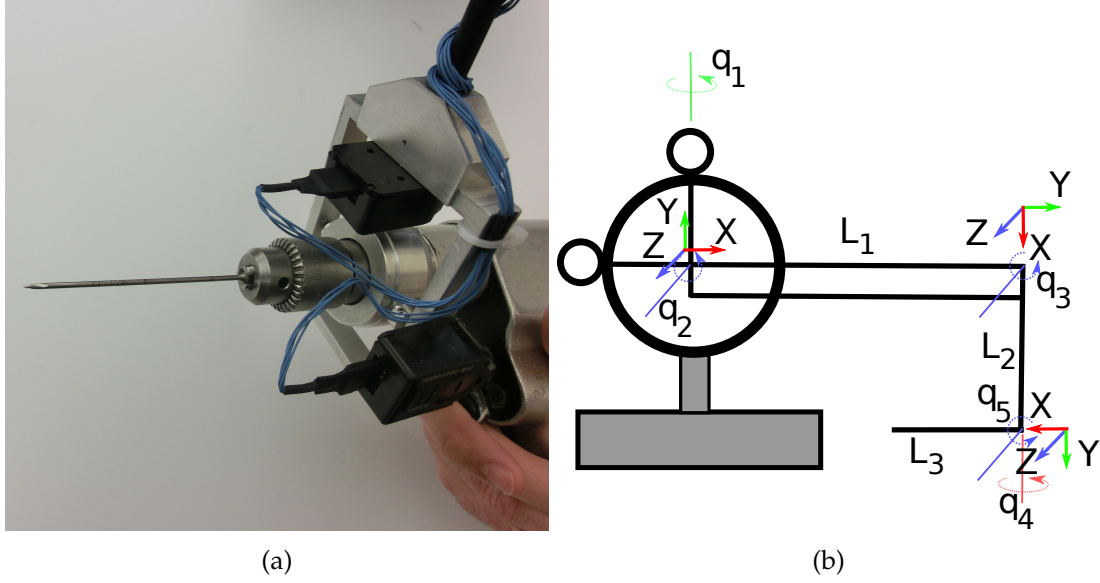


Figure 3.1: (a) Phantom Premium 1.5HF mounted to the Stryker System 5 drill via a customized gimbal. Yaw and pitch angle are captured using an Arduino Mega and two Avago HEDM-5500 encoders. (b) The forward-kinematics for the modified device use the length and angle definitions shown. The joint angles $\{q_1, q_2, \dots, q_5\}$ of device are defined with the device in the home configuration.

In order to find the absolute location and orientation of the drill, the forward-kinematics needed to be recalculated taking into account changes to the structure of the haptic device. We define relative joint angles $\{q_1, q_2, \dots, q_5\}$ as shown in Figure 3.1(b) in order to capture the kinematics associated with the standard proximal structure as well as the distal structure including the custom gimbal and drill geometry (Figure 3.2). Accordingly, the drill-tip position and orientation can be determined using the homogeneous transformation matrix (using notation by Spong [68]):

$$H = Rot_{y,q_1} Rot_{z,q_2} Trans_{x,L_1} Rot_{z,q_3} \dots \dots Trans_{x,L_2} Rot_{x,q_4} Rot_{z,q_5} Trans_{x,L_3} \quad (3.1)$$

Because of the relatively stiff surface of the bone and the desire to apply no force before contact, forward-kinematics must be calculated with accuracy and

precision. An external metrology system (an 8-camera Optitrak Flex13 system) was used to verify drill-tip location in various configurations. No errors exceeding 1 mm were observed in any configuration. Note that this is not much greater than the uncertainty introduced by the metrology system itself (0.6 mm in plane, 0.7 mm out of plane).

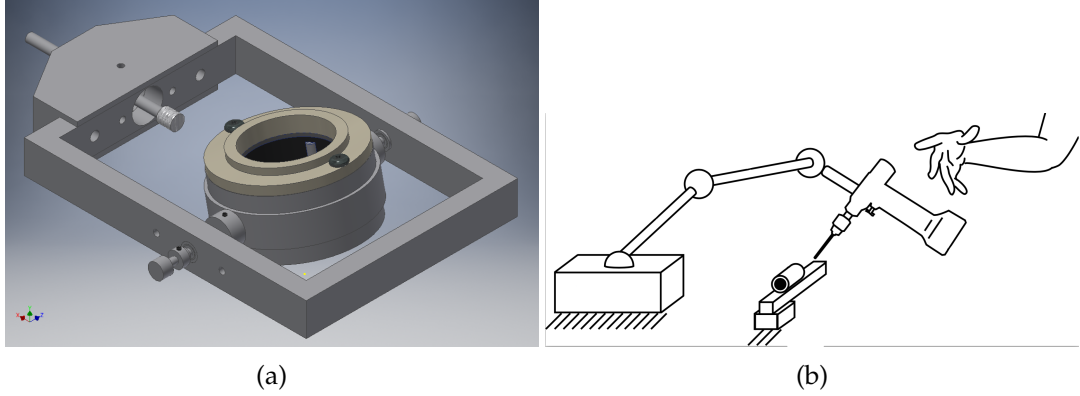


Figure 3.2: (a) 3D model of the gimbal. (b) The schematic of the drill

The forward kinematic model was then used to derive the manipulator Jacobian. Its terms (partial derivatives) were obtained using Maple and are included in Appendix C.1. To verify the accuracy of the result, the actual versus commanded forces were compared at various configurations and found to agree well (Fig. 3.3).

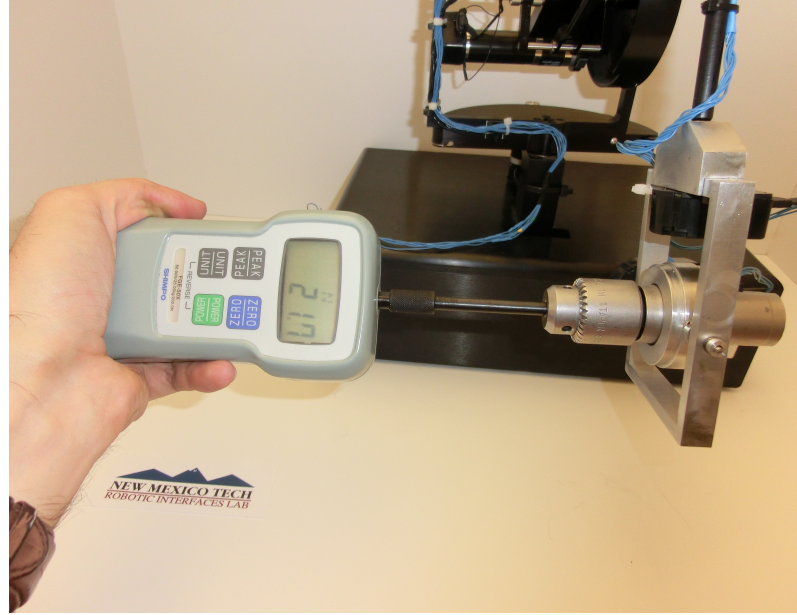


Figure 3.3: To validate the Jacobian matrix, the output force of the device was measured by a Shimpo force gage, relative to the commanded value at various configurations.

3.2.2 Bone Drilling Mechanical Model

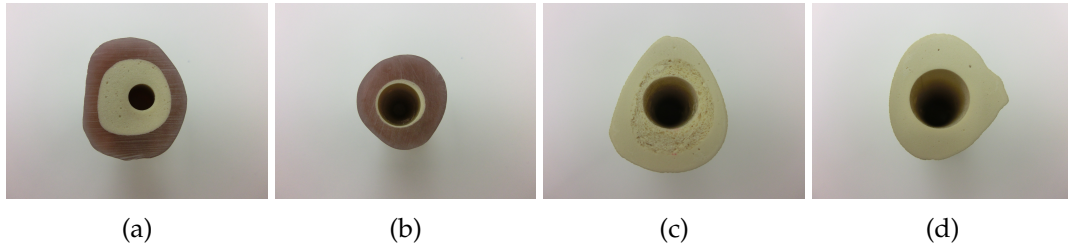


Figure 3.4: Cross-sections of two types of synthetic bone were used for the purpose of modeling each with differing thickness of cortical and cancellous (trabecular) bone. (a) Hard bone with cancellous , (b) hard bone without cancellous , (c) softbone with cancellous and, (d) softbone without cancellous

Two major parameters related to the mechanics of drilling are thickness and hardness of the cortical layer. Synthetic bone specimens with these variations were prepared (Fig. 3.4). Multiple holes were drilled in each specimen using the apparatus shown in Figure 3.5. The force during drilling was measured with a Futek force sensor (model LLB400) and a NI data logger (cDAQ-9184) with a sampling frequency of 100 Hz. The Phantom Premium device (for $\{q_1 \dots q_3\}$)

in conjunction with an Arduino Mega (for q_4 and q_5) were used to measure the location of the drill bit with a frequency of 50 Hz. The kinematic data was post-processed using a 6th order Butterworth filter with 0.1 Hz cut-off frequency.

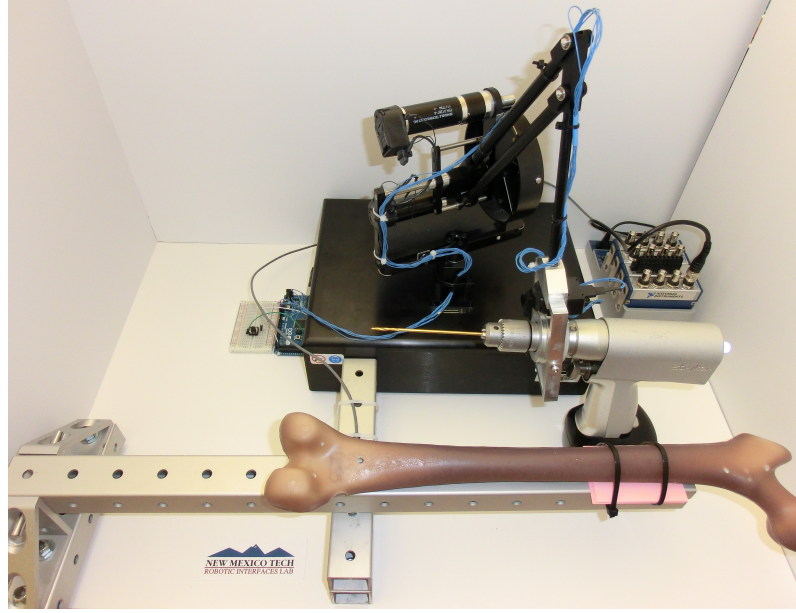


Figure 3.5: Test setup for measuring the force during the drilling.

Initially, a linear, velocity-dependent model was used to fit the data, as per the recommendations in the literature mentioned previously. This effort resulted in a poor fit to the data. Instead a phenomenological approach was taken, using the non-linear objective function:

$$f = a_4x^4 + a_3x^3 + \dots + a_0 + b_4\dot{x}^4 + b_3\dot{x}^3 + \dots + a_0 \quad (3.2)$$

with the corresponding multiple regression model:

$$\begin{bmatrix} f_1 \\ f_2 \\ \vdots \\ f_n \end{bmatrix} = \begin{bmatrix} x_1^4 & x_1^3 & x_1^2 & x_1 & 1 & \dot{x}_1^4 & \dot{x}_1^3 & \dot{x}_1^2 & \dot{x}_1 & 1 \\ x_2^4 & x_2^3 & x_2^2 & x_2 & 1 & \dot{x}_2^4 & \dot{x}_2^3 & \dot{x}_2^2 & \dot{x}_2 & 1 \\ \vdots & \vdots & \vdots & \vdots & \ddots & \vdots & \vdots & \vdots & \vdots & \vdots \\ x_n^4 & x_n^3 & x_n^2 & x_n & 1 & \dot{x}_n^4 & \dot{x}_n^3 & \dot{x}_n^2 & \dot{x}_n & 1 \end{bmatrix} \begin{bmatrix} a_4 \\ a_3 \\ \vdots \\ b_1 \\ a_0 \end{bmatrix} \quad (3.3)$$

where n is the number of data points gathered in *all trials* for a particular bone specimen and x is defined normal to the surface of the bone with the origin at the surface and with up (away from bone) being positive. In order to create simulate the mechanics of drilling into bone with sufficient accuracy for the sake

of training, we sought to create a phenomenological model with optimized accuracy, with focus on position- and velocity-dependent parameters. Position and velocity have been shown previously to critically underlie drilling mechanics [11]. Favoring simplicity, in light of the need for real-time performance, and iterative algorithm started with a first order polynomial model in x and \dot{x} , ($F = a_1x + a_0 + b_1\dot{x} + b_0$). Higher order terms of both x and \dot{x} were added and a regression was run to calculate the root-mean-square error (RMSE). This RMSE was compared to that from the previous step (simpler model) until the improvement in error dropped to below 10%." The final models produced were found describe the respective bone types with the RMSE errors (given in Figures 3.6 - 3.9).

3.3 Results

3.3.1 Force Modeling

Using equation(3.3), model parameters were obtained for each bone sample (Table 3.1). As expected, the various trials for the same sample showed some variability, but were well described by the respective models nonetheless (Figs. 3.6, 3.7, 3.8, 3.9). By contrast, the models (surfaces) found for the various samples were quite distinct from each other (Fig. 3.10), suggesting that the samples tested are indeed mechanically distinct. It can be further conjectured that the role of the thickness of the cortical and cancellous regions play a significant role.

It should be noted that the domain used in fitting the surface is not thoroughly explored by the data obtained. The extra domain is somewhat unavoidable as certain combinations are difficult to attain, such as high velocity at the initial position. This is not a significant limitation, as such a combination is not relevant to this application.

parameter	Sample A	Sample B	Sample C	Sample D
a_4	-9010	-5220	-5080	-19060
a_3	-11900	-6280	-7030	-17100
a_2	-5440	-2730	-3080	-5200
a_1	-939	-516	-454	-601
a_0	0.351	10.9	2.10	3.55
b_4	792	-14800	-1880	-48900
b_3	393	-19100	-1930	-24700
b_2	-42.8	4330	-583	-3460
b_1	-28.8	-95.4	-55.9	-130
a_0	0.351	10.9	2.10	3.55

Table 3.1: Model (surface) parameters, where the units of each term are such that when multiplied by the corresponding position-, velocity-, or offset-based parameter (e.g. x) the result is in Newtons. Note that the kinematic equations were derived using inches as the length unit to match design and manufacturing around imperial units.

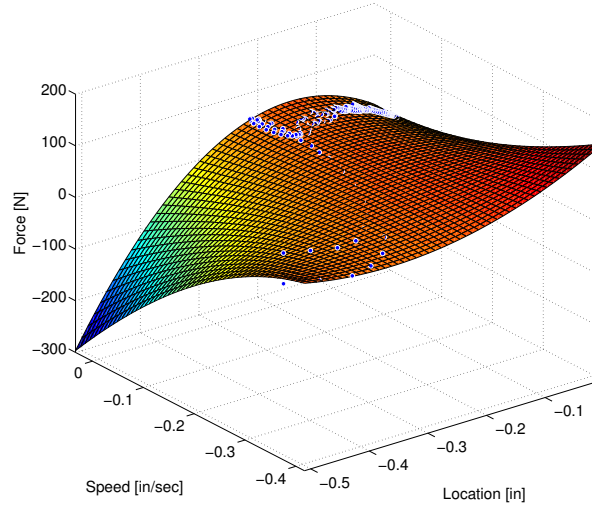


Figure 3.6: Plot of the force model with respect to the measured data sets (multiple trials) are shown for the sample comprised of hard bone with a cancellous region (Sample A), RMSE 8%. The model is shown to fit the data well; however, it is critical to note that the model extends well beyond the domain actually sampled. This is also true for the models shown in the immediately following figures.

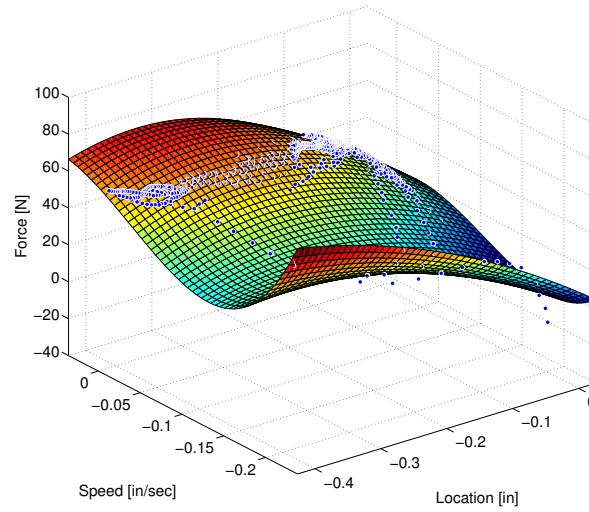


Figure 3.7: Plot of the force model with respect to the measured data sets (multiple trials) are shown for the sample comprised of hard bone without a cancellous region (Sample B), RMSE 9%.

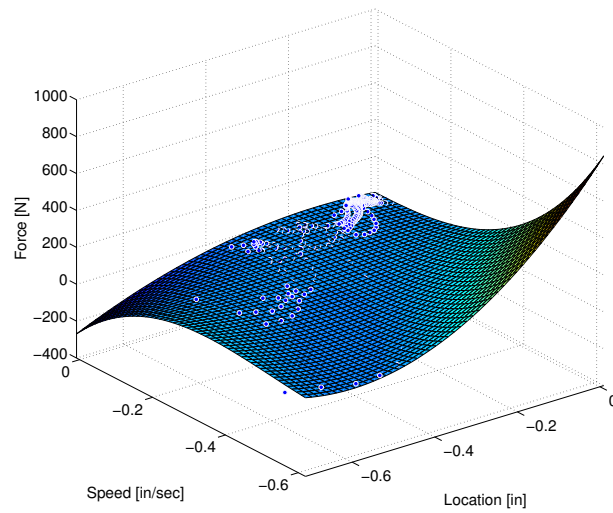


Figure 3.8: Plot of the force model with respect to the measured data sets (multiple trials) are shown for the sample comprised of soft bone with a cancellous region (Sample C), RMSE 11%.

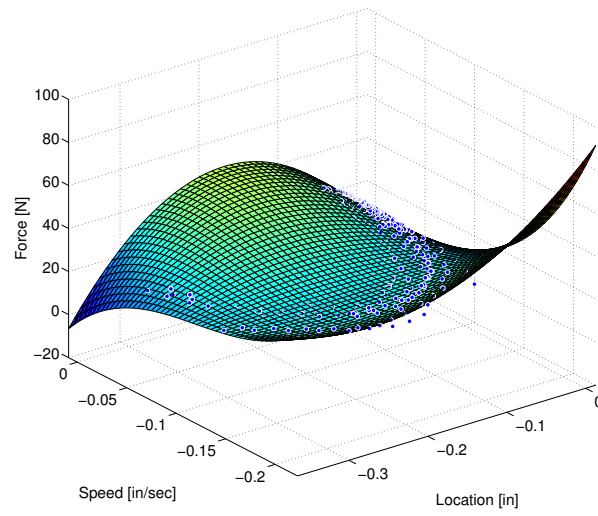


Figure 3.9: Plot of the force model with respect to the measured data sets (multiple trials) are shown for the sample comprised of soft bone without a cancellous region (Sample D), RMSE 13%.

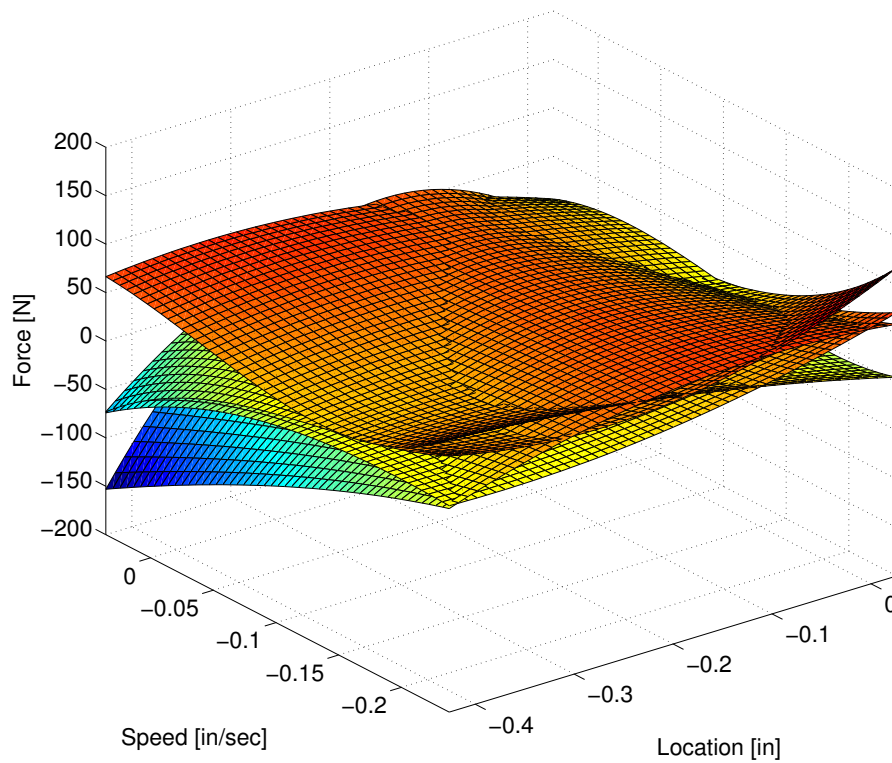


Figure 3.10: Comparison of the four force models, each resulting from one of the bone samples tested, also shown in figures 3.6 - 3.9.

Figures. 3.11, 3.12, 3.13 and 3.14 compare multiple trials for each material. Although the error in some areas is considerable, most of these areas are not reachable for location and velocity.

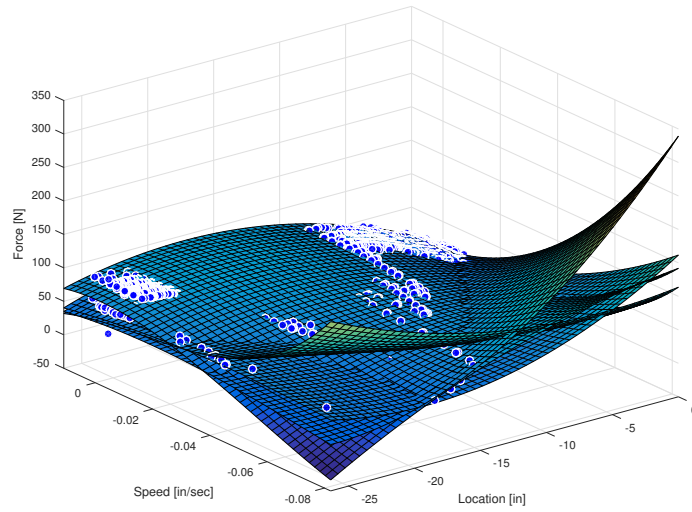


Figure 3.11: Comparing the four force models with respect to the measured data sets are shown for the sample comprised of hard bone with a cancellous region (Sample A)

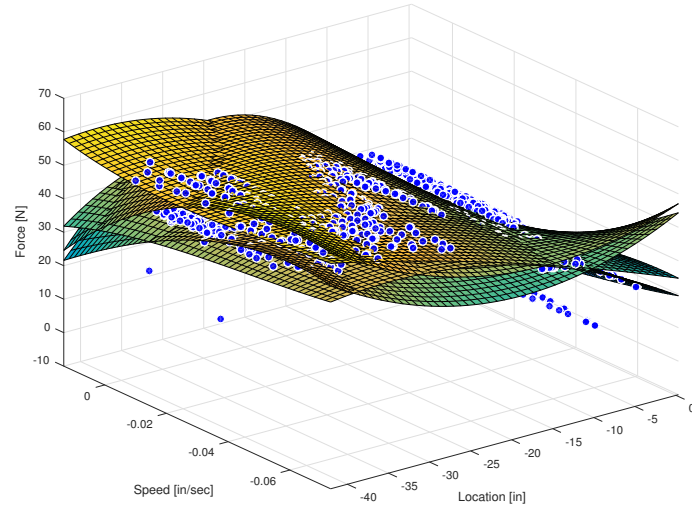


Figure 3.12: Comparing the four force models with respect to the measured data sets are shown for the sample comprised of hard bone without a cancellous region (Sample B)

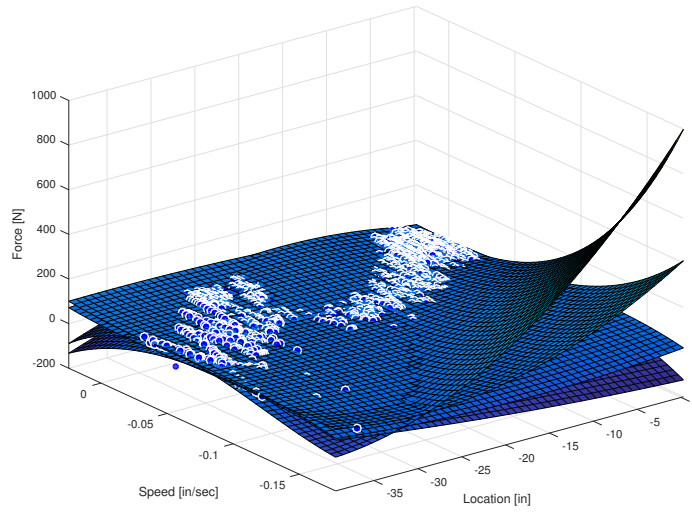


Figure 3.13: Comparing the four force models with respect to the measured data sets are shown for the sample comprised of soft bone with a cancellous region (Sample C)

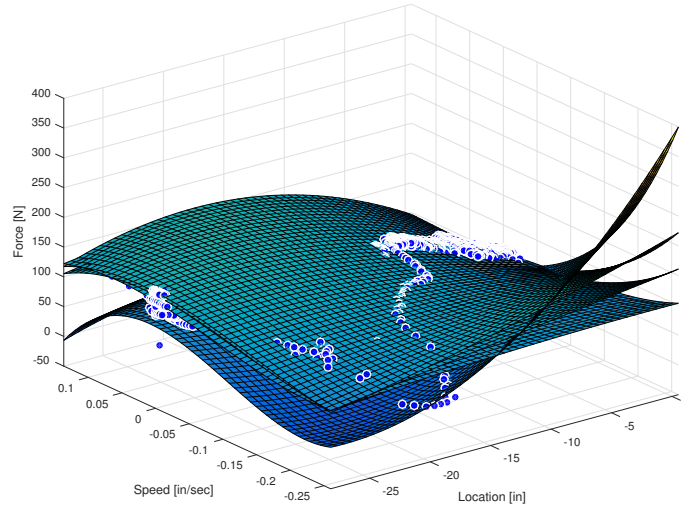


Figure 3.14: Comparing the four force models with respect to the measured data sets are shown for the sample comprised of soft bone without a cancellous region (Sample D)

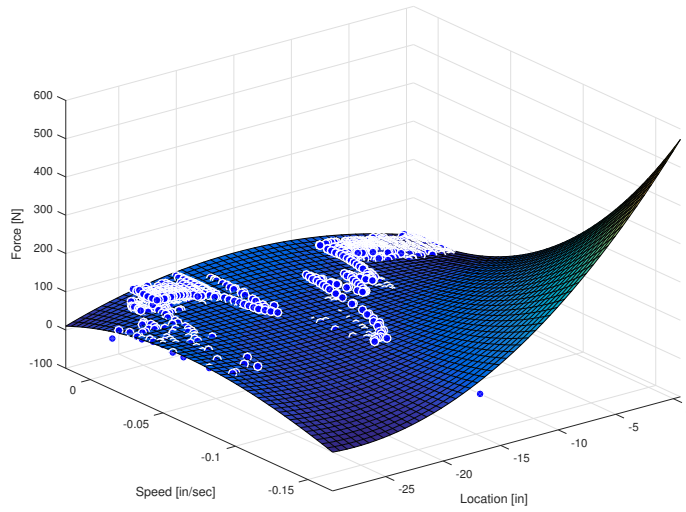


Figure 3.15: Plot of the average force model with respect to the measured data sets (all trials) are shown for the sample comprised of hard bone with a cancellous region (Sample A)

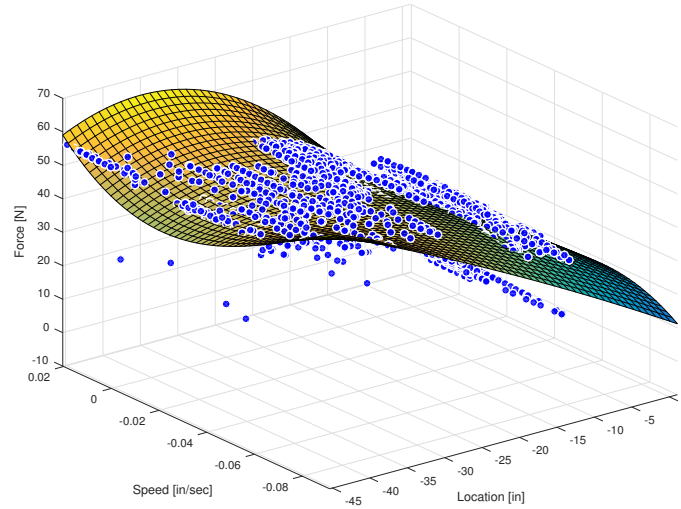


Figure 3.16: Plot of the average force model with respect to the measured data sets (all trials) are shown for the sample comprised of hard bone without a cancellous region (Sample B)

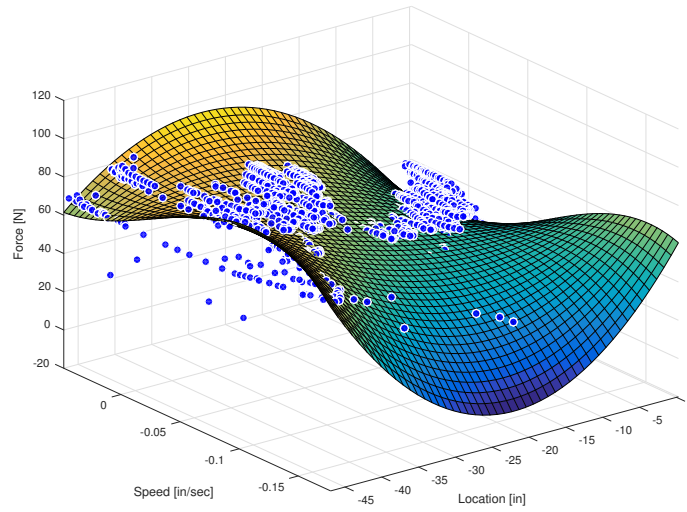


Figure 3.17: Plot of the average force model with respect to the measured data sets (all trials) are shown for the sample comprised of soft bone with a cancellous region (Sample C)

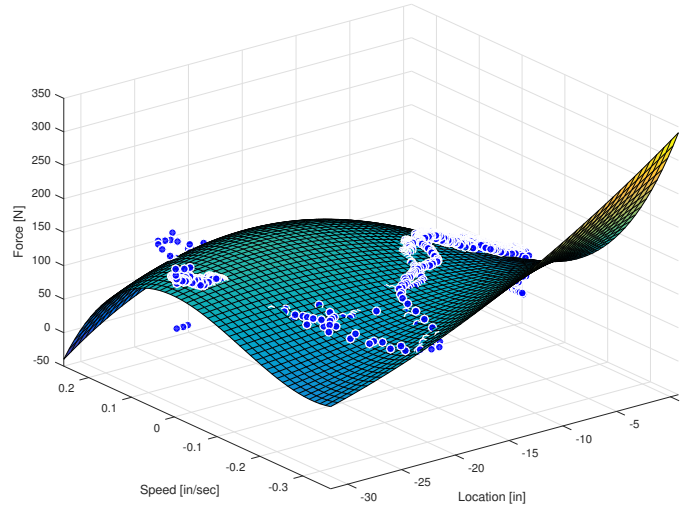


Figure 3.18: Plot of the average force model with respect to the measured data sets (all trials) are shown for the sample comprised of soft bone without a cancellous region (Sample D)

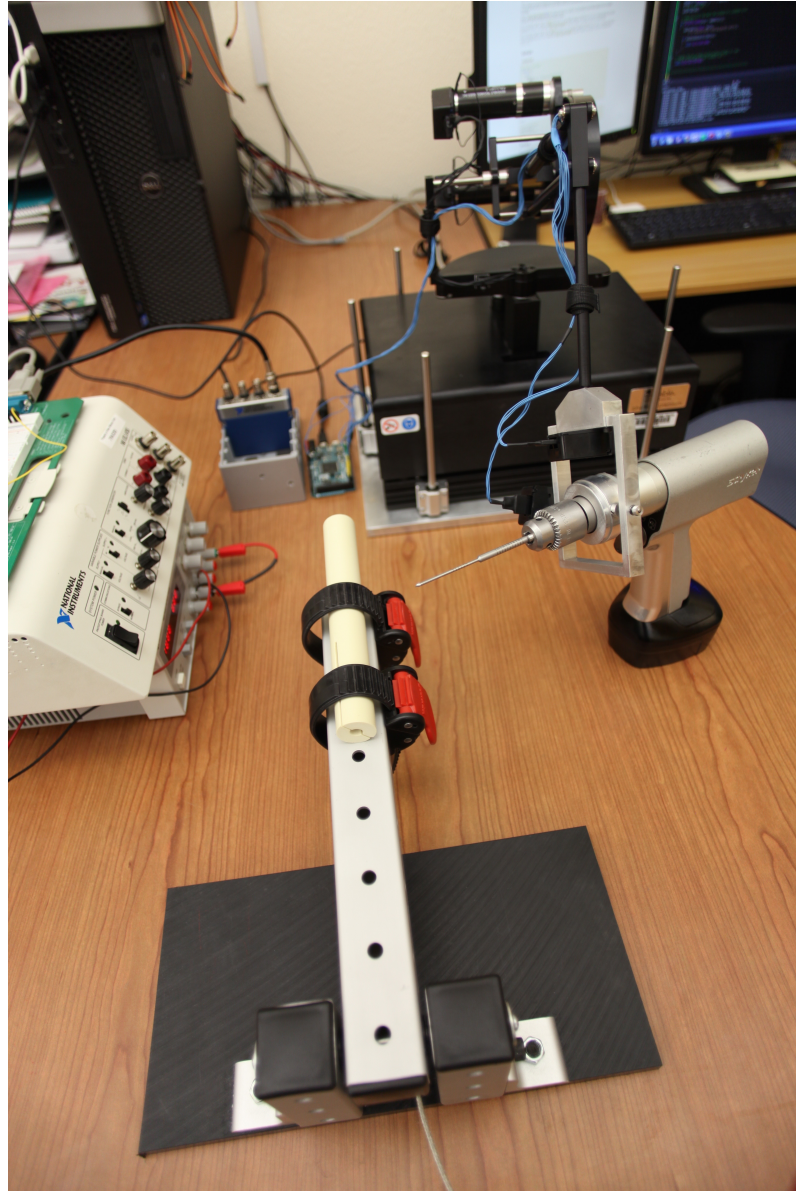


Figure 3.19: The modified haptic device (right) is shown with the force-gage-embedded bone fixture (bottom) and data acquisition system (right). In order to obtain the kinematic parameters (x, \dot{x}), the raw encoder values were read using a custom C++ script and then fed into the inverse kinematic equations we derived. The force sensor was driven by and read using an National Instruments data acquisition system.

3.3.2 Test Evaluation

To check the performance of the method, a custom chassis was constructed. As a first step to check the modified Jacobian, a vertically sliding table was designed and the robot set on top of it. The force sensor under the sliding table, measured the vertical load that was applied from the robot during the drilling (Figs. 3.20).

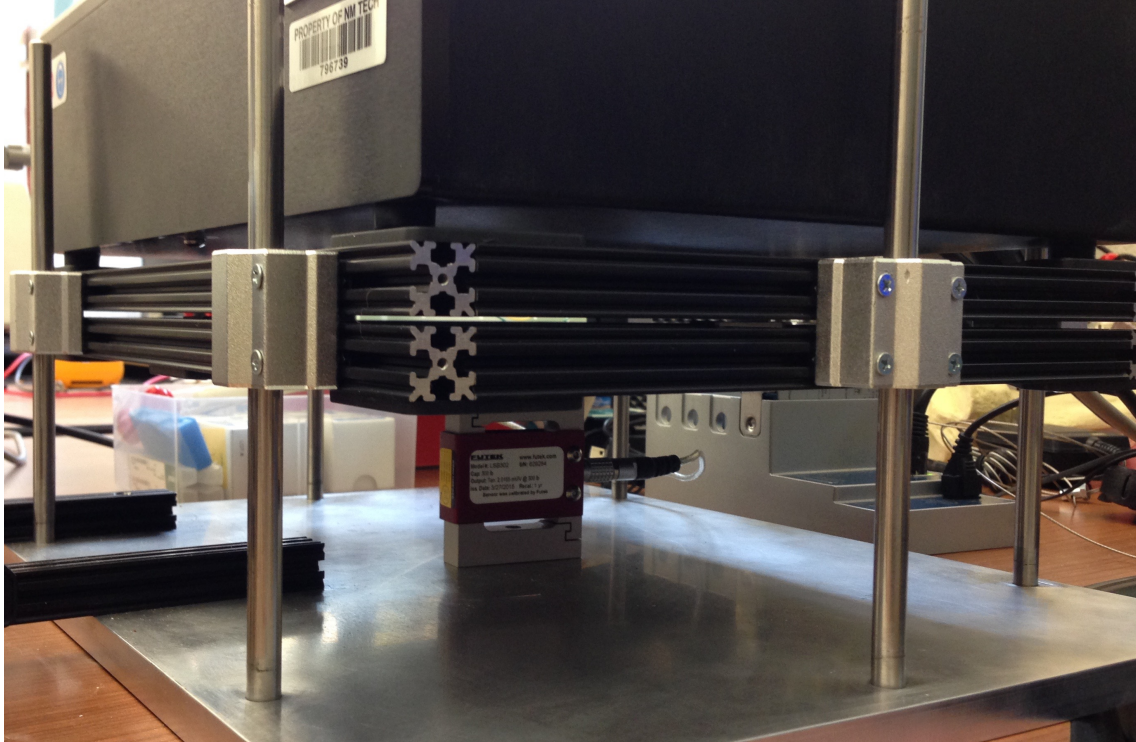


Figure 3.20: The test setup to check the modified Jacobian. By putting the robot on a force sensor in a vertically slider table, during the evaluation test, the applied force from the robot was continuously measured and compared with the calculated force.

As an experiment, in the case where bone B is meant to feel like A, the algorithm would:

- Measure the location x , and the speed \dot{x} .
- Estimate the current force associated with drilling into B, given the current kinematics.
- Calculate the necessary difference in force to make B feel like A.
- Apply this force to the user.

Figure 3.21 shows the result of the validation proses.

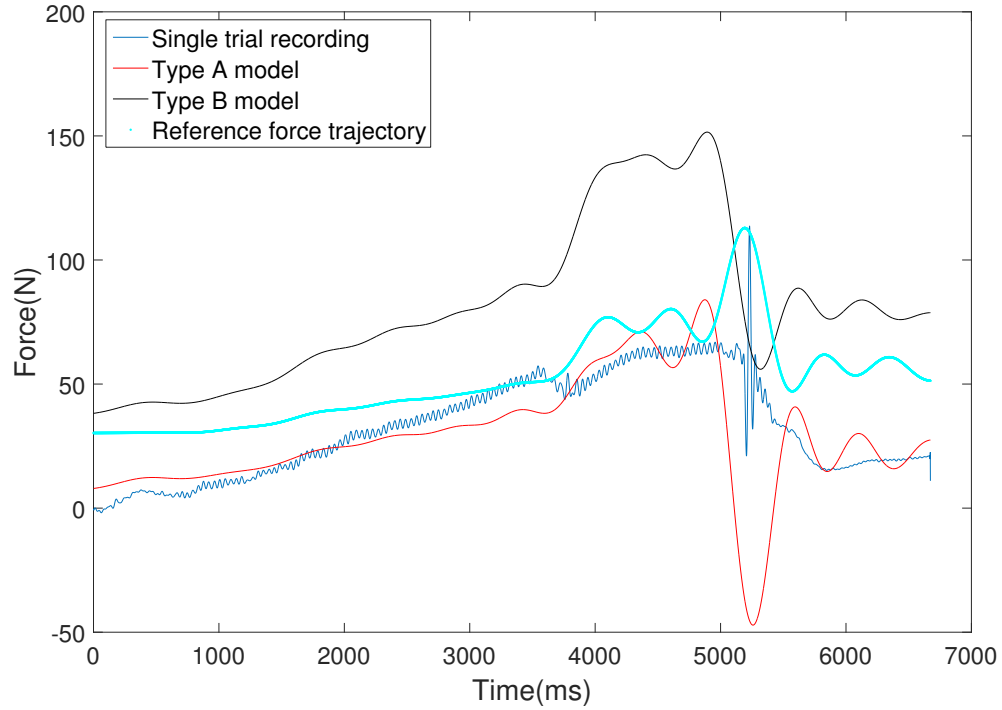


Figure 3.21: The applied force in validation study.

To make the system stable, the reference force trajectory was overlaid on a signal ramp function.

3.4 Conclusions

The force model which was used in this study is a function of drill bit's position and velocity relative to the bone surface. This model is more complex than those presented by others in the prior work described and better fit the data we obtained, by a significant margin, than these simpler models. It may be that the position dependence relates to frictional forces, which increase with depth. In particular, these simpler models did not contain the non-linear terms present in our model. This suggests that better fit provided by our model points to drilling mechanics being more complicated than previously thought. It should again be mentioned that the cross-sections are non-uniform.

These results suggest that accurate predictive models of drilling can be obtained. These models may be used to augmented one bone sample, to "feel"

like some target bone type. To effectively harden the cortical or cancellous region, this model can predict the necessary increase in force against the drilling direction, and visa versa.

Future work will extend the types of bone tested to include flat, irregular, and short bones as well as cadaveric samples. Future work will investigate the quantitative and perceived realism of augmented bone drilling through user studies with surgical residents and experts. This preliminary success does, in fact, suggest that low-cost (e.g. PVC pipe) materials might be used to reduce cost without sacrificing fidelity.

Future work might also explore the use of augmenting torque feedback during drilling. In addition, it may prove to be useful to intentionally distort what is felt to exaggerate certain effects for the purpose of training (e.g. making the bone surface especially slippery). Force perturbation might elicit reductions in toggling, decreased surface friction may improve tactics related to avoiding skivvyng, and so forth. We will also explore rendering soft tissue that would be adjacent to the bones, further increasing the realism of the simulation.

CHAPTER 4

CONCLUSIONS AND RECOMMENDATIONS

4.1 Summary

This thesis explored the potential benefits of using robotics tools to improve training methods in surgical drilling. Modern tools such as motion capture systems and haptic robots may enhance the precision and fidelity of training tools. Even subtle improvements, might play a significant role in the utility of bone drilling training. Moreover, improvement to training may significantly reduce risk during surgical procedures. Here, through quantification of mechanical and “human moto” parameters we present an improved understanding of how a surgeons control of a drill affects relevant outcomes.

4.1.1 Skill Assessment

Clearly a surgeons ability to correctly execute a surgical path relies on some combination of dexterity, clinical knowledge, and prior experience. It is worth considering to what extent skill assessments such as those presented here specifically address each of these areas. As there was no significant improvement in recorded parameters during the traditional training, this study suggests adding more effective and modern methods.

The fact that the performance parameters measured were not significantly different over the course of the focused training course like SWOTA, suggests that either substantial improvements in the training method is required or the assessment tool must be revised to better capture the differences between and novice and expert performance.

4.1.2 Augmented Haptics

The use of virtual reality for surgical training could yield many exciting benefits. However, limitations exist in the accuracy of the mechanical models as well as the capability of existing commercial haptic devices for surgical training.

To improve realism, VR systems for bone drilling need a more accurate mechanical model. Here we were able to demonstrate an accurate mechanical model. The use of augmented haptics was shown to critically extend the capability of standard, impedance-type haptic devices for tasks like training bone drilling.

4.2 Future Work

4.2.1 Skill Assessment

In this thesis a case for additional studies on the skill assessment of bone drilling was presented. This study demonstrated that there are limitations in the sensitivity of the measurement tools used here relative to the surgical skill evaluation and/or specificity of training events like SWOTA. It stands to reason that focused training on a particular skill, such as avoiding over-penetration, would result in more significant/rapid improvements in that particular aspect. Clearly this is difficult to accomplish at these events given the wide range of skills that need to be acquired in the relatively short time. Some of the assumptions, such as the effect of vibration and the angle of penetration, did not show a strong correlation with over-penetration or other clinically important parameters. The current trial design is too bulky, but before being able to make the design simpler and more compact, we must understand which parameters may be neglected. It is necessary to conduct more tests and prioritize the measured parameters. More than simplification, having more data and participants can significantly improve the quality and accuracy of the data.

Having clear definitions for parameters can help to generate a more accurate index. This study used traditional definitions for the measured parameters; as an example, we assigned the “expert surgeon” class to a practitioner past their residency. Literature showed that spending more time in the OR does not necessarily make an expert surgeon, therefore making better definitions of parameters can improve the quality of the training significantly. Experts participated in the studies during different conferences and events, and occasionally the team had difficulties explaining the task clearly due to the lack of time subject focus. Not being consistent with the explanation of the task, as well as letting participants communicate during the trial may have added error. Defining a more routine task may magnify the difference between experts and novices, and experimenting with bones of various mechanical properties is also recommended.

Future work might include the use of complex Neural Network to further elucidate the connection between clinically relevant outcome of performance parameters. So far only a simple, single hidden layer Neural Network was used but this study did not produce any significant results suggesting that a more complicated Neural Network maybe required. Data-mining and big-data methods can also be beneficial for future work[69].

4.2.2 Augmented Haptics

The physical model can easily move compared to the registered location in the VR coordinate system. Therefore, adding a physical collision detection system can help with the performance of the device, providing superior accuracy over a location estimate. As another approach, adding an image processing base setup can continuously register the location of the model via virtual coordinates.

The force model presented here for drilling has only modest error. Additional work related to fine tuning the model can result significant improvement. Additionally conducting trials on wider range of materials and drill bit could expand the utility of this model.

To generate a more realistic virtual reality it is necessary to add a second and third dimension to the model. Furthermore, adding torque feedback maybe critical to realism, although it is worth noting that most commercial haptic devices are incapable of providing the level of torque required, if any at all. The available haptic devices capable of torque feedback tend to have much smaller work space than their equivalent without torque feedback.

APPENDIX A

SURVEYING RESULT FROM NOVICE PARTICIPANTS

Id	Record Name	Date Created	Date Updated	Record Stat	1. Years in F	2. Sex	3. Handedn
1	Record_1	5/14/15 9:06	5/14/15 13:55	Saved	5	1	1
2	Record_2	5/14/15 10:57	5/14/15 13:55	Saved	1	1	1
3	Record_3	5/14/15 11:15	5/14/15 11:19	Saved	1	1	1
4	Record_4	5/14/15 11:33	5/14/15 11:54	Saved	1	1	1
5	Record_5	5/14/15 11:55	5/14/15 11:58	Saved	1	0	1
6	Record_6	5/14/15 12:09	5/14/15 12:13	Saved	1	1	1
7	Record_7	5/14/15 12:13	5/14/15 12:36	Saved	1	1	1
8	Record_8	5/14/15 12:42	5/14/15 12:45	Saved	1	1	1
9	Record_9	5/14/15 12:45	5/14/15 12:48	Saved	1	1	1
10	Record_10	5/14/15 13:49	5/14/15 14:26	Saved	1	1	1
11	Record_11	5/14/15 13:58	5/14/15 14:27	Saved	1	0	1
12	Record_12	5/14/15 14:43	5/14/15 14:48	Saved	1	0	1
13	Record_13	5/14/15 14:49	5/14/15 14:53	Saved	1	1	1
14	Record_14	5/14/15 15:04	5/14/15 15:07	Saved	1	0	1
15	Record_15	5/14/15 15:09	5/14/15 15:12	Saved	1	1	1
16	Record_16	5/14/15 15:22	5/14/15 15:25	Saved	1	1	1
17	Record_17	5/14/15 15:25	5/14/15 15:29	Saved	1	1	0
18	Record_18	5/14/15 15:37	5/14/15 17:01	Saved	1	1	1
19	Record_19	5/14/15 15:58	5/14/15 17:01	Saved	1	0	1
20	Record_20	5/14/15 16:02	5/14/15 17:18	Saved	1	1	1
21	Record_21	5/14/15 16:20	5/14/15 17:17	Saved	1	0	1
22	Record_22	5/14/15 16:53	5/14/15 17:17	Saved	1	1	1
23	Record_23	5/14/15 17:14	5/14/15 17:17	Saved	1	1	1

4. Height (in)	5. How many hols	6. How mar	7. How mar	8. Does you	9. Do you b	10. Does yc
72	100	10	1		1	1 nan
70	1	1	90	0	1	1 0
73	5	0	2	1	1 1,2	1
71	3	1	28	0	1	1 0
68	10	10	3	1	1	1 0
70	230	1	30	0	1 1,2	0
75	10	1	4	1	1 1,2	1
70	2	2	5	0	1 1,2	0
75	10	100	2	1	0 nan	1
66	2	0	5	1	1 1,2	1
67	1	0	2	1	1	1 1
68	1	1	4	0	1	1 0
69	3	0	1	1	1	1 1
64	10	0	7	1	1	1 1
69	4	0	14	0	0 nan	1
68	20	5	1	1	1	1 1
73	10	0	1	1	0 nan	1
70	5	0	10	1	1	1 1
69	10	10	2	0	1	1 1
69	20	0	2	1	1	1 1
64	20	0	2	1	1 1,2	1
72	1	0	90	0	1 1,2,3,4,5	0
72	1	0	90	0	1	1 0

11. Does yc	12. Does yc	13. Does yc	14. How are your su	other:	15. Do you	16. Do you
nan	nan	nan	nan	nan	nan	nan
1	0	1	a. Faculty Evaluation		0	0
1	1	1	a. Faculty Evaluation		0	1
1	1	1	a. Faculty Evaluation		1	0
1	1	1	c. Objective Structured Assessment of Technical		1	0
1	0	1	d. other	Ot	0	0
1	0	1	a. Faculty Evaluation		0	1
1	1	1	a. Faculty Evaluation		0	0
1	1	1	a. Faculty Evaluation		1	1
1	1	1	a. Faculty Evaluation		0	1
1	1	1	d. other	Month training was second,	0	1
1	1	1	a. Faculty Evaluation		0	0
1	1	1	d. other	all three	1	0
0	1	1	a. Faculty Evaluation		1	0
1	1	1	a. Faculty Evaluation		0	0
1	1	1	a. Faculty Evaluation		0	0
1	1	1	a. Faculty Evaluation		1	1
1	1	1	a. Faculty Evaluation		0	0
1	1	1	a. Faculty Evaluation		1	0
1	1	1	d. other	a and c	1	1
1	1	1	a. Faculty Evaluation		1	1
1	0	1	a. Faculty Evaluation		1	0
1	1	1	a. Faculty Evaluation		1	0

17. Do you a. If 1, did y	18. Do you a. If 1, how	19. On a sc	20. (21. Participant Number	Addition
1 nan	1 nan	8	8	5	1 Ot in resi
1	1	1	400	8	8 7
1	1	0		7	8 7
1 nan	1	1	150	5	5 3
1	1	1	20	6	6 6
1	1	0		6	4 3
1	1	1	200	7	7 7
1	1	1	100	7	7 5
1	1	1	1000	5	4 2
1	1	1	8	7	6 8
1	1	0		4	4 2
1	1	0		5	4 6
1	1	0		6	5 6
1	1	0		3	3 4
1	1	1	100	8	4 4
1	1	0		5	6 6
1	1	1	1000	5	5 3
1	1	0		4	6 3
1	1	1	24	8	8 8
1	1	0		8	8 6
1	1	0		4	5 6
1	1	0		3	3 4
1	1	1	4	5	6 6
					22
					21
					20 Had resi
					23
					19
					16
					18
					15
					17
					14
					12
					13
					11
					10
					4
					9
					8 Multiple
					3
					7
					6 Done bo
					5
					2 UNM stu
					1 Ot in resi

Id	Record	Nan	Date Create	Date Update	Record Stat	1. Do you have a...	2. On a scale...
8	Record_8	#####	#####	Saved	1	100	8
4	Record_4	#####	#####	Saved	0		7
th models First year in this residency, did one year general prior to this one E6 - 0 handed							
19	Record_19	#####	#####	Saved	1	40	6
1	Record_1	#####	#####	Saved	0		5
14	Record_14	#####	#####	Saved	1	200	7
7	Record_7	#####	#####	Saved	1		7
11	Record_11	#####	#####	Saved	1	2500	6
3	Record_3	#####	#####	Saved	0		7
2	Record_2	#####	#####	Saved	0		4
22	Record_22	#####	#####	Saved	0		6
5	Record_5	#####	#####	Saved	0		5
26	Record_26	#####	#####	Saved	0		4
9	Record_9	#####	#####	Saved	1	100	8
16	Record_16	#####	#####	Saved	0		6
27	Record_27	#####	#####	Saved	0		4
13	Record_13	#####	#####	Saved	0		8
10	Record_10	#####	#####	Saved	1	24	8
18	Record_18	#####	#####	Saved	0		5
6	Record_6	#####	#####	Saved	0		4
12	Record_12	#####	#####	Saved	1	4	6

3. On a scal	4. On a scal	Previous Re	Current Res	Additional Ote	Id	Record Nan	Date Create	Date Updat
8	8	2	30			8 Record_8	#####	#####
7	7	5	26	New rigid defi		4 Record_4	#####	#####
6	6	7	43			20 Record_20	#####	#####
5	6	3	24	First hole - tab		1 Record_1	#####	#####
7	5	8	38	After c, drill bi		15 Record_15	#####	#####
7	8	9	31			7 Record_7	#####	#####
7	5	4	35			11 Record_11	#####	#####
7	8	10	27			3 Record_3	#####	#####
4	3	11	25	Problem with		2 Record_2	#####	#####
5	6	13	47					
5	4	12	28			5 Record_5	#####	#####
4	5	14	50	Used step stoc		27 Record_27	#####	#####
7	7	17	33	Right side		9 Record_9	#####	#####
6	7	15	39			17 Record_17	#####	#####
						14 Record_14	#####	#####
6	5	16	51	starting on B		28 Record_28	#####	#####
7	8	19	36	Drill bit is getti		13 Record_13	#####	#####
8	8	23	32			10 Record_10	#####	#####
6	7	20	41	Standing on st		19 Record_19	#####	#####
4	5	21	29			6 Record_6	#####	#####
6	7	22	34					

Record Stat 1. Do you f a. If 1, whic 2. On a scal 3. On a scal 4. On a scal 5. Do you b 6. Do you f 7. Do you b

Saved	1 markers on	8	8	8	1	1	1
Saved	0	8	6	7	0	1	1
Saved	0	6	7	6	1	1	1
Saved	1 tracker ball	5	4	6	1	0	1
Saved	1 drill was du	8	9	8	1	1	1
Saved	0	7	7	8	1	1	1
Saved	1 location an	5	9	5	1	1	0
Saved	0	7	7	8	1	1	1
Saved	1 markers on	4	4	3	1	1	1
Saved	0	5	3	5	1	1	1
Saved	0	4	4	5	1	1	1
Saved	0	8	8	7	1	1	1
Saved	0	6	7	7	1	1	1
Saved	0	6	6	4	1	1	1
Saved	0	4	6	4	1	1	1
Saved	0	5	8	8	1	0	1
Saved	1 hand on dri	8	8	8	1	1	1
Saved	1 height was	6	6	7	1	0	1
Saved	0	5	6	6	1	1	1

a. If 1, in wl 8. Do you h Sides Driller Previous Re Current Res Additional Otes

	1	Markers obstructing av	2	30
	1	0	5	26
	1	First Time l	7	43
1,2		More clearly define obj	3	24
1,2		First Time l	8	38
1,2			9	31 Different side
		Wires and p First Time l	4	35
1,2			10	27
	1		11	25
	1	Getting drill more	12	28
1,2,3,4,5		First Time l	14	50
1,2,3,4,5		First Time l	17	33
	1	First Time l	15	39
	1	First Time l	18	37
1,2,3,4,5		First Time l	16	51
	1	First Time l	19	36
	1	Limited abil First Time l	23	32
1,2		Adjustable First Time l	20	41
1,2,3,4,5			21	29

APPENDIX B

MATLAB CODES AND FUNCTIONS

B.1 Skill assessment project

B.1.1 Main file 1

```
1 clc
2 clear all
3 [data_lv,h_lv,min_lv,sec_lv]=Dataanalyze('test.lvm');
4 data_lv(:,1)=data_lv(:,1)+str2num(sec_lv)+str2num(min_lv)*60+...
    str2num(h_lv)*3600;
5 %data_omni=csvread('example.txt');
6 %data_omni(:,10)=12;
7 %data_omni(:,14)=data_omni(:,13)/1000+data_omni(:,12)+data_omni...
    (:,11)*60+data_omni(:,10)*3600;
8 subplot(4,1,1);
9 plot(data_lv(:,1),data_lv(:,2));
10 subplot(4,1,2);
11 plot(data_lv(:,1),data_lv(:,3));
12 subplot(4,1,3);
13 plot(data_lv(:,1),data_lv(:,4));
14 subplot(4,1,4);
15 plot(data_lv(:,1),data_lv(:,5));
16 %subplot(5,1,5);
17 %plot(data_lv(:,1),data_lv(:,3));
18 %hold on
19 %plot(data_omni(:,1),data_lv(:,14));
```

B.1.2 Costume correlation function 1

```
1 function [corr_out]=costume_corr(input_data)
2 %input is [m,n]; m: length of each arr, n=numbers of arr.
3 [~,n]=size(input_data);
4 w=diag(ones(1,n));
```

```

5 corr_out=zeros(n);
6     for mm=1:n
7         for mm2=mm:n
8             corr_out(mm,mm2)=nancorrcoef(input_data(:,mm),...
                                           input_data(:,mm2));
9         end
10    end
11    corr_out=corr_out+flipud(rot90(corr_out))-w;
12 end

```

B.1.3 Costume correlation function 2

```

1  clc
2  close all
3  clear all
4  load('matlab.mat')
5  load('matlab_data.mat')
6  load('matlab_numbers.mat')
7  Total_finaldata=[Finaldata_nmtday1,Finaldata_NMTday2,...
                    Finaldata_UNMday2];
8  Total_finalNumb=[Finaldata_nmtday1,Finaldata_NMTday2,...
                   Finaldata_UNMday2];
9  list_load
10 %%
11 clc
12 conver=[1 2 6 9 3 4 5 7 8 10 11 13 12 14 16 18 15 17 19 21 22 23 ...
          20 6 11 3 10 13 22 2 8 20 1 23 9 19 24 7 16 24 21 24 5 24 24 ...
          24 12 24 24 14 18];
13 ii=[1:125];
14 yy=[1 5 8 13 14 19 20 21 22 23 1 8 9 14 16 19 21 22 23 1 6 10 14 ...
      15 19 21 22 1 6 13 14 19 20 23 1 6 8 9 14 22 25 29 30 32 34 ...
      36 38 39 41 43 45 47 48 49 50 25 26 29 30 32 34 36 38 39 41 ...
      43 45 47 48 49 50 25 29 30 32 34 36 38 39 41 45 47 48 49 50 ...
      51 25 29 30 32 34 36 38 41 43 45 47 48 49 29 30 32 34 36 38 ...
      41 43 47 48 49 50 24 28 37 42 28 46 28 27 28 31 35 27 28 31];
15 for d=1:length(yy)
16     i=ii(d);
17     nn=Total_finaldata(i).Name ;
18     for qq=2:length(BoneLettering)
19         e=BoneLettering(qq);
20         w=e{1};
21         if (strncmpi(w,nn,min([length(w) length(nn)])))
22             test=1;
23             match_numb=qq;
24         end
25     end

```

```

26 y=conver(yy(d));
27 if (Total_finaldata(i).Name(1)=='A')
28     Total_finaldata(i).HoleType=1;
29 elseif (Total_finaldata(i).Name(1)=='B')
30     Total_finaldata(i).HoleType=2;
31 elseif (Total_finaldata(i).Name(1)=='C')
32     Total_finaldata(i).HoleType=3;
33 elseif (Total_finaldata(i).Name(1)=='D')
34     Total_finaldata(i).HoleType=4;
35 elseif (Total_finaldata(i).Name(1)=='E')
36     Total_finaldata(i).HoleType=5;
37 end
38 Total_finaldata(i).ID_UNMname=BoneLettering(match_numb);
39 Total_finaldata(i).DistancetoMark=DistancetoMark(match_numb);
40 Total_finaldata(i).FinalMajorAxis=FinalMajorAxis(match_numb);
41 Total_finaldata(i).FinalMinorAxis=FinalMinorAxis(match_numb);
42 Total_finaldata(i).InitialMajorAxisBoneplane=...
    InitialMajorAxisBoneplane(match_numb);
43 Total_finaldata(i).InitialMinorAxisPerpendiculartoBone=...
    InitialMinorAxisPerpendiculartoBone(match_numb);
44 Total_finaldata(i).ID_number=form.ParticipantNumber_Old(y);
45 Total_finaldata(i).Years_in_residency=form....
    Years_in_Residency(y);
46 Total_finaldata(i).Sex=form.sex(y);
47 Total_finaldata(i).Height=form.Height(y);
48 Total_finaldata(i).Sex=form.sex(y);
49 Total_finaldata(i).How_many_holes=form.How_many_holes(y);
50 Total_finaldata(i).days_since_your_last_bone_drilling=form....
    days_since_your_last_bone_drilling(y);
51 Total_finaldata(i).residency_program_include=form....
    residency_program_include(y);
52 Total_finaldata(i)....
    program_have_dedicated_surgical_skills_training=form....
    program_have_dedicated_surgical_skills_training(y);
53 Total_finaldata(i).PVC=form.PVC(y);
54 Total_finaldata(i).have_extensive_0n_surgical_experience=form...
    .have_extensive_0n_surgical_experience(y);
55 Total_finaldata(i).rate_your_drill_overpenetration=form....
    rate_your_drill_overpenetration(y);
56 %Total_finaldata(i).rate_your_drill_overpenetration=form....
    rate_your_drill_overpenetration(y);
57 if (i<41)
58     Total_finaldata(i).Time_lv_2ndcliped=Total_finaldata(i)....
        C_drilling_dataLV(:,1);
59     Total_finaldata(i).Force_lv_2ndcliped=Total_finaldata(i)....
        C_drilling_dataLV(:,2);
60     Total_finaldata(i).RPM_lv_2ndcliped=Total_finaldata(i)....
        C_drilling_dataLV(:,3);
61     Total_finaldata(i).bar_lv_2ndcliped=Total_finaldata(i)....
        C_drilling_dataLV(:,4);

```



```

62         Total_finaldata(i).drill_lv_2ndclipped=Total_finaldata(i)....
           C_drilling_dataLV(:,5);
63     elseif (i<112)
64         Total_finaldata(i).Time_lv_2ndclipped=Total_finaldata(i)....
           C_drilling_dataLV(:,1);
65         Total_finaldata(i).Force_lv_2ndclipped=Total_finaldata(i)....
           C_drilling_dataLV(:,4);
66         Total_finaldata(i).RPM_lv_2ndclipped=Total_finaldata(i)....
           C_drilling_dataLV(:,5);
67         Total_finaldata(i).bar_lv_2ndclipped=Total_finaldata(i)....
           C_drilling_dataLV(:,2);
68         Total_finaldata(i).drill_lv_2ndclipped=Total_finaldata(i)....
           C_drilling_dataLV(:,3);
69     else
70         Total_finaldata(i).Time_lv_2ndclipped=Total_finaldata(i)....
           C_drilling_dataLV(:,1);
71         Total_finaldata(i).Force_lv_2ndclipped=Total_finaldata(i)....
           C_drilling_dataLV(:,4);
72         Total_finaldata(i).RPM_lv_2ndclipped=Total_finaldata(i)....
           C_drilling_dataLV(:,2);
73         Total_finaldata(i).bar_lv_2ndclipped=Total_finaldata(i)....
           C_drilling_dataLV(:,5);
74         Total_finaldata(i).drill_lv_2ndclipped=Total_finaldata(i)....
           C_drilling_dataLV(:,3);
75     end
76     [res]=rpm_final(Total_finaldata(i).RPM_lv_2ndclipped,...
           Total_finaldata(i).Time_lv_2ndclipped);
77     Total_finaldata(i).RPM_ave_2ndclipped=mean(res(1,:));
78     [w,~]=size(Total_finaldata(i).C_Overpen_fixed_dataMT);
79     Total_finaldata(i).maxpen=sqrt((Total_finaldata(i)....
           C_Overpen_fixed_dataMT(1,27)-Total_finaldata(i)....
           C_Overpen_fixed_dataMT(w,27))^2+(Total_finaldata(i)....
           C_Overpen_fixed_dataMT(1,28)-Total_finaldata(i)....
           C_Overpen_fixed_dataMT(w,28))^2+(Total_finaldata(i)....
           C_Overpen_fixed_dataMT(1,29)-Total_finaldata(i)....
           C_Overpen_fixed_dataMT(w,29))^2);
80     %Total_finaldata(i).avg_RPM=mean(Total_finaldata(i).C_RPM...
           (:,2));
81     if (Total_finaldata(i).RPM_ave_2ndclipped==0)
82         Total_finaldata(i).RPM_ave_2ndclipped=NaN;
83     end
84     Total_finaldata(i).avg_force=mean(Total_finaldata(i)....
           Force_lv_2ndclipped);
85     Total_finaldata(i).max_force=max(Total_finaldata(i)....
           Force_lv_2ndclipped);
86     Total_finaldata(i).std_force=std(Total_finaldata(i)....
           Force_lv_2ndclipped);
87     Total_finaldata(i).std_bar_vib=std(Total_finaldata(i)....
           bar_lv_2ndclipped);

```

```

88     Total_finaldata(i).std_drill_vib=std(Total_finaldata(i)...
        drill_lv_2ndclipped);
89     Total_finaldata(i).tog_drill=nanmean([nanstd(Total_finaldata(...
        i).C_drilling_fixed_dataMT(:,27)),nanstd(Total_finaldata(...
        i).C_drilling_fixed_dataMT(:,28)),nanstd(Total_finaldata(...
        i).C_drilling_fixed_dataMT(:,29))]));
90     Total_finaldata(i).mean_roll_drill=nanmean(Total_finaldata(i)...
        .C_drilling_fixed_dataMT(:,30));
91     Total_finaldata(i).mean_pitch_drill=nanmean(Total_finaldata(i)...
        ).C_drilling_fixed_dataMT(:,31));
92     Total_finaldata(i).mean_yaw_drill=nanmean(Total_finaldata(i)...
        C_drilling_fixed_dataMT(:,32));
93     %plot3(Total_finaldata(i).C_drilling_fixed_dataMT(:,27),...
        Total_finaldata(i).C_drilling_fixed_dataMT(:,28),...
        Total_finaldata(i).C_drilling_fixed_dataMT(:,29),'.'); ...
        axis equal; grid on
94     %im=getframe;
95     %imwrite(im.cdata, strcat(Total_finaldata(i).Name, '.JPG'));
96 end
97 for i=112:125
98     Total_finaldata(i).std_drill_vib=Total_finaldata(i)...
        std_drill_vib/10;
99 end
100 %%
101
102 Total_finaldata(51).Years_in_residency=10;
103 Total_finaldata(53).Years_in_residency=10;
104 Total_finaldata(54).Years_in_residency=10;
105 Total_finaldata(67).Years_in_residency=10;
106 Total_finaldata(69).Years_in_residency=10;
107 Total_finaldata(70).Years_in_residency=10;
108 Total_finaldata(81).Years_in_residency=10;
109 Total_finaldata(83).Years_in_residency=10;
110 Total_finaldata(84).Years_in_residency=10;
111 Total_finaldata(96).Years_in_residency=10;
112 Total_finaldata(98).Years_in_residency=10;
113 Total_finaldata(99).Years_in_residency=10;
114 Total_finaldata(109).Years_in_residency=10;
115 Total_finaldata(110).Years_in_residency=10;
116 Total_finaldata(114).Years_in_residency=10;
117 Total_finaldata(115).Years_in_residency=10;
118 Total_finaldata(117).Years_in_residency=10;
119
120 %%
121 finalp=costume_corr([Total_finaldata.HoleType;Total_finaldata....
    DistancetoMark;Total_finaldata.FinalMajorAxis;Total_finaldata...
    .FinalMinorAxis;Total_finaldata.ID.number;Total_finaldata....
    Years_in_residency;Total_finaldata.Sex;Total_finaldata....
    Height;Total_finaldata.How_many_holes; Total_finaldata....
    days_since_your_last_bone_drilling; Total_finaldata....

```

```

    residency_program_include; Total_finaldata....
    program_have_dedicated_surgical_skills_training; ...
    Total_finaldata.PVC; Total_finaldata....
    have_extensive_0n_surgical_experience; Total_finaldata....
    RPM_ave_2ndcliped; Total_finaldata.maxpen; Total_finaldata....
    avg_force; Total_finaldata.max_force; Total_finaldata.std_force...
    ; Total_finaldata.std_bar_vib; Total_finaldata.std_drill_vib; ...
    Total_finaldata.tog_drill; Total_finaldata.mean_roll_drill; ...
    Total_finaldata.mean_pitch_drill; Total_finaldata....
    mean_yaw_drill]);
122 % 1-Total_finaldata.HoleType;
123 % 2-Total_finaldata.DistanceToMark;
124 % 3-Total_finaldata.FinalMajorAxis;
125 % 4-Total_finaldata.FinalMinorAxis;
126 % 5-Total_finaldata.ID-number;
127 % 6-Total_finaldata.Years_in_residency;
128 % 7-Total_finaldata.Sex;
129 % 8-Total_finaldata.Height;
130 % 9-Total_finaldata.How_many_holes;
131 % 10-Total_finaldata.days_since_your_last_bone_drilling;
132 % 11-Total_finaldata.residency_program_include;
133 % 12-Total_finaldata....
    program_have_dedicated_surgical_skills_training;
134 % 13-Total_finaldata.PVC;
135 % 14-Total_finaldata.have_extensive_0n_surgical_experience;
136 % 15-Total_finaldata.RPM_ave_2ndcliped;
137 % 16-Total_finaldata.maxpen;
138 % 17-Total_finaldata.avg_force;
139 % 18-Total_finaldata.max_force;
140 % 19-Total_finaldata.std_force;
141 % 20-Total_finaldata.std_bar_vib;
142 % 21-Total_finaldata.std_drill_vib;
143 % 22-Total_finaldata.tog_drill;
144 % 23-Total_finaldata.mean_roll_drill;
145 % 24-Total_finaldata.mean_pitch_drill;
146 % 25-Total_finaldata.mean_yaw_drill;
147 imagesc((finalp)) %plot the
148 %%
149 figure
150 pre_Total_finaldata=Total_finaldata(1:40);
151 figure;pre_finalp=costume_corr([pre_Total_finaldata.HoleType;...
    pre_Total_finaldata.DistanceToMark;pre_Total_finaldata....
    FinalMajorAxis;pre_Total_finaldata.FinalMinorAxis;...
    pre_Total_finaldata.ID-number;pre_Total_finaldata....
    Years_in_residency;pre_Total_finaldata.Sex;...
    pre_Total_finaldata.Height;pre_Total_finaldata.How_many_holes...
    ; pre_Total_finaldata.days_since_your_last_bone_drilling; ...
    pre_Total_finaldata.residency_program_include; ...
    pre_Total_finaldata....
    program_have_dedicated_surgical_skills_training; ...

```

```

pre.Total_finaldata.PVC; pre.Total_finaldata....
have_extensive_0n_surgical_experience;pre.Total_finaldata....
RPM_ave_2ndclipped;pre.Total_finaldata.maxpen;...
pre.Total_finaldata.avg_force;pre.Total_finaldata.max_force;...
pre.Total_finaldata.std_force;pre.Total_finaldata.std_bar_vib...
;pre.Total_finaldata.std_drill_vib;pre.Total_finaldata....
tog_drill;pre.Total_finaldata.mean_roll_drill;...
pre.Total_finaldata.mean_pitch_drill;pre.Total_finaldata....
mean_yaw_drill]);
152 imagesc((pre_finalp))
153 %title('PRE')
154 post.Total_finaldata=Total_finaldata(41:125);
155 figure;Post_finalp=costume_corr([post.Total_finaldata.HoleType;...
post.Total_finaldata.DistancetoMark;post.Total_finaldata....
FinalMajorAxis;post.Total_finaldata.FinalMinorAxis;...
post.Total_finaldata.ID_number;post.Total_finaldata....
Years_in_residency;post.Total_finaldata.Sex;...
post.Total_finaldata.Height;post.Total_finaldata....
How_many_holes; post.Total_finaldata....
days_since_your_last_bone_drilling; post.Total_finaldata....
residency_program_include; post.Total_finaldata....
program_have_dedicated_surgical_skills_training; ...
post.Total_finaldata.PVC; post.Total_finaldata....
have_extensive_0n_surgical_experience;post.Total_finaldata....
RPM_ave_2ndclipped;post.Total_finaldata.maxpen;...
post.Total_finaldata.avg_force;post.Total_finaldata.max_force...
;post.Total_finaldata.std_force;post.Total_finaldata....
std_bar_vib;post.Total_finaldata.std_drill_vib;...
post.Total_finaldata.tog_drill;post.Total_finaldata....
mean_roll_drill;post.Total_finaldata.mean_pitch_drill;...
post.Total_finaldata.mean_yaw_drill]);
156 imagesc((Post_finalp))
157 title('POST')
158 diff_finalp=Post_finalp-pre_finalp;
159 figure
160 imagesc((diff_finalp))
161 title('diff_finalp')
162 %%
163 figure
164 hold on
165 for i=1:125
166     if (i<40)
167         switch Total_finaldata(i).HoleType
168             case 1
169                 plot(Total_finaldata(i).ID_number,Total_finaldata(i)....
DistancetoMark,'c*')
170             case 2
171                 plot(Total_finaldata(i).ID_number,Total_finaldata(i)....
DistancetoMark,'*m')
172             case 3

```

```

173         plot (Total_finaldata(i).ID_number,Total_finaldata(i)....
174             DistancetoMark, 'b*')
175     case 4
176         plot (Total_finaldata(i).ID_number,Total_finaldata(i)....
177             DistancetoMark, 'r*')
178     case 5
179         plot (Total_finaldata(i).ID_number,Total_finaldata(i)....
180             DistancetoMark, 'g*')
181     end
182 else
183     switch Total_finaldata(i).HoleType
184     case 1
185         plot (Total_finaldata(i).ID_number,Total_finaldata(i)....
186             DistancetoMark, '.c')
187     case 2
188         plot (Total_finaldata(i).ID_number,Total_finaldata(i)....
189             DistancetoMark, '.m')
190     case 3
191         plot (Total_finaldata(i).ID_number,Total_finaldata(i)....
192             DistancetoMark, '.b')
193     case 4
194         plot (Total_finaldata(i).ID_number,Total_finaldata(i)....
195             DistancetoMark, '.r')
196     case 5
197         plot (Total_finaldata(i).ID_number,Total_finaldata(i)....
198             DistancetoMark, '.g')
199     end
200 end
201 title('Distanc2marker')
202 im=getframe;
203 imwrite(im.cdata, strcat('Distanc2marker', '.JPG'));
204
205 figure
206 hold on
207 for i=1:125
208     if (i<40)
209         switch Total_finaldata(i).HoleType
210         case 1
211             plot (Total_finaldata(i).ID_number,Total_finaldata(i)....

```

```

212         plot (Total_finaldata(i).ID_number,Total_finaldata(i)....
                FinalMajorAxis,'r*')
213     case 5
214     plot (Total_finaldata(i).ID_number,Total_finaldata(i)....
                FinalMajorAxis,'g*')
215
216     end
217 else
218     switch Total_finaldata(i).HoleType
219     case 1
220     plot (Total_finaldata(i).ID_number,Total_finaldata(i)....
                FinalMajorAxis,'.c')
221     case 2
222     plot (Total_finaldata(i).ID_number,Total_finaldata(i)....
                FinalMajorAxis,'.m')
223     case 3
224     plot (Total_finaldata(i).ID_number,Total_finaldata(i)....
                FinalMajorAxis,'.b')
225     case 4
226     plot (Total_finaldata(i).ID_number,Total_finaldata(i)....
                FinalMajorAxis,'.r')
227     case 5
228     plot (Total_finaldata(i).ID_number,Total_finaldata(i)....
                FinalMajorAxis,'.g')
229
230     end
231 end
232 end
233 title('FinalMajorAxis')
234 im=getframe;
235 imwrite(im.cdata, strcat('FinalMajorAxis','.JPG'));
236
237 figure
238 hold on
239 for i=1:125
240     if (i<40)
241         switch Total_finaldata(i).HoleType
242         case 1
243         plot (Total_finaldata(i).ID_number,Total_finaldata(i)....
                FinalMinorAxis,'c*')
244         case 2
245         plot (Total_finaldata(i).ID_number,Total_finaldata(i)....
                FinalMinorAxis,'m*')
246         case 3
247         plot (Total_finaldata(i).ID_number,Total_finaldata(i)....
                FinalMinorAxis,'b*')
248         case 4
249         plot (Total_finaldata(i).ID_number,Total_finaldata(i)....
                FinalMinorAxis,'r*')
250         case 5

```

```

251         plot (Total_finaldata(i).ID_number,Total_finaldata(i)....
                FinalMinorAxis,'g*')
252
253     end
254 else
255     switch Total_finaldata(i).HoleType
256     case 1
257         plot (Total_finaldata(i).ID_number,Total_finaldata(i)....
                FinalMinorAxis,'.c')
258     case 2
259         plot (Total_finaldata(i).ID_number,Total_finaldata(i)....
                FinalMinorAxis,'.m')
260     case 3
261         plot (Total_finaldata(i).ID_number,Total_finaldata(i)....
                FinalMinorAxis,'.b')
262     case 4
263         plot (Total_finaldata(i).ID_number,Total_finaldata(i)....
                FinalMinorAxis,'.r')
264     case 5
265         plot (Total_finaldata(i).ID_number,Total_finaldata(i)....
                FinalMinorAxis,'.g')
266
267     end
268 end
269 end
270 title('FinalMinorAxis')
271 im=getframe;
272 imwrite(im.cdata, strcat('FinalMinorAxis','.JPG'));
273 figure
274 hold on
275 for i=1:125
276     if (i<40)
277         switch Total_finaldata(i).HoleType
278         case 1
279             plot (Total_finaldata(i).ID_number,Total_finaldata(i)....
                    RPM_ave_2ndclipped,'c*')
280         case 2
281             plot (Total_finaldata(i).ID_number,Total_finaldata(i)....
                    RPM_ave_2ndclipped,'m*')
282         case 3
283             plot (Total_finaldata(i).ID_number,Total_finaldata(i)....
                    RPM_ave_2ndclipped,'b*')
284         case 4
285             plot (Total_finaldata(i).ID_number,Total_finaldata(i)....
                    RPM_ave_2ndclipped,'r*')
286         case 5
287             plot (Total_finaldata(i).ID_number,Total_finaldata(i)....
                    RPM_ave_2ndclipped,'g*')
288
289     end

```

```

290     else
291         switch Total_finaldata(i).HoleType
292             case 1
293                 plot(Total_finaldata(i).ID-number,Total_finaldata(i)....
                     RPM_ave_2ndclipped,'.c')
294             case 2
295                 plot(Total_finaldata(i).ID-number,Total_finaldata(i)....
                     RPM_ave_2ndclipped,'.m')
296             case 3
297                 plot(Total_finaldata(i).ID-number,Total_finaldata(i)....
                     RPM_ave_2ndclipped,'.b')
298             case 4
299                 plot(Total_finaldata(i).ID-number,Total_finaldata(i)....
                     RPM_ave_2ndclipped,'.r')
300             case 5
301                 plot(Total_finaldata(i).ID-number,Total_finaldata(i)....
                     RPM_ave_2ndclipped,'.g')
302
303         end
304     end
305 end
306 title('RPM_ave_2ndclipped')
307 im=getframe;
308 imwrite(im.cdata, strcat('RPM_ave_2ndclipped','.JPG'));
309 figure
310 hold on
311 for i=1:125
312     if (i<40)
313         switch Total_finaldata(i).HoleType
314             case 1
315                 plot(Total_finaldata(i).ID-number,Total_finaldata(i)....
                     maxpen,'c*')
316             case 2
317                 plot(Total_finaldata(i).ID-number,Total_finaldata(i)....
                     maxpen,'m*')
318             case 3
319                 plot(Total_finaldata(i).ID-number,Total_finaldata(i)....
                     maxpen,'b*')
320             case 4
321                 plot(Total_finaldata(i).ID-number,Total_finaldata(i)....
                     maxpen,'r*')
322             case 5
323                 plot(Total_finaldata(i).ID-number,Total_finaldata(i)....
                     maxpen,'g*')
324
325         end
326     else
327         switch Total_finaldata(i).HoleType
328             case 1

```



```

329         plot (Total_finaldata(i).ID_number,Total_finaldata(i)....
            maxpen, '.c')
330     case 2
331     plot (Total_finaldata(i).ID_number,Total_finaldata(i)....
            maxpen, '.m')
332     case 3
333     plot (Total_finaldata(i).ID_number,Total_finaldata(i)....
            maxpen, '.b')
334     case 4
335     plot (Total_finaldata(i).ID_number,Total_finaldata(i)....
            maxpen, '.r')
336     case 5
337     plot (Total_finaldata(i).ID_number,Total_finaldata(i)....
            maxpen, '.g')
338
339     end
340 end
341 end
342 title('maxpen')
343 im=getframe;
344 imwrite(im.cdata, strcat('maxpen', '.JPG'));
345 figure
346 hold on
347 for i=1:125
348     if (i<40)
349         switch Total_finaldata(i).HoleType
350             case 1
351                 plot (Total_finaldata(i).ID_number,Total_finaldata(i)....
                    avg_force, 'c*')
352             case 2
353                 plot (Total_finaldata(i).ID_number,Total_finaldata(i)....
                    avg_force, 'm*')
354             case 3
355                 plot (Total_finaldata(i).ID_number,Total_finaldata(i)....
                    avg_force, 'b*')
356             case 4
357                 plot (Total_finaldata(i).ID_number,Total_finaldata(i)....
                    avg_force, 'r*')
358             case 5
359                 plot (Total_finaldata(i).ID_number,Total_finaldata(i)....
                    avg_force, 'g*')
360
361             end
362         else
363             switch Total_finaldata(i).HoleType
364                 case 1
365                     plot (Total_finaldata(i).ID_number,Total_finaldata(i)....
                        avg_force, '.c')
366                 case 2

```

```

367         plot (Total_finaldata(i).ID_number,Total_finaldata(i)....
          avg_force, 'm')
368     case 3
369     plot (Total_finaldata(i).ID_number,Total_finaldata(i)....
          avg_force, 'b')
370     case 4
371     plot (Total_finaldata(i).ID_number,Total_finaldata(i)....
          avg_force, 'r')
372     case 5
373     plot (Total_finaldata(i).ID_number,Total_finaldata(i)....
          avg_force, 'g')
374
375     end
376 end
377 end
378 title('avg_force')
379 im=getframe;
380 imwrite(im.cdata, strcat('avg_force', '.JPG'));
381 figure
382 hold on
383 for i=1:125
384     if (i<40)
385         switch Total_finaldata(i).HoleType
386             case 1
387                 plot (Total_finaldata(i).ID_number,Total_finaldata(i)....
                    std_bar_vib, 'c*')
388             case 2
389                 plot (Total_finaldata(i).ID_number,Total_finaldata(i)....
                    std_bar_vib, 'm*')
390             case 3
391                 plot (Total_finaldata(i).ID_number,Total_finaldata(i)....
                    std_bar_vib, 'b*')
392             case 4
393                 plot (Total_finaldata(i).ID_number,Total_finaldata(i)....
                    std_bar_vib, 'r*')
394             case 5
395                 plot (Total_finaldata(i).ID_number,Total_finaldata(i)....
                    std_bar_vib, 'g*')
396
397             end
398         else
399             switch Total_finaldata(i).HoleType
400                 case 1
401                     plot (Total_finaldata(i).ID_number,Total_finaldata(i)....
                        std_bar_vib, 'c')
402                 case 2
403                     plot (Total_finaldata(i).ID_number,Total_finaldata(i)....
                        std_bar_vib, 'm')
404                 case 3

```

```

405         plot(Total_finaldata(i).ID_number,Total_finaldata(i)....
               std_bar_vib, '.b')
406     case 4
407         plot(Total_finaldata(i).ID_number,Total_finaldata(i)....
               std_bar_vib, '.r')
408     case 5
409         plot(Total_finaldata(i).ID_number,Total_finaldata(i)....
               std_bar_vib, '.g')
410
411     end
412 end
413 end
414 title('std_bar_vib')
415 im=getframe;
416 imwrite(im.cdata, strcat('std_bar_vib', '.JPG'));
417 figure
418 hold on
419 for i=1:125
420     if (i<40)
421         switch Total_finaldata(i).HoleType
422             case 1
423                 plot(Total_finaldata(i).ID_number,Total_finaldata(i)....
                       mean_roll_drill, 'c*')
424             case 2
425                 plot(Total_finaldata(i).ID_number,Total_finaldata(i)....
                       mean_roll_drill, 'm*')
426             case 3
427                 plot(Total_finaldata(i).ID_number,Total_finaldata(i)....
                       mean_roll_drill, 'b*')
428             case 4
429                 plot(Total_finaldata(i).ID_number,Total_finaldata(i)....
                       mean_roll_drill, 'r*')
430             case 5
431                 plot(Total_finaldata(i).ID_number,Total_finaldata(i)....
                       mean_roll_drill, 'g*')
432
433         end
434     else
435         switch Total_finaldata(i).HoleType
436             case 1
437                 plot(Total_finaldata(i).ID_number,Total_finaldata(i)....
                       mean_roll_drill, '.c')
438             case 2
439                 plot(Total_finaldata(i).ID_number,Total_finaldata(i)....
                       mean_roll_drill, '.m')
440             case 3
441                 plot(Total_finaldata(i).ID_number,Total_finaldata(i)....
                       mean_roll_drill, '.b')
442             case 4

```

```

443         plot (Total_finaldata(i).ID_number,Total_finaldata(i)....
              mean_roll_drill, 'r')
444     case 5
445     plot (Total_finaldata(i).ID_number,Total_finaldata(i)....
              mean_roll_drill, 'g')
446
447     end
448 end
449 end
450 title('mean_roll_drill')
451 im=getframe;
452 imwrite(im.cdata, strcat('mean_roll_drill', '.JPG'));
453
454 %%
455 figure
456 hold on
457 for i=1:125
458     if (i<40)
459         switch Total_finaldata(i).HoleType
460             case 1
461                 plot (Total_finaldata(i).HoleType,Total_finaldata(i)....
462                     DistancetoMark, 'c*')
463             case 2
464                 plot (Total_finaldata(i).HoleType,Total_finaldata(i)....
465                     DistancetoMark, 'm*')
466             case 3
467                 plot (Total_finaldata(i).HoleType,Total_finaldata(i)....
468                     DistancetoMark, 'b*')
469             case 4
470                 plot (Total_finaldata(i).HoleType,Total_finaldata(i)....
471                     DistancetoMark, 'r*')
472             case 5
473                 plot (Total_finaldata(i).HoleType,Total_finaldata(i)....
474                     DistancetoMark, 'g*')
475
476         end
477     else
478         switch Total_finaldata(i).HoleType
479             case 1
480                 plot (Total_finaldata(i).HoleType+5,Total_finaldata(i)...
481                     .DistancetoMark, 'c')
482             case 2
483                 plot (Total_finaldata(i).HoleType+5,Total_finaldata(i)...
484                     .DistancetoMark, 'm')
485             case 3
486                 plot (Total_finaldata(i).HoleType+5,Total_finaldata(i)...
487                     .DistancetoMark, 'b')
488             case 4

```

```

482         plot (Total_finaldata(i).HoleType+5,Total_finaldata(i)...
483             .DistancetoMark, 'r')
484     case 5
485         plot (Total_finaldata(i).HoleType+5,Total_finaldata(i)...
486             .DistancetoMark, 'g')
487     end
488 end
489 title('Distanc2marker')
490 im=getframe;
491 imwrite(im.cdata, strcat('Distanc2marker+5', '.JPG'));
492
493 figure
494 hold on
495 for i=1:125
496     if (i<40)
497         switch Total_finaldata(i).HoleType
498             case 1
499                 plot (Total_finaldata(i).HoleType,Total_finaldata(i)...
500                     FinalMajorAxis, 'c*')
501             case 2
502                 plot (Total_finaldata(i).HoleType,Total_finaldata(i)...
503                     FinalMajorAxis, 'm*')
504             case 3
505                 plot (Total_finaldata(i).HoleType,Total_finaldata(i)...
506                     FinalMajorAxis, 'b*')
507             case 4
508                 plot (Total_finaldata(i).HoleType,Total_finaldata(i)...
509                     FinalMajorAxis, 'r*')
510             case 5
511                 plot (Total_finaldata(i).HoleType,Total_finaldata(i)...
512                     FinalMajorAxis, 'g*')
513         end
514     else
515         switch Total_finaldata(i).HoleType
516             case 1
517                 plot (Total_finaldata(i).HoleType+5,Total_finaldata(i)...
518                     .FinalMajorAxis, '.c')
519             case 2
520                 plot (Total_finaldata(i).HoleType+5,Total_finaldata(i)...
521                     .FinalMajorAxis, '.m')
522             case 3
523                 plot (Total_finaldata(i).HoleType+5,Total_finaldata(i)...
524                     .FinalMajorAxis, '.b')
525             case 4
526                 plot (Total_finaldata(i).HoleType+5,Total_finaldata(i)...
527                     .FinalMajorAxis, '.r')
528             case 5

```

```

521         plot (Total_finaldata(i).HoleType+5,Total_finaldata(i)...
               .FinalMajorAxis, 'g')
522
523     end
524 end
525 end
526 title('FinalMajorAxis')
527 im=getframe;
528 imwrite(im.cdata, strcat('FinalMajorAxis+5', '.JPG'));
529
530 figure
531 hold on
532 for i=1:125
533     if (i<40)
534         switch Total_finaldata(i).HoleType
535             case 1
536                 plot (Total_finaldata(i).HoleType,Total_finaldata(i)...
                       FinalMinorAxis, 'c*')
537             case 2
538                 plot (Total_finaldata(i).HoleType,Total_finaldata(i)...
                       FinalMinorAxis, 'm*')
539             case 3
540                 plot (Total_finaldata(i).HoleType,Total_finaldata(i)...
                       FinalMinorAxis, 'b*')
541             case 4
542                 plot (Total_finaldata(i).HoleType,Total_finaldata(i)...
                       FinalMinorAxis, 'r*')
543             case 5
544                 plot (Total_finaldata(i).HoleType,Total_finaldata(i)...
                       FinalMinorAxis, 'g*')
545
546         end
547     else
548         switch Total_finaldata(i).HoleType
549             case 1
550                 plot (Total_finaldata(i).HoleType+5,Total_finaldata(i)...
                       .FinalMinorAxis, '.c')
551             case 2
552                 plot (Total_finaldata(i).HoleType+5,Total_finaldata(i)...
                       .FinalMinorAxis, '.m')
553             case 3
554                 plot (Total_finaldata(i).HoleType+5,Total_finaldata(i)...
                       .FinalMinorAxis, '.b')
555             case 4
556                 plot (Total_finaldata(i).HoleType+5,Total_finaldata(i)...
                       .FinalMinorAxis, '.r')
557             case 5
558                 plot (Total_finaldata(i).HoleType+5,Total_finaldata(i)...
                       .FinalMinorAxis, '.g')
559

```

```

560         end
561     end
562 end
563 title('FinalMinorAxis')
564 im=getframe;
565 imwrite(im.cdata, strcat('FinalMinorAxis+5', '.JPG'));
566 figure
567 hold on
568 for i=1:125
569     if (i<40)
570         switch Total_finaldata(i).HoleType
571             case 1
572                 plot(Total_finaldata(i).HoleType, Total_finaldata(i)...
573                     RPM_ave_2ndclipped, 'c*')
574             case 2
575                 plot(Total_finaldata(i).HoleType, Total_finaldata(i)...
576                     RPM_ave_2ndclipped, 'm*')
577             case 3
578                 plot(Total_finaldata(i).HoleType, Total_finaldata(i)...
579                     RPM_ave_2ndclipped, 'b*')
580             case 4
581                 plot(Total_finaldata(i).HoleType, Total_finaldata(i)...
582                     RPM_ave_2ndclipped, 'r*')
583             case 5
584                 plot(Total_finaldata(i).HoleType, Total_finaldata(i)...
585                     RPM_ave_2ndclipped, 'g*')
586         end
587     else
588         switch Total_finaldata(i).HoleType
589             case 1
590                 plot(Total_finaldata(i).HoleType+5, Total_finaldata(i)...
591                     .RPM_ave_2ndclipped, '.c')
592             case 2
593                 plot(Total_finaldata(i).HoleType+5, Total_finaldata(i)...
594                     .RPM_ave_2ndclipped, '.m')
595             case 3
596                 plot(Total_finaldata(i).HoleType+5, Total_finaldata(i)...
597                     .RPM_ave_2ndclipped, '.b')
598             case 4
599                 plot(Total_finaldata(i).HoleType+5, Total_finaldata(i)...
600                     .RPM_ave_2ndclipped, '.r')
601             case 5
602                 plot(Total_finaldata(i).HoleType+5, Total_finaldata(i)...
603                     .RPM_ave_2ndclipped, '.g')
604         end
605     end
606 end
607 title('RPM_ave_2ndclipped')

```

```

600 im=getframe;
601 imwrite(im.cdata, strcat('RPM_ave_2ndclipped+5', '.JPG'));
602 figure
603 hold on
604 for i=1:125
605     if (i<40)
606         switch Total_finaldata(i).HoleType
607             case 1
608                 plot(Total_finaldata(i).HoleType, Total_finaldata(i)...
609                     maxpen, 'c*')
610             case 2
611                 plot(Total_finaldata(i).HoleType, Total_finaldata(i)...
612                     maxpen, 'm*')
613             case 3
614                 plot(Total_finaldata(i).HoleType, Total_finaldata(i)...
615                     maxpen, 'b*')
616             case 4
617                 plot(Total_finaldata(i).HoleType, Total_finaldata(i)...
618                     maxpen, 'r*')
619             case 5
620                 plot(Total_finaldata(i).HoleType, Total_finaldata(i)...
621                     maxpen, 'g*')
622         end
623     else
624         switch Total_finaldata(i).HoleType
625             case 1
626                 plot(Total_finaldata(i).HoleType+5, Total_finaldata(i)...
627                     .maxpen, '.c')
628             case 2
629                 plot(Total_finaldata(i).HoleType+5, Total_finaldata(i)...
630                     .maxpen, '.m')
631             case 3
632                 plot(Total_finaldata(i).HoleType+5, Total_finaldata(i)...
633                     .maxpen, '.b')
634             case 4
635                 plot(Total_finaldata(i).HoleType+5, Total_finaldata(i)...
636                     .maxpen, '.r')
637             case 5
638                 plot(Total_finaldata(i).HoleType+5, Total_finaldata(i)...
639                     .maxpen, '.g')
640         end
641     end
642 end
643 title('maxpen')
644 im=getframe;
645 imwrite(im.cdata, strcat('maxpen+5', '.JPG'));
646 figure
647 hold on

```



```

640 for i=1:125
641     if (i<40)
642         switch Total_finaldata(i).HoleType
643             case 1
644                 plot(Total_finaldata(i).HoleType,Total_finaldata(i)...
645                     avg_force,'c*')
646             case 2
647                 plot(Total_finaldata(i).HoleType,Total_finaldata(i)...
648                     avg_force,'m*')
649             case 3
650                 plot(Total_finaldata(i).HoleType,Total_finaldata(i)...
651                     avg_force,'b*')
652             case 4
653                 plot(Total_finaldata(i).HoleType,Total_finaldata(i)...
654                     avg_force,'r*')
655             case 5
656                 plot(Total_finaldata(i).HoleType,Total_finaldata(i)...
657                     avg_force,'g*')
658         end
659     else
660         switch Total_finaldata(i).HoleType
661             case 1
662                 plot(Total_finaldata(i).HoleType+5,Total_finaldata(i)...
663                     .avg_force,'.c')
664             case 2
665                 plot(Total_finaldata(i).HoleType+5,Total_finaldata(i)...
666                     .avg_force,'.m')
667             case 3
668                 plot(Total_finaldata(i).HoleType+5,Total_finaldata(i)...
669                     .avg_force,'.b')
670             case 4
671                 plot(Total_finaldata(i).HoleType+5,Total_finaldata(i)...
672                     .avg_force,'.r')
673             case 5
674                 plot(Total_finaldata(i).HoleType+5,Total_finaldata(i)...
675                     .avg_force,'.g')
676         end
677     end
678 end
679 title('avg_force')
680 im=getframe;
681 imwrite(im.cdata, strcat('avg_force+5','JPG'));
682 figure
683 hold on
684 for i=1:125
685     if (i<40)
686         switch Total_finaldata(i).HoleType
687             case 1

```

```

680         plot (Total_finaldata(i).HoleType,Total_finaldata(i)...
681             std_bar_vib,'c*')
682     case 2
683         plot (Total_finaldata(i).HoleType,Total_finaldata(i)...
684             std_bar_vib,'m*')
685     case 3
686         plot (Total_finaldata(i).HoleType,Total_finaldata(i)...
687             std_bar_vib,'b*')
688     case 4
689         plot (Total_finaldata(i).HoleType,Total_finaldata(i)...
690             std_bar_vib,'r*')
691     case 5
692         plot (Total_finaldata(i).HoleType,Total_finaldata(i)...
693             std_bar_vib,'g*')
694
695     end
696 else
697     switch Total_finaldata(i).HoleType
698     case 1
699         plot (Total_finaldata(i).HoleType+5,Total_finaldata(i)...
700             .std_bar_vib,'.c')
701     case 2
702         plot (Total_finaldata(i).HoleType+5,Total_finaldata(i)...
703             .std_bar_vib,'.m')
704     case 3
705         plot (Total_finaldata(i).HoleType+5,Total_finaldata(i)...
706             .std_bar_vib,'.b')
707     case 4
708         plot (Total_finaldata(i).HoleType+5,Total_finaldata(i)...
709             .std_bar_vib,'.r')
710     case 5
711         plot (Total_finaldata(i).HoleType+5,Total_finaldata(i)...
712             .std_bar_vib,'.g')
713
714     end
715 end
716 title('std_bar_vib')
717 im=getframe;
718 imwrite(im.cdata, strcat('std_bar_vib+5','JPG'));
719 figure
720 hold on
721 for i=1:125
722     if (i<40)
723         switch Total_finaldata(i).HoleType
724         case 1
725             plot (Total_finaldata(i).HoleType,Total_finaldata(i)...
726                 mean_roll_drill,'c*')
727         case 2

```

```

718         plot (Total_finaldata(i).HoleType,Total_finaldata(i)...
              mean_roll_drill,'m*')
719     case 3
720     plot (Total_finaldata(i).HoleType,Total_finaldata(i)...
              mean_roll_drill,'b*')
721     case 4
722     plot (Total_finaldata(i).HoleType,Total_finaldata(i)...
              mean_roll_drill,'r*')
723     case 5
724     plot (Total_finaldata(i).HoleType,Total_finaldata(i)...
              mean_roll_drill,'g*')
725
726     end
727 else
728     switch Total_finaldata(i).HoleType
729     case 1
730     plot (Total_finaldata(i).HoleType+5,Total_finaldata(i)...
              .mean_roll_drill,'.c')
731     case 2
732     plot (Total_finaldata(i).HoleType+5,Total_finaldata(i)...
              .mean_roll_drill,'.m')
733     case 3
734     plot (Total_finaldata(i).HoleType+5,Total_finaldata(i)...
              .mean_roll_drill,'.b')
735     case 4
736     plot (Total_finaldata(i).HoleType+5,Total_finaldata(i)...
              .mean_roll_drill,'.r')
737     case 5
738     plot (Total_finaldata(i).HoleType+5,Total_finaldata(i)...
              .mean_roll_drill,'.g')
739
740     end
741 end
742 end
743 title('mean_roll_drill')
744 im=getframe;
745 imwrite(im.cdata, strcat('mean_roll_drill+5','JPG'));
746 %%
747 pullout=[1:51; 2447 1809 2122 2447 2447 2876 2695 2780 2366 3075 ...
            2409 2765 2568 2945 2932 nan 2423 2887 3398 2376 2371 2839 ...
            2715 2428 2145 2075 3089 3204 2626 2851 2525 2362 2787 2714 ...
            2497 3096 2209 3185 2613 2985 3032 2825 1937 3528 2623 3409 ...
            2933 2439 3341 3343 2905]';
748 plot (pullout(:,1),pullout(:,2),'.')
749 ii=1;
750 for i=1:125
751     if (Total_finaldata(i).HoleType==3)
752         PulloutTotal_finaldata(ii)=Total_finaldata(i);
753         PulloutTotal_finaldata(ii).HoleType=3;
754         ii=ii+1;

```

```

755     end
756 end
757 %%
758 %%
759 figure
760 finalp=costume_corr([Total_finaldata.HoleType;Total_finaldata....
    DistancetoMark;Total_finaldata.FinalMajorAxis;Total_finaldata....
    .FinalMinorAxis;Total_finaldata.ID-number;Total_finaldata....
    Years_in_residency;Total_finaldata.Sex;Total_finaldata....
    Height;Total_finaldata.How_many_holes; Total_finaldata....
    days_since_your_last_bone_drilling; Total_finaldata....
    residency_program_include; Total_finaldata....
    program_have_dedicated_surgical_skills_training; ...
    Total_finaldata.PVC; Total_finaldata....
    have_extensive_0n_surgical_experience;Total_finaldata....
    RPM_ave_2ndcliped;Total_finaldata.maxpen;Total_finaldata....
    avg_force;Total_finaldata.max_force;Total_finaldata.std_force...
    ;Total_finaldata.std_bar_vib;Total_finaldata.std_drill_vib;...
    Total_finaldata.tog_drill;Total_finaldata.mean_roll_drill;...
    Total_finaldata.mean_pitch_drill;Total_finaldata....
    mean_yaw_drill]);
761 imagesc((finalp)) %plot the
762 % 1-Total_finaldata.HoleType;
763 % 2-Total_finaldata.DistancetoMark;
764 % 3-Total_finaldata.FinalMajorAxis;
765 % 4-Total_finaldata.FinalMinorAxis;
766 % 5-Total_finaldata.ID-number;
767 % 6-Total_finaldata.Years_in_residency;
768 % 7-Total_finaldata.Sex;
769 % 8-Total_finaldata.Height;
770 % 9-Total_finaldata.How_many_holes;
771 % 10-Total_finaldata.days_since_your_last_bone_drilling;
772 % 11-Total_finaldata.residency_program_include;
773 % 12-Total_finaldata....
    program_have_dedicated_surgical_skills_training;
774 % 13-Total_finaldata.PVC;
775 % 14-Total_finaldata.have_extensive_0n_surgical_experience;
776 % 15-Total_finaldata.RPM_ave_2ndcliped;
777 % 16-Total_finaldata.maxpen;
778 % 17-Total_finaldata.avg_force;
779 % 18-Total_finaldata.max_force;
780 % 19-Total_finaldata.std_force;
781 % 20-Total_finaldata.std_bar_vib;
782 % 21-Total_finaldata.std_drill_vib;
783 % 22-Total_finaldata.tog_drill;
784 % 23-Total_finaldata.mean_roll_drill;
785 % 24-Total_finaldata.mean_pitch_drill;
786 % 25-Total_finaldata.mean_yaw_drill;
787
788 %%

```

```

789 figure
790 for i=1:length(PulloutTotal_finaldata)
791     PulloutTotal_finaldata(i).ID_number
792     PulloutTotal_finaldata(i).Pullout=pullout(...
        PulloutTotal_finaldata(i).ID_number,2);
793 end
794 %PulloutTotal_finaldata.HoleType;
795 finalp=costume_corr([PulloutTotal_finaldata.DistancetoMark;...
    PulloutTotal_finaldata.FinalMajorAxis;PulloutTotal_finaldata....
    FinalMinorAxis;PulloutTotal_finaldata.ID_number;...
    PulloutTotal_finaldata.Years_in_residency;...
    PulloutTotal_finaldata.Sex;PulloutTotal_finaldata.Height;...
    PulloutTotal_finaldata.How_many_holes; PulloutTotal_finaldata...
    .days_since_your_last_bone_drilling; PulloutTotal_finaldata....
    residency_program_include; PulloutTotal_finaldata....
    program_have_dedicated_surgical_skills_training; ...
    PulloutTotal_finaldata.PVC; PulloutTotal_finaldata....
    have_extensive_On_surgical_experience;PulloutTotal_finaldata....
    RPM_ave_2ndclipped;PulloutTotal_finaldata.maxpen;...
    PulloutTotal_finaldata.avg_force;PulloutTotal_finaldata....
    max_force;PulloutTotal_finaldata.std_force;...
    PulloutTotal_finaldata.std_bar_vib;PulloutTotal_finaldata....
    std_drill_vib;PulloutTotal_finaldata.tog_drill;...
    PulloutTotal_finaldata.mean_roll_drill;PulloutTotal_finaldata...
    .mean_pitch_drill;PulloutTotal_finaldata.mean_yaw_drill;...
    PulloutTotal_finaldata.Pullout]);
796 imagesc((finalp))
797 im=getframe;
798 imwrite(im.cdata, strcat('COV_with_pull_out','.JPG'));

```

B.1.4 Data fitter function

```

1 function [a]=data_fit(lavbiefile,hapticfile)
2 [dataLV_A,H,MIN,SEC]=Labview2var(lavbiefile);
3 haptic_A=csvread(hapticfile);
4 %%
5 [dataLV_A(:,2)]=Low_filter_force(dataLV_A(:,2));
6 dataLV_A(:,2)=5601.7*dataLV_A(:,2)+6208.7;
7 figure;plot(dataLV_A(:,1),dataLV_A(:,2));
8 haptic_A(:,3)=str2num(H);
9 haptic_A(:,7)=haptic_A(:,3)*3600+haptic_A(:,4)*60+haptic_A(:,5)+...
    haptic_A(:,6)*0.001;
10 hold on; plot(haptic_A(:,7),haptic_A(:,1)*10,'r');plot(haptic_A...
    (:,7),haptic_A(:,2)*10000,'g')
11 %%
12 clip_A=[6.398e+04 1.464e+05];

```

```

13 [OUTPUT]=syncer(dataLV_A,haptic_A,clip_A);
14 figure
15 sf = fit([OUTPUT(:,1), OUTPUT(:,2)],OUTPUT(:,3),'poly23')
16 plot(sf,[OUTPUT(:,1), OUTPUT(:,2)],OUTPUT(:,3))
17 a=1;
18 end

```

B.1.5 Row data adder function

```

1 clc
2 clear all
3 %[data_lv,h_lv,min_lv,sec_lv]=Dataanalyze('test.lvm');
4 %data_lv(:,1)=data_lv(:,1)+str2num(sec_lv)+str2num(min_lv)*60+...
   str2num(h_lv)*3600;
5 data_omni=csvread('2.txt');
6 %data_omni(:,10)=12;
7 data_omni(:,17)=data_omni(:,13)/1000+data_omni(:,12)+data_omni...
   (:,11)*60+data_omni(:,10)*3600;
8 for q=1:length(data_omni)
9     [x,y,z]=trans_omni([data_omni(q,10),data_omni(q,11),data_omni...
   (q,12)],[data_omni(q,1),data_omni(q,2),data_omni(q,3)],[...
   data_omni(q,7),data_omni(q,8),data_omni(q,9)],[-174 -81 ...
   0]);
10    Location_drill(q,1)=x;Location_drill(q,2)=y;Location_drill(q...
   ,3)=z;
11 end
12 plot3(Location_drill(:,1),Location_drill(:,2),Location_drill(:,3)...
   )
13 grid on
14 axis equal

```

B.1.6 General analyzer function

```

1 function [dataLV,H,MIN,SEC]=LTFO(filename)
2 fileID = fopen(filename);
3 fid=fileID;
4 C = textscan(fileID,'%s %s');
5 Timeloc=11;
6 data_start=30;
7 com=strfind(C{1,1}{Timeloc,1},',');
8 colo=strfind(C{1,1}{Timeloc,1},':');
9 H= C{1,1}{Timeloc,1}((com+1):(colo(1,1)-1));

```

```

10 MIN= C{1,1}{Timeloc,1}((colo(1,1)+1):(colo(1,2)-1));
11 SEC= C{1,1}{Timeloc,1}((colo(1,2)+1):(colo(1,2)+8));
12 fid=fopen(filename);
13 fid2=fopen('newfile.txt','wt');
14 id=0;
15 a=fgets(fid);
16 while(ischar(a))
17     id=id+1;
18     if id<24
19         a=fgets(fid);
20         continue
21     else
22         fprintf(fid2,a);
23     end
24     a=fgets(fid);
25 end
26 dataLV=csvread('newfile.txt');

```

B.1.7 Low pass filter function 1

```

1 d = designfilt('lowpassfir');
2 y = filtfilt(d,data);
3 y1 = filter(d,data);
4 subplot(2,1,1)
5 plot([y y1])
6 title('Filtered Waveforms')
7 legend('Zero-phase Filtering','Conventional Filtering')
8
9 subplot(2,1,2)
10 plot(data)
11 title('Original Waveform')

```

B.1.8 Main file 2

```

1 clc
2 clear all
3 %List of data files to import:
4 list=['R54 ','R53 ','R52 ','R43P','R43 ','R42P','R42 ','R41P';'...
      R41 ','R2P3','R2P2','R2P1','R23 ','R22 ','R21 ','R13P','R13 ','...
      'R12P','R12 ','R11P','R11 ','MS43'];
5 List=cellstr(list);
6 Points=[96344 119417 120446 1;

```

```

7         96297 126726 127559 2;
8         121617 138161 138161 3;
9         66880 123987 124686 4;
10        65301 150367 152001 5;
11        84015 137039 139502 6;
12        99682 162385 164541 7;
13        112468 167029 168706 8;
14        65276 122882 133961 9;
15        57996 101332 104183 10;
16        102031 113035 113617 11;
17        65935 99735 100861 12;
18        105174 123514 124200 13;
19        57503 67468 70365 14;
20        67010 88523 89537 15;
21        111229 129450 130126 16;
22        87093 126329 142184 17;
23        75894 116583 117238 18;
24        75426 105250 106975 19;
25        86157 121960 122882 20;
26        104253 151079 153191 21;
27        83437 103411 105106 22];
28 for i=1:length(list);
29     data(i).name = char(List(i,1));
30     data(i).test = Points(i,:);
31     [data(i).NI,h_lv,min_lv,sec_lv]=Dataanalyze(strcat(char(List(...
32         i,1)),'.lvm'));
33     data(i).NI(:,1)=data(i).NI(:,1)+str2num(sec_lv)+str2num(...
34         min_lv)*60+str2num(h_lv)*3600;
35     data(i).Omni=csvread(strcat(char(List(i,1)),'.txt'));
36     data(i).Omni(:,17)=data(i).Omni(:,13)/1000+data(i).Omni(:,12)...
37         +data(i).Omni(:,11)*60+data(i).Omni(:,10)*3600;
38     for q=1:length(data(i).Omni)
39         [x,y,z]=trans_omni([data(i).Omni(q,10),data(i).Omni(q,11)...
40             ,data(i).Omni(q,12)], [data(i).Omni(q,1),data(i).Omni(...
41                 q,2),data(i).Omni(q,3)], [data(i).Omni(q,7),data(i)...
42                     Omni(q,8),data(i).Omni(q,9)], [-174 -81 0]);
43         data(i).Location(q,1)=x;data(i).Location(q,2)=y;data(i)...
44             Location(q,3)=z;
45     end
46     data(i).Holelength=((data(i).Location(Points(i,1),1)-data(i)...
47         Location(Points(i,2),1))^2+(data(i).Location(Points(i,1)...
48             ,2)-data(i).Location(Points(i,2),2))^2 +(data(i).Location...
49                 (Points(i,1),3)-data(i).Location(Points(i,2),3))^2)^.5;
50     data(i).Overpenetrationlength=((data(i).Location(Points(i,2)...
51         ,1)-data(i).Location(Points(i,3),1))^2+(data(i).Location(...
52             Points(i,2),2)-data(i).Location(Points(i,3),2))^2 +(data(...
53                 i).Location(Points(i,2),3)-data(i).Location(Points(i,3)...
54                     ,3))^2)^.5;
55     for num=Points(i,1):Points(i,2)

```



```

42         data(i).Penetrationspeed(num-Points(i,1)+1)=(data(i).Omni...
            (num,4)^2+data(i).Omni(num,5)^2+data(i).Omni(num,6)...
            ^2)^.5;
43     end
44     data(i).MaxPenetrationspeed=max(abs(data(i).Penetrationspeed...
        ));
45     data(i).MinPenetrationspeed=min(abs(data(i).Penetrationspeed...
        ));
46 end

```

B.1.9 File loader (Customized Matlab generated code)

```

1 function [BoneLettering,InitialMajorAxisBoneplane,...
    InitialMinorAxisPerpendiculartoBone,FinalMajorAxis,...
    FinalMinorAxis,DistancetoMark,NOTE] = importfile(workbookFile...
    ,sheetName,startRow,endRow)
2 %IMPORTFILE Import data from a spreadsheet
3 % [BoneLettering,InitialMajorAxisBoneplane,...
    InitialMinorAxisPerpendiculartoBone,FinalMajorAxis,...
    FinalMinorAxis,DistancetoMark,NOTE]
4 % = IMPORTFILE(FILE) reads data from the first worksheet in the...
    Microsoft
5 % Excel spreadsheet file named FILE and returns the data as ...
    column
6 % vectors.
7 %
8 % [BoneLettering,InitialMajorAxisBoneplane,...
    InitialMinorAxisPerpendiculartoBone,FinalMajorAxis,...
    FinalMinorAxis,DistancetoMark,NOTE]
9 % = IMPORTFILE(FILE,SHEET) reads from the specified worksheet.
10 %
11 % [BoneLettering,InitialMajorAxisBoneplane,...
    InitialMinorAxisPerpendiculartoBone,FinalMajorAxis,...
    FinalMinorAxis,DistancetoMark,NOTE]
12 % = IMPORTFILE(FILE,SHEET,STARTROW,ENDROW) reads from the ...
    specified
13 % worksheet for the specified row interval(s). Specify STARTROW...
    and
14 % ENDROW as a pair of scalars or vectors of matching size for
15 % dis-contiguous row intervals. To read to the end of the file ...
    specify an
16 % ENDROW of inf.%
17 % Example:
18 % [BoneLettering,InitialMajorAxisBoneplane,...
    InitialMinorAxisPerpendiculartoBone,FinalMajorAxis,...
    FinalMinorAxis,DistancetoMark,NOTE] = importfile('SWOTA BONE ...
    TABLE - OFFICE (1).xls','Sheet1',2,256);

```

```

19 %
20 % See also XLSREAD.
21
22 % Auto-generated by MATLAB on 2015/07/08 12:32:21
23
24 %% Input handling
25
26 % If no sheet is specified, read first sheet
27 if nargin == 1 || isempty(sheetName)
28     sheetName = 1;
29 end
30
31 % If row start and end points are not specified, define defaults
32 if nargin ≤ 3
33     startRow = 2;
34     endRow = 256;
35 end
36
37 %% Import the data
38 [~, ~, raw] = xlsread(workbookFile, sheetName, sprintf('A%d:G%d', ...
    startRow(1), endRow(1)));
39 for block=2:length(startRow)
40     [~, ~, tmpRowBlock] = xlsread(workbookFile, sheetName, ...
    sprintf('A%d:G%d', startRow(block), endRow(block)));
41     raw = [raw; tmpRowBlock]; %#ok<AGROW>
42 end
43 raw(cellfun(@(x) ~isempty(x) && isnumeric(x) && isnan(x), raw)) = ...
    {' '});
44 cellVectors = raw(:, [1, 7]);
45 raw = raw(:, [2, 3, 4, 5, 6]);
46
47 %% Create output variable
48 I = cellfun(@(x) ischar(x), raw);
49 raw(I) = {NaN};
50 data = reshape([raw{:}], size(raw));
51
52 %% Allocate imported array to column variable names
53 BoneLettering = cellVectors(:, 1);
54 InitialMajorAxisBoneplane = data(:, 1);
55 InitialMinorAxisPerpendiculartoBone = data(:, 2);
56 FinalMajorAxis = data(:, 3);
57 FinalMinorAxis = data(:, 4);
58 DistancetoMark = data(:, 5);
59 NOTE = cellVectors(:, 2);

```

B.1.10 List loader

```

1 %% Import data from spreadsheet
2 % Script for importing data from the following spreadsheet:
3 %
4 %     Workbook: C:\Users\Ashkan\Google Drive\Code\Matlab\Bone ...
        drilling project\General\SWOTA BONE TABLE - OFFICE (1).xls
5 %     Worksheet: Sheet1
6 %
7 % To extend the code for use with different selected data or a ...
        different
8 % spreadsheet, generate a function instead of a script.
9
10 % Auto-generated by MATLAB on 2015/07/08 12:37:04
11
12 %% Import the data
13 [~, ~, raw] = xlsread('C:\Users\Ashkan\Google Drive\Code\Matlab\...
        Bone drilling project\General\SWOTA BONE TABLE - OFFICE (1)....
        xls', 'Sheet1');
14 raw(cellfun(@(x) ~isempty(x) && isnumeric(x) && isnan(x), raw)) = ...
        {' '};
15 cellVectors = raw(:, [1, 7, 8, 9]);
16 raw = raw(:, [2, 3, 4, 5, 6]);
17
18 %% Replace non-numeric cells with NaN
19 R = cellfun(@(x) ~isnumeric(x) && ~islogical(x), raw); % Find non-...
        numeric cells
20 raw(R) = {NaN}; % Replace non-numeric cells
21
22 %% Create output variable
23 data = reshape([raw{:}], size(raw));
24
25 %% Allocate imported array to column variable names
26 BoneLettering = cellVectors(:, 1);
27 InitialMajorAxisBoneplane = data(:, 1);
28 InitialMinorAxisPerpendiculartoBone = data(:, 2);
29 FinalMajorAxis = data(:, 3);
30 FinalMinorAxis = data(:, 4);
31 DistancetoMark = data(:, 5);
32 NOTE = cellVectors(:, 2);
33 VarName8 = cellVectors(:, 3);
34 VarName9 = cellVectors(:, 4);
35
36 %% Clear temporary variables
37 clearvars data raw cellVectors R;

```

B.1.11 Low pass filter function 2

```

1 function [y]=Low_filter_force(data)
2 rng default;
3 %x=data(:,4); %noisy waveform
4 x=data;
5 h=fdesign.lowpass('Fp,Fst,Ap,Ast',0.15,0.2,1,60);
6 d=design(h,'equiripple'); %Lowpass FIR filter
7 h=fdesign.lowpass('N,F3dB',12,0.0003);
8 d1 = design(h,'butter');
9 y = filtfilt(d1.sosMatrix,d1.ScaleValues,x);
10 %plot(x,'b-.'); hold on;
11 %plot(y,'r','linewidth',3);

```

B.1.12 Labview oppener

```

1 function [dataLV,H,MIN,SEC]=LTFO(filename)
2 fileID = fopen(filename);
3 fid=fileID;
4 C = textscan(fileID,'%s %s');
5 Timeloc=11;
6 data.start=30;
7 com=strfind(C{1,1}{Timeloc,1},',');
8 colo=strfind(C{1,1}{Timeloc,1},':');
9 H= C{1,1}{Timeloc,1}((com+1):(colo(1,1)-1));
10 MIN= C{1,1}{Timeloc,1}((colo(1,1)+1):(colo(1,2)-1));
11 SEC= C{1,1}{Timeloc,1}((colo(1,2)+1):(colo(1,2)+8));
12 fid=fopen(filename);
13 fid2=fopen('newfile.txt','wt');
14 id=0;
15 a=fgets(fid);
16 while(ischar(a))
17     id=id+1;
18     if id<24
19         a=fgets(fid);
20         continue
21     else
22         fprintf(fid2,a);
23     end
24     a=fgets(fid);
25 end
26 dataLV=csvread('newfile.txt');

```

B.1.13 Nan available correlation function

```

1 function r = nancorrcoef(x,y)
2 %NANCCORRcoef - Compute Pearson's correlation for input vectors ...
   that contain NaN values
3 %
4 %Syntax:  r = nancorrcoef(x,y);
5 %
6 %Inputs: X - First input vector
7 %         Y - Second input vector
8 %
9 %Output: R - Correlation coefficient
10 %          (Note: R is a scalar, not a 2 x 2
11 %               matrix as in CORRCOEf)
12 %
13 %Example: x = randn(20,1); y = randn(20,1);
14 %         r = nancorrcoef(x,y);
15 %
16 %Other m-files required: none
17 %Subfunctions: none
18 %mat-files required: none
19 %
20 %See also: CORRCOEf
21
22 %Author: Denis Gilbert, Ph.D., physical oceanography
23 %Maurice Lamontagne Institute, Dept. of Fisheries and Oceans ...
   Canada
24 %email: gilbertd@dfo-mpo.gc.ca Web: http://www.qc.dfo-mpo.gc.ca/...
   iml/
25 %September 2001; Last revision: 13-Sep-2001 by D. Gilbert
26
27 %Check number of input vectors
28 if nargin ≠ 2
29     error('Two input vectors are required');
30 end
31
32 %Conditions that must be satisfied to continue the calculations
33 if size(x) ≠ size(y)
34     error('Dimensions of input vectors must be the same !!!');
35 elseif (sum(isnan(x))/length(x)) > 0.20 | (sum(isnan(y))/length(y...
   )) > 0.20
36     disp('Input vectors have more than 20% NaN values...')
37     disp('Verify if you could eliminate a few NaNs')
38     disp('by interpolation or some other method')
39     error('Too many NaNs, processing stopped !!!');
40 elseif (sum(isnan(x))/length(x)) > 0.05 | (sum(isnan(y))/length(y...
   )) > 0.05
41     warning('Vectors have more than 5% NaN values, results may be...
   inaccurate !!!')
42 end
43
44 %Only keep the common valid values in both input vectors

```

```

45 tf = ~isnan(x) & ~isnan(y); %Logical flag
46 x = x(tf); y = y(tf);
47
48 meanx = mean(x); %Compute mean value of X
49 meany = mean(y); %Compute mean value of Y
50
51 %Compute the arguments that go into the mathematical formula of R
52 sx2 = sum((x-meanx).^2);
53 sy2 = sum((y-meany).^2);
54 sxy = sum((x-meanx).*(y-meany));
55
56 % Mathematical definition of Pearson's product moment correlation...
    coefficient
57 r = sxy./sqrt(sx2*sy2);

```

B.1.14 Omni data cutter

```

1  clc
2  clear all
3  %[data_lv,h_lv,min_lv,sec_lv]=Dataanalyze('test.lvm');
4  %data_lv(:,1)=data_lv(:,1)+str2num(sec_lv)+str2num(min_lv)*60+...
    str2num(h_lv)*3600;
5  data_omni=csvread('R54.txt');
6  points=[94169,119449,120426];
7  %data_omni(:,10)=12;
8  data_omni(:,17)=data_omni(:,13)/1000+data_omni(:,12)+data_omni...
    (:,11)*60+data_omni(:,10)*3600;
9  for q=1:length(data_omni)
10     [x,y,z]=trans_omni([data_omni(q,10),data_omni(q,11),data_omni...
        (q,12)], [data_omni(q,1),data_omni(q,2),data_omni(q,3)], [...
        data_omni(q,7),data_omni(q,8),data_omni(q,9)], [-174 -81 ...
        0]);
11     Location_drill(q,1)=x;Location_drill(q,2)=y;Location_drill(q...
        ,3)=z;
12 end
13
14 lenght_1_2=((Location_drill(points(1,1),1)-Location_drill(points...
    (1,2),1))^2+(Location_drill(points(1,1),2)-Location_drill(...
    points(1,2),2))^2 +(Location_drill(points(1,1),3)-...
    Location_drill(points(1,2),3))^2)^.5
15 lenght_1_2=((Location_drill(points(1,2),1)-Location_drill(points...
    (1,3),1))^2+(Location_drill(points(1,2),2)-Location_drill(...
    points(1,3),2))^2 +(Location_drill(points(1,2),3)-...
    Location_drill(points(1,3),3))^2)^.5
16 for num=points(1,1):points(1,2)
17     v(num-points(1,1)+1)=(data_omni(num,4)^2+data_omni(num,5)^2+...
        data_omni(num,6)^2)^.5;

```

```

18 end
19 max_v=max(v)
20 min_v=min(v)

```

B.1.15 Plot generator function

```

1 %% force plot
2 d=[1 2 3 4 5 6 7 9 10 11 12 13 14 16 18 19 20 21 22 23 24 25 26 ...
    27 28 29 30 31 32 34 35 36 37 38 39 40 41 43 44 45 46 47 49 ...
    50 51 52 53 54 55 56 57 60 61 62 63 65 66 67 68 69 70 71 73 ...
    75 76 77 78 79 80 82 83 84 85 86 87 90 91 92 93 94 95 97 98 ...
    99 101 102 103 104 105 016 107 108 110 111 113];
3 for i=1:length(d)
4     x=Total_finaldata(d(i)).Time_lv_2ndclipped;
5     y=Low_filter_force(Low_filter_force(Low_filter_force(...
        Total_finaldata(d(i)).Force_lv_2ndclipped)));
6     x=x-min(x);
7     y=y-min(y);
8     x=x./max(x);
9     y=y./max(y);
10    plot(x,y,'b. ');
11    hold on
12    %title(num2str(d(i)))
13    %pause(1)
14 end
15 dd=[49 50 51 52 53 54 55 65 66 69 67 68 69 70 80 82 83 84 85 105]
16 for i=1:length(dd)
17     x=Total_finaldata(dd(i)).Time_lv_2ndclipped;
18     y=Low_filter_force(Low_filter_force(Low_filter_force(...
        Total_finaldata(dd(i)).Force_lv_2ndclipped)));
19     x=x-min(x);
20     y=y-min(y);
21     x=x./max(x);
22     y=y./max(y);
23     plot(x,y,'r. ');
24     hold on
25     %title(num2str(d(i)))
26     %pause(1)
27 end

```

B.1.16 RPM function 1

```

1 function [res]=rpm_final(w,t)
2 n=10000;
3 for i=1:length(w)/n
4     tim(i)=mean(t(((i-1)*n+1):(i)*n)));
5     ddd(i)=rpm2(w(((i-1)*n+1):(i)*n))*60;
6 end
7 res=[ddd;tim];

```

B.1.17 RPM function 2

```

1 function [dd]=rpm2(data)
2 y=data-mean(data)/2;
3 %[y]=Low_filter_rpm(data);
4 d=0;
5 for i=1:(length(y)-1)
6     if ((y(i)*y(i+1))<0)
7         d=d+1;
8     end
9 end
10 dd=d/2;

```

B.1.18 General SYNC function

```

1 function [OUTPUT]=syncer(dataLV_A,haptic_A,clip_A)
2 %OUTPUT=[Time,X,V,Force];
3 %clip LV:
4 newLV=dataLV_A(clip_A(1,1):clip_A(1,2),:);
5 plot(dataLV_A(:,1),dataLV_A(:,2));hold on ; plot(newLV(:,1),newLV...
6     (:,2),'r');
7 [¬,haptic_clip_1]=min(sqrt(newLV(1,1)-haptic_A(:,7)));
8 [¬,haptic_clip_2]=min(sqrt(newLV(length(newLV),1)-haptic_A(:,7)))...
9     ;
10 new_data_LV=resample(newLV,haptic_clip_2-haptic_clip_1,clip_A...
11     (1,2)-clip_A(1,1));
12 %figure;plot(newLV(:,1),newLV(:,2));hold on; plot(new_data_LV...
13     (:,1),new_data_LV(:,2),'r');
14 size(new_data_LV);
15 size(haptic_A(haptic_clip_1:haptic_clip_2,2));
16 size(haptic_A(haptic_clip_1:haptic_clip_2,3));
17 OUTPUT=[haptic_A(haptic_clip_1:haptic_clip_2,7),haptic_A(...
18     haptic_clip_1:haptic_clip_2,1),haptic_A(haptic_clip_1:...
19     haptic_clip_2,2),new_data_LV(:,2)];

```



```

14 figure;
15 plot(OUTPUT(:,2)*10); hold on; plot(OUTPUT(:,3)*10000,'r');plot(...
    OUTPUT(:,4),'g')

```

B.2 Augmented haptic project

B.2.1 General code for type A

```

1  clc
2  clear all
3  %close all
4  %%
5  [dataLV_A,H,MIN,SEC]=Labview2var('A_1.lvm');
6  haptic_A=csvread('A_1.txt');
7  %%
8  [dataLV_A(:,2)]=Low_filter_force(dataLV_A(:,2));
9  dataLV_A(:,2)=(5601.7*dataLV_A(:,2)+6208.7)*0.00980665002864;
10 m=figure;plot(dataLV_A(:,1),dataLV_A(:,2));
11 haptic_A(:,3)=str2num(H);
12 haptic_A(:,7)=haptic_A(:,3)*3600+haptic_A(:,4)*60+haptic_A(:,5)+...
    haptic_A(:,6)*0.001;
13 hold on; plot(haptic_A(:,7),haptic_A(:,1)*10,'r');plot(haptic_A...
    (:,7),haptic_A(:,2)*10000,'g')
14 %%
15 clip_A=[6.398e+04 1.464e+05];
16 [m,OUTPUT]=syncer(dataLV_A,haptic_A,clip_A);
17 saveas(m,'A_1_clip','fig')
18 h=figure;
19 sf_A_1 = fit([OUTPUT(:,2), OUTPUT(:,3)],OUTPUT(:,4),'poly23')
20 plot(sf_A_1,[OUTPUT(:,2), OUTPUT(:,3)],OUTPUT(:,4))
21 save('A_1','sf_A_1')
22 saveas(h,'A_1','fig')
23 X=OUTPUT(:,2);
24 dX=OUTPUT(:,3);
25 F=OUTPUT(:,4);

```

B.2.2 Force filter function

```

1 d = designfilt('lowpassfir');
2 y = filtfilt(d,data);
3 y1 = filter(d,data);

```

```

4 subplot(2,1,1)
5 plot([y y1])
6 title('Filtered Waveforms')
7 legend('Zero-phase Filtering','Conventional Filtering')
8
9 subplot(2,1,2)
10 plot(data)
11 title('Original Waveform')

```

B.2.3 Location filter function

```

1 function [ data ] = fitrev( sf,x,y )
2 %UNTITLED5 Summary of this function goes here
3 % Detailed explanation goes here
4 data = sf.p00 + sf.p10*x + sf.p01*y + sf.p20*x.^2 + sf.p11*x.*y +...
        sf.p02*y.^2 + sf.p21*x.^2.*y
5         + sf.p12*x.*y.^2 + sf.p03*y.^3;
6 end

```

B.2.4 Labview opener

```

1 function [dataLV,H,MIN,SEC]=Labview2var(filename)
2 %The 6th culomn is the ABS time. The function creates a 'newfile....
   txt'.
3 fileID = fopen(filename);
4 fid=fileID;
5 C = textscan(fileID,'%s %s');
6 Timeloc=11;
7 data.start=30;
8 com=strfind(C{1,1}{Timeloc,1},',');
9 colo=strfind(C{1,1}{Timeloc,1},':');
10 H= C{1,1}{Timeloc,1}((com+1):(colo(1,1)-1));
11 MIN= C{1,1}{Timeloc,1}((colo(1,1)+1):(colo(1,2)-1));
12 SEC= C{1,1}{Timeloc,1}((colo(1,2)+1):(colo(1,2)+8));
13 fid=fopen(filename);
14 fid2=fopen('newfile.txt','w');
15 id=0;
16 a=fgets(fid);
17 while(ischar(a))
18     id=id+1;
19     if id<24
20         a=fgets(fid);

```

```

21         continue
22     else
23         fprintf(fid2,a);
24     end
25     a=fgets(fid);
26 end
27 xx=csvread('newfile.txt');
28 xy=xx(:,1)+(str2num(SEC)+60*str2num(MIN)+3600*str2num(H));
29 %Be sure the trend is accelerometer 0 ,accelerometer 1, Voltage ...
    0, Voltage 1
30 %The structure is : ABS TIME ; Acceleration 0 ; Acceleration 1 ; ...
    Filtered
31 %force ; RPM
32 dataLV=[xy , xx(:,2)];
33 %dataLV=csvread('newfile.txt');

```

B.2.5 File opener

```

1 d = designfilt('lowpassfir');
2 y = filtfilt(d,data);
3 y1 = filter(d,data);
4 subplot(2,1,1)
5 plot([y y1])
6 title('Filtered Waveforms')
7 legend('Zero-phase Filtering','Conventional Filtering')
8
9 subplot(2,1,2)
10 plot(data)
11 title('Original Waveform')

```

B.2.6 Calculator

```

1 function [r_sq]=R_SQ_REG(input)
2 %needs the data str made in clip_data_fix
3 force=input.sf.p00+input.sf.p10.*input.OUTPUT(:,2)+input.sf.p01.*...
    input.OUTPUT(:,3)+input.sf.p20.*(input.OUTPUT(:,2).^2)+input....
    sf.p11.*input.OUTPUT(:,2).*input.OUTPUT(:,3)+input.sf.p02.*...
    input.OUTPUT(:,3).^2+input.sf.p21.*(input.OUTPUT(:,2).^2).*...
    input.OUTPUT(:,3)+input.sf.p12.*input.OUTPUT(:,2).*(input....
    OUTPUT(:,3).^2)+input.sf.p03.*input.OUTPUT(:,3).^3;
4 r_sq=(sum((force-mean(input.OUTPUT(:,4))).^2)/sum((input.OUTPUT...
    (:,4)-mean(input.OUTPUT(:,4))).^2));

```

B.2.7 Error calculator

```
1 A.sf.p00=mean([A_1.sf.p00 A_2.sf.p00 A_3.sf.p00 A_4.sf.p00]);
2 B.sf.p00=mean([B_1.sf.p00 B_2.sf.p00 B_3.sf.p00 B_4.sf.p00]);
3 C.sf.p00=mean([C_1.sf.p00 C_2.sf.p00 C_3.sf.p00 C_4.sf.p00]);
4 D.sf.p00=mean([D_1.sf.p00 D_2.sf.p00 D_3.sf.p00 D_4.sf.p00]);
5
6 A.sf.p01=mean([A_1.sf.p01 A_2.sf.p01 A_3.sf.p01 A_4.sf.p01]);
7 B.sf.p01=mean([B_1.sf.p01 B_2.sf.p01 B_3.sf.p01 B_4.sf.p01]);
8 C.sf.p01=mean([C_1.sf.p01 C_2.sf.p01 C_3.sf.p01 C_4.sf.p01]);
9 D.sf.p01=mean([D_1.sf.p01 D_2.sf.p01 D_3.sf.p01 D_4.sf.p01]);
10
11 A.sf.p10=mean([A_1.sf.p10 A_2.sf.p10 A_3.sf.p10 A_4.sf.p10]);
12 B.sf.p10=mean([B_1.sf.p10 B_2.sf.p10 B_3.sf.p10 B_4.sf.p10]);
13 C.sf.p10=mean([C_1.sf.p10 C_2.sf.p10 C_3.sf.p10 C_4.sf.p10]);
14 D.sf.p10=mean([D_1.sf.p10 D_2.sf.p10 D_3.sf.p10 D_4.sf.p10]);
15
16 A.sf.p20=mean([A_1.sf.p20 A_2.sf.p20 A_3.sf.p20 A_4.sf.p20]);
17 B.sf.p20=mean([B_1.sf.p20 B_2.sf.p20 B_3.sf.p20 B_4.sf.p20]);
18 C.sf.p20=mean([C_1.sf.p20 C_2.sf.p20 C_3.sf.p20 C_4.sf.p20]);
19 D.sf.p20=mean([D_1.sf.p20 D_2.sf.p20 D_3.sf.p20 D_4.sf.p20]);
20
21
22 A.sf.p11=mean([A_1.sf.p11 A_2.sf.p11 A_3.sf.p11 A_4.sf.p11]);
23 B.sf.p11=mean([B_1.sf.p11 B_2.sf.p11 B_3.sf.p11 B_4.sf.p11]);
24 C.sf.p11=mean([C_1.sf.p11 C_2.sf.p11 C_3.sf.p11 C_4.sf.p11]);
25 D.sf.p11=mean([D_1.sf.p11 D_2.sf.p11 D_3.sf.p11 D_4.sf.p11]);
26
27 A.sf.p02=mean([A_1.sf.p02 A_2.sf.p02 A_3.sf.p02 A_4.sf.p02]);
28 B.sf.p02=mean([B_1.sf.p02 B_2.sf.p02 B_3.sf.p02 B_4.sf.p02]);
29 C.sf.p02=mean([C_1.sf.p02 C_2.sf.p02 C_3.sf.p02 C_4.sf.p02]);
30 D.sf.p02=mean([D_1.sf.p02 D_2.sf.p02 D_3.sf.p02 D_4.sf.p02]);
31
32 A.sf.p21=mean([A_1.sf.p21 A_2.sf.p21 A_3.sf.p21 A_4.sf.p21]);
33 B.sf.p21=mean([B_1.sf.p21 B_2.sf.p21 B_3.sf.p21 B_4.sf.p21]);
34 C.sf.p21=mean([C_1.sf.p21 C_2.sf.p21 C_3.sf.p21 C_4.sf.p21]);
35 D.sf.p21=mean([D_1.sf.p21 D_2.sf.p21 D_3.sf.p21 D_4.sf.p21]);
36
37 A.sf.p12=mean([A_1.sf.p12 A_2.sf.p12 A_3.sf.p12 A_4.sf.p12]);
38 B.sf.p12=mean([B_1.sf.p12 B_2.sf.p12 B_3.sf.p12 B_4.sf.p12]);
39 C.sf.p12=mean([C_1.sf.p12 C_2.sf.p12 C_3.sf.p12 C_4.sf.p12]);
40 D.sf.p12=mean([D_1.sf.p12 D_2.sf.p12 D_3.sf.p12 D_4.sf.p12]);
41
42 A.sf.p03=mean([A_1.sf.p03 A_2.sf.p03 A_3.sf.p03 A_4.sf.p03]);
43 B.sf.p03=mean([B_1.sf.p03 B_2.sf.p03 B_3.sf.p03 B_4.sf.p03]);
44 C.sf.p03=mean([C_1.sf.p03 C_2.sf.p03 C_3.sf.p03 C_4.sf.p03]);
45 D.sf.p03=mean([D_1.sf.p03 D_2.sf.p03 D_3.sf.p03 D_4.sf.p03]);
46
47
```

```
48 A.OUTPUT=[A_1.OUTPUT' A_2.OUTPUT' A_3.OUTPUT' A_4.OUTPUT']';  
49 B.OUTPUT=[B_1.OUTPUT' B_2.OUTPUT' B_3.OUTPUT' B_4.OUTPUT']';  
50 C.OUTPUT=[C_1.OUTPUT' C_2.OUTPUT' C_3.OUTPUT' C_4.OUTPUT']';  
51 D.OUTPUT=[D_1.OUTPUT' D_2.OUTPUT' D_3.OUTPUT' D_4.OUTPUT']';
```

APPENDIX C

C++ CODES AND FUNCTIONS

C.1 Augmented Haptic

```
1  /*The modified template code from open haptics library
2   Library generated for haptic onmi device 2008
3   */
4  #include <QHHeadersGLUT.h> //Include all necessary headers
5  #include <HDU/hduMath.h>
6  #ifdef _WIN64
7  #pragma warning (disable:4996)
8  #endif
9
10 #include <cstdio>
11 #include <iostream>
12 #include <fstream>
13 using namespace std;
14
15 #include <HL/hl.h>
16 #include <HD/hd.h>
17
18 #include <HDU/hduVector.h>
19 #include <HDU/hduError.h>
20 struct PointMass
21 {
22
23 };
24 hduVector3Dd m_position;
25 hduVector3Dd m_velocity;
26 HDdouble m_mass;
27 HDdouble m_kStiffness;
28 HDdouble m_kDamping;
29 hduVector3Dd springForce;
30 hduVector3Dd damperForce;
31 hduVector3Dd inertiaForce;
32 hduVector3Dd v_location;
33
34 void HLCALLBACK buttonCB(HLenum event, HLuint object, HLenum ...
    thread,
```

```

35         HLcache *cache, void *userdata);
36  /*...
37  Servo loop thread callback. Computes a force effect.
38  ****
39  void HLCALLBACK computeForceCB(HDdouble force[3], HLcache *cache,...
    void *userdata)
40  {
41      PointMass *pPointMass = static_cast<PointMass *>(userdata);
42
43      // Get the time  $\Delta$  since the last update.
44      HDdouble instRate;
45      hdGetDoublev(HD_INSTANTANEOUS_UPDATE_RATE, &instRate);
46      HDdouble  $\Delta T$  = 1.0 / instRate;
47
48      // Set Variable Values
49      m_mass = 0.01;
50      hdGetDoublev(HD_NOMINAL_MAX_STIFFNESS, &m_kStiffness);
51      m_kStiffness *= 0.5;
52      m_kDamping = 2 * sqrt(m_mass * m_kStiffness);
53      // Get the current proxy position from the state cache.
54      // Note that the effect state cache is maintained in ...
55      // workspace coordinates,
56      // so we don't need to do any transformations in using the ...
57      // proxy
58      // position for computing forces.
59      hduVector3Dd proxyPos;
60      hlCacheGetDoublev(cache, HL_PROXY_POSITION, proxyPos);
61
62      // Compute the inertia force based on pulling the point mass ...
63      // around
64      // by a spring.
65      //std::cout<< m_kStiffness;
66      springForce = m_kStiffness * (proxyPos - m_position);
67
68      damperForce = -m_kDamping * m_velocity;
69      inertiaForce = springForce + damperForce;
70
71      // Perform Euler integration of the point mass state.
72      hduVector3Dd acceleration = inertiaForce / m_mass;
73      m_velocity += acceleration *  $\Delta T$ ;
74      m_position += m_velocity *  $\Delta T$ ;
75
76      // Send the opposing force to the device.
77      force[0] += -inertiaForce[0];
78      force[1] += -inertiaForce[1];
79      force[2] += -inertiaForce[2];
80  }

```

```

78
79
80 /*...
    *****

81 Servo loop thread callback called when the effect is started.
82 *****...
    */
83 void HLCALLBACK startEffectCB(HLcache *cache, void *userdata)
84 {
85     fprintf(stdout, "Custom effect started\n");
86
87     // Initialize the position of the mass to be at the proxy ...
88     position.
89     hlCacheGetDoublev(cache, HL_PROXY_POSITION, m_position);
90
91     m_velocity.set(0, 0, 0);
92 }
93
94 /*...
    *****

95 Servo loop thread callback called when the effect is stopped.
96 *****...
    */
97 void HLCALLBACK stopEffectCB(HLcache *cache, void *userdata)
98 {
99     fprintf(stdout, "Custom effect stopped\n");
100 }
101
102
103
104
105 int main(int argc, char *argv[]) //initializes the function "main"
106 {
107     ofstream myfile;
108     myfile.open ("example.txt");
109     HHD hHD;
110     HHLRC hHLRC;
111     //HDErrorInfo error;
112
113     hHD = hdInitDevice(HD_DEFAULT_DEVICE);
114     /*if (HD_DEVICE_ERROR(error = hdGetError()))
115     {
116         hduPrintError(stderr, &error, "Failed to initialize ...
            haptic device");
117         fprintf(stderr, "\nPress any key to quit.\n");
118         getch();
119         return -1;

```



```

120     */
121     hdMakeCurrentDevice(hHD);
122
123     hHLRC = hlCreateContext(hHD);
124     hlMakeCurrent(hHLRC);
125
126     HLuInt effect = hlGenEffects(1);
127
128
129
130     /* Add a callback to handle button down in the collision ...
131        thread. */
132     hlAddEventCallback(HLEVENT_1BUTTONDOWN, HL_OBJECT_ANY, ...
133         HL_CLIENT_THREAD,
134         buttonCB, 0);
135     hlAddEventCallback(HLEVENT_1BUTTONUP, HL_OBJECT_ANY, ...
136         HL_CLIENT_THREAD,
137         buttonCB, 0);
138     hlAddEventCallback(HLEVENT_2BUTTONDOWN, HL_OBJECT_ANY, ...
139         HL_CLIENT_THREAD,
140         buttonCB, 0);
141
142     hlBeginFrame();
143
144     hlCallback(HLEFFECT_COMPUTE_FORCE, (HLcallbackProc) ...
145         computeForceCB, 0);
146     hlCallback(HLEFFECT_START, (HLcallbackProc) startEffectCB, ...
147         0);
148     hlCallback(HLEFFECT_STOP, (HLcallbackProc) stopEffectCB, 0);
149
150     hlStartEffect(HLEFFECT_CALLBACK, effect);
151
152     hlEndFrame(); */
153
154     fprintf(stdout, "Press any key to stop the effect\n");
155     //fprintf("Press any key to stop the effect\n");
156     HDdouble key;
157     key = 1.0;
158     while (key = 1)
159     {
160         hduVector3Dd proxyPos;
161         HLcache *cache;
162         hlCacheGetDoublev(cache, HL_PROXY_POSITION, proxyPos);
163
164         std::cout << "proxy position = " << proxyPos[0] << ", " << ...
165             proxyPos[1] << ", " << proxyPos[2] << " " << std::endl;
166         */
167         std::cout << "mass position = " << m.position[0] << ", " ...
168             << m.position[1] << ", " << m.position[2] << " " << ...
169             std::endl; */

```

```

160         hlBeginFrame();
161         hlCheckEvents();
162         hlEndFrame();
163     };
164
165     hlBeginFrame();
166     hlStopEffect(effect);
167     hlEndFrame();
168
169     //fprintf(stdout, "Shutting down...\n");
170     //getch();
171
172     hlDeleteEffects(effect, 1);
173
174     hlDeleteContext(hHLRC);
175     hdDisableDevice(hHD);
176
177     //return 0;
178
179     //qhStart(); //Set everything in motion
180 }
181
182 void HLCALLBACK buttonCB(HLenum event, HLuInt object, HLenum ...
    thread,
183                             Hlcache *cache, void *userdata)
184 {
185     if (event == HLEVENT_1BUTTONDOWN)
186     {
187         /*fprintf(stdout, "Button 1 has been pressed.\n");
188         float h;
189         h = 150.0;
190         //std::cout << "Angle 1 = " << pAngles->Th1 << "\n";
191         //fprintf(stdout, "Angle 1 = %f\n", pAngles->Th1);
192         hduVector3Dd proxyPos;
193         hlCacheGetDoublev(cache, HL_PROXY_POSITION, proxyPos);
194         std::cout << "Proxy x position = " << proxyPos[0] << " \n...
195             " <<
196             "Proxy y position = " << proxyPos[1] << " \n...
197             " <<
198             "Proxy z position = " << proxyPos[2] << " " ...
199             << std::endl;/**/
200         //std::cout << "velocity = " << newVelFilt[0] << ", " << ...
201             newVelFilt[1] << ", " << newVelFilt[2] << " " << std:...
202             :endl;/**/
203         //std::cout << "acceleration = " << accel[0] << ", " << ...
204             accel[1] << ", " << accel[2] << " " << std::endl;/**/
205         //std::cout << "force = " << inertiaForce[0] << ", " << ...
206             inertiaForce[1] << ", " << inertiaForce[2] << " " << ...
207             std::endl;/**/
208         //fprintf(stdout, "Stiffness = %f\n", m_kStiffness);

```

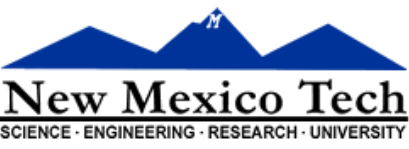
```

201         fprintf(stdout, "Mass = %f\n", m_mass);
202     }
203     else if (event == HLEVENT_1BUTTONUP)
204     {
205     }
206 }
207 else if (event == HLEVENT_2BUTTONDOWN)
208 {
209     /*fprintf(stdout, "Button 2 has been pressed.\n");
210     hduVector3Dd currentPos;
211     hdGetDoublev(HD_CURRENT_POSITION, currentPos);
212     std::cout << "Current x position = " << currentPos[0] << ...
213         " mm\n" <<
214         "Current y position = " << currentPos[1] << ...
215         " mm\n" <<
216         "Current z position = " << currentPos[2] << ...
217         " mm" << std::endl;
218     /*std::cout << "COM x position = " << COM[0] << " \n" <<
219         "COM y position = " << COM[1] << " \n" <<
220         "COM z position = " << COM[2] << " " << std:...
221         :endl;*/
222     //std::cout << "damping force = " << damperForce[0] << ", ...
223         " << damperForce[1] << ", " << damperForce[2] << " " ...
224         << std::endl;*/
225     //std::cout << "spring force = " << springForce[0] << ", ...
226         << springForce[1] << ", " << springForce[2] << " " <<...
227         std::endl;*/
228     hduVector3Dd proxyPos;
229     hlCacheGetDoublev(cache, HL_PROXY_POSITION, proxyPos);
230
231     std::cout << "proxy position = " << proxyPos[0] << ", " <<...
232         proxyPos[1] << ", " << proxyPos[2] << " " << std::end...
233         l;*/
234     std::cout << "mass position = " << m_position[0] << ", " ...
235         << m_position[1] << ", " << m_position[2] << " " << ...
236         std::endl;*/
237     // basic file operations
238     ofstream myfile;
239     myfile.open ("example.txt");
240     myfile << "proxy position = " << proxyPos[0] << ", " << ...
241         proxyPos[1] << ", " << proxyPos[2] << " " << std::end...
242         l;
243     myfile.close();
244 }
245 }

```


APPENDIX D

IRB APPLICATION

 <p>New Mexico Tech SCIENCE · ENGINEERING · RESEARCH · UNIVERSITY</p>	<p align="center">Institutional Review Board for the Protection of Human Subjects in Research</p> <p align="center">IRB Approval of Research Project</p> <p align="center">REV. March 2013 PAGE 1 OF 2</p>	
	<p align="center">NMT's Institutional/Organization Number (assigned by DHHS): FWA00006606 Valid Through: 12 July 2016</p>	<p align="center">IRB DATABASE No.: <u>2014-10-004</u></p>



<p>Title of research project: Robotic tools for bone drilling training and assessment</p>	
<p>Primary researcher name and title: David Grow</p>	
<p>Type of review sought by PI: <input checked="" type="checkbox"/> Initial Review of new research project <input type="checkbox"/> Continuing Review for ongoing project </p>	
<p>Type of Initial Review performed: <input checked="" type="checkbox"/> Full Board Review <input type="checkbox"/> Expedited Review – list IRB Members participating in review: </p>	<p>Recommended Interval for Continuing Review: <input type="checkbox"/> Every 6 months <input checked="" type="checkbox"/> Every 12 months <input type="checkbox"/> Further review not required unless protocol changes </p>
<p>Research project qualifies for expedited IRB Review, according to the NMT IRB Policy, Appendix B, Category:</p> <p> <input type="checkbox"/> Collection of small samples of blood (<50 ml) <input type="checkbox"/> Prospective collection of biological specimens for research purposes by non-invasive means <input type="checkbox"/> Collection of data through non-invasive procedures, including sensors, weighing, exercise testing, EEG, EKG, etc. <input type="checkbox"/> Research involving personally identifiable data, documents, or specimens collected solely for classroom/lab purposes <input type="checkbox"/> Collection of data from voice, video, digital, or image recordings made for research purposes <input checked="" type="checkbox"/> Research on group characteristics or behaviors that also collects personally identifiable data <input type="checkbox"/> Continuing review of research previously approved by the IRB: <input type="checkbox"/> Where no additional subjects have been used and no additional risks have been identified <input type="checkbox"/> Where the remaining research activities are limited to data analysis </p>	

IRB Review Findings:	YES	N/A
1. The scientific questions addressed in this project have adequate merit to justify experimenting with human subjects.	<input checked="" type="checkbox"/>	<input type="checkbox"/>
2. The risks to subjects are minimized and reasonable in relation to the anticipated benefits.	<input checked="" type="checkbox"/>	<input type="checkbox"/>
3. The selection of subjects is reasonable in relation to anticipated benefits.	<input checked="" type="checkbox"/>	<input type="checkbox"/>
4. The PI's choice of consent documentation (e.g., written, oral, waived) is appropriate.	<input checked="" type="checkbox"/>	<input type="checkbox"/>
5. The project has appropriate protections to ensure the privacy of subjects and confidentiality of data.	<input checked="" type="checkbox"/>	<input type="checkbox"/>
6. No vulnerable populations are being used, OR there are appropriate safeguards for vulnerable populations.	<input checked="" type="checkbox"/>	<input type="checkbox"/>

 New Mexico Tech <small>SCIENCE · ENGINEERING · RESEARCH · UNIVERSITY</small>	Institutional Review Board for the Protection of Human Subjects in Research IRB Approval of Research Project REV. March 2013 PAGE 2 OF 2	
NMT's Institutional/Organization Number (assigned by DHHS): FWA00006606 Valid Through: 12 July 2016		IRB DATABASE No.: <u>2014-10-004</u>

Protocol has been reviewed by New Mexico Tech's IRB and is approved for 365 days from the date given below.

Research must **NOT** continue after this date without continuing review and approval from the IRB. Research conducted without such review and approval runs the risk of being shut down and having all collected data destroyed.

MONTH: October	DAY: 24	YEAR: 2014
IRB Member (Printed) _____ Jacob Carrillo _____ Signature of IRB Member: 		Date Signed: 23 Oct 2014
IRB Member (Printed) _____ Troylyn Zimmerly _____ Signature of IRB Member: 		Date Signed: 10.23.14

Patient Code _____

Date _____

Surgical Skill Assessment Survey

The Institutional Review Board for the Protection of Human Subjects at NM Tech has reviewed and approved this research project. By completing this survey, you agree to participate in this project. Your participation in this research project is strictly voluntary and you may choose not to participate by simply not completing the survey. You may also refuse to answer specific questions on this survey if you so desire. If you have any questions or concerns about this survey, please contact the researcher at 505-307-2918 or the New Mexico Tech IRB Administrator at 575-835-5690.

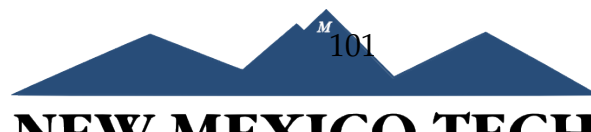
Basic Information

1. Gender: _____
2. Age: _____
3. Handedness: _____

Previous Experience

1. What is your current training level (e.g. 2nd year resident)?
2. Roughly, how many hours of training do you have in drilling real or synthetic bone?
3. Do you have any prior experience working with haptic (force-feedback) robotic devices? If so,

how many hours and what is this experience?



Subject Feedback

1. Please rate the realism of the bone drilling experience compared to normally drilling in

synthetic bone (1 [not at all realistic] – 10 [perfectly realistic]): ____ (score)

2. Please rate the realism of the bone drilling experience compared to normally drilling in human

bone (1 [not at all realistic] – 10 [perfectly realistic]): ____ (score)

3. Please describe any sensations produced by the haptic (force-feedback) device that you found to significantly add to or detract from the realism of this training.

Sample Recruiting Letter

Dear Colleagues,

We are currently conducting a human/machine interactive experiment in Dr. Grow's Human Robot Interfaces Laboratory. As part of this work, I will be conducting an experiment that investigates the use of robotic tools to measure skill in surgical drilling procedures and explore the use of these same tools for training of relevant skills. Results may lead to improved methods for assessing and training orthopaedic surgeons.

This experiment will last 20-60 minutes. Only those who are 18 or over, and right-handed with no neurological disorders or injuries to their dominant hand are eligible to participate. If you are interested in being an experiment subject please contact me via email at pourkand@nmt.edu.

Your participation in this experiment is entirely voluntary. If you have any questions or concerns, feel free to contact me or Dr. Grow at dgrow@nmt.edu or extension 5109. Your assistance in helping us meet our research goals would be greatly appreciated.

Thank You,
Ashkan Pourkand

IRB Protocol Number: XXXX



REFERENCES

- [1] W.-Y. Lee and C.-L. Shih, "Control and breakthrough detection of a three-axis robotic bone drilling system," *Mechatronics*, vol. 16, no. 2, pp. 73–84, Mar. 2006. [Online]. Available: <http://www.sciencedirect.com/science/article/pii/S0957415805001352>
- [2] H. Jin, Y. Hu, W. Tian, P. Zhang, J. Zhang, and B. Li, "Safety analysis and control of a robotic spinal surgical system," *Mechatronics*, vol. 24, no. 1, pp. 55–65, Feb. 2014. [Online]. Available: <http://www.sciencedirect.com/science/article/pii/S0957415813002286>
- [3] P. Poddar, N. Ahmidi, S. S. Vedula, L. Ishii, G. D. Hager, and M. Ishii, "Automated Objective Surgical Skill Assessment in the Operating Room Using Unstructured Tool Motion," *arXiv:1412.6163 [cs]*, Dec. 2014, arXiv: 1412.6163. [Online]. Available: <http://arxiv.org/abs/1412.6163>
- [4] D. W. Overby and R. A. Watson, "Hand motion patterns of Fundamentals of Laparoscopic Surgery certified and noncertified surgeons," *The American Journal of Surgery*, vol. 207, no. 2, pp. 226–230, Feb. 2014. [Online]. Available: <http://www.sciencedirect.com/science/article/pii/S0002961013005989>
- [5] M. Uemura, M. Tomikawa, R. Kumashiro, T. Miao, R. Souzaki, S. Ieiri, K. Ohuchida, A. T. Lefor, and M. Hashizume, "Analysis of hand motion differentiates expert and novice surgeons," *Journal of Surgical Research*, vol. 188, no. 1, pp. 8–13, May 2014. [Online]. Available: <http://www.sciencedirect.com/science/article/pii/S0022480413021744>
- [6] M. Louredo, I. Daz, and J. J. Gil, "DRIBON: A mechatronic bone drilling tool," *Mechatronics*, vol. 22, no. 8, pp. 1060–1066, Dec. 2012. [Online]. Available: <http://www.sciencedirect.com/science/article/pii/S0957415812001304>
- [7] R. K. Pandey and S. S. Panda, "Multi-performance optimization of bone drilling using Taguchi method based on membership function," *Measurement*, vol. 59, pp. 9–13, Jan. 2015. [Online]. Available: <http://www.sciencedirect.com/science/article/pii/S0263224114004187>
- [8] —, "Optimization of multiple quality characteristics in bone drilling using grey relational analysis," *Journal of Orthopaedics*, vol. 12, no. 1, pp. 39–45, Mar. 2015. [Online]. Available: <http://www.sciencedirect.com/science/article/pii/S0972978X14000543>

- [9] —, "Optimization of bone drilling parameters using grey-based fuzzy algorithm," *Measurement*, vol. 47, pp. 386–392, Jan. 2014. [Online]. Available: <http://www.sciencedirect.com/science/article/pii/S0263224113004430>
- [10] B. B. Gilmer, D. M. Guerrero, N. W. Coleman, A. M. Chamberlain, and W. J. Warne, "Orthopaedic Residents Improve Confidence and Knot-Tying Speed With a Skills Course," *Arthroscopy: The Journal of Arthroscopic & Related Surgery*, vol. 31, no. 7, pp. 1343–1348.e2, Jul. 2015. [Online]. Available: <http://www.sciencedirect.com/science/article/pii/S0749806315001024>
- [11] R. V. O'Toole III, B. Jaramaz, A. M. DiGioia III, C. D. Visnic, and R. H. Reid, "Biomechanics for preoperative planning and surgical simulations in orthopaedics," *Computers in Biology and Medicine*, vol. 25, no. 2, pp. 183–191, Mar. 1995. [Online]. Available: <http://www.sciencedirect.com/science/article/pii/001048259400043P>
- [12] F. R. Ong and K. Bouazza-Marouf, "The detection of drill bit break-through for the enhancement of safety in mechatronic assisted orthopaedic drilling," *Mechatronics*, vol. 9, no. 6, pp. 565–588, Sep. 1999. [Online]. Available: <http://www.sciencedirect.com/science/article/pii/S0957415899000197>
- [13] I. Daz, J. J. Gil, and M. Louredo, "Bone drilling methodology and tool based on position measurements," *Computer Methods and Programs in Biomedicine*, vol. 112, no. 2, pp. 284–292, Nov. 2013. [Online]. Available: <http://www.sciencedirect.com/science/article/pii/S0169260713000539>
- [14] A. Kapoor, M. Li, and R. Taylor, "Constrained control for surgical assistant robots," in *Proceedings 2006 IEEE International Conference on Robotics and Automation, 2006. ICRA 2006*, May 2006, pp. 231–236.
- [15] M. T. Hillery and I. Shuaib, "Temperature effects in the drilling of human and bovine bone," *Journal of Materials Processing Technology*, vol. 9293, pp. 302–308, Aug. 1999. [Online]. Available: <http://www.sciencedirect.com/science/article/pii/S0924013699001557>
- [16] G. Augustin, T. Zigman, S. Davila, T. Udilljak, T. Staroveski, D. Brezak, and S. Babic, "Cortical bone drilling and thermal osteonecrosis," *Clinical Biomechanics*, vol. 27, no. 4, pp. 313–325, May 2012. [Online]. Available: <http://www.sciencedirect.com/science/article/pii/S0268003311002786>
- [17] F. Karaca, B. Aksakal, and M. Kom, "Influence of orthopaedic drilling parameters on temperature and histopathology of bovine tibia: An in vitro study," *Medical Engineering & Physics*, vol. 33, no. 10, pp. 1221–1227, Dec. 2011. [Online]. Available: <http://www.sciencedirect.com/science/article/pii/S1350453311001263>
- [18] G. Gonzalez-Badillo, H. I. Medellin-Castillo, and T. Lim, "Development of a Haptic Virtual Reality System for Assembly Planning and Evaluation," *Procedia Technology*, vol. 7, pp. 265–272, 2013. [Online]. Available: <http://www.sciencedirect.com/science/article/pii/S2212017313000340>

- [19] R. K. Pandey and S. S. Panda, "Drilling of bone: A comprehensive review," *Journal of Clinical Orthopaedics and Trauma*, vol. 4, no. 1, pp. 15–30, Mar. 2013. [Online]. Available: <http://www.sciencedirect.com/science/article/pii/S0976566213000039>
- [20] J. Lee, O. B. Ozdoganlar, and Y. Rabin, "An experimental investigation on thermal exposure during bone drilling," *Medical Engineering & Physics*, vol. 34, no. 10, pp. 1510–1520, Dec. 2012. [Online]. Available: <http://www.sciencedirect.com/science/article/pii/S1350453312000501>
- [21] H. Esen, K. Yano, and M. Buss, "Bone Drilling Medical Training System," in *The Sense of Touch and its Rendering*, ser. Springer Tracts in Advanced Robotics, A. Bicchi, M. Buss, M. O. Ernst, and A. Peer, Eds. Springer Berlin Heidelberg, 2008, no. 45, pp. 245–278. [Online]. Available: <http://link.springer.com/chapter/10.1007/978354079035812>
- [22] R. Phillips, "(ii) The accuracy of surgical navigation for orthopaedic surgery," *Current Orthopaedics*, vol. 21, no. 3, pp. 180–192, Jun. 2007. [Online]. Available: <http://www.sciencedirect.com/science/article/pii/S0268089007001120>
- [23] R. A. Robb, "Virtual endoscopy: Development and evaluation using the Visible Human Datasets," *Computerized medical imaging and graphics : the official journal of the Computerized Medical Imaging Society*, vol. 24, no. 3, pp. 133–51, 2000.
- [24] I. Lee, K. Siu, D. Katsavelis, and N. Stergiou, "Nonlinear Analysis Quantifies Learning in Robot-assisted Laproscopic Surgery." *Surgical Endoscopy*, vol. 22, no. 5, p. 288, 2008.
- [25] A. Eversbusch and T. P. Grantcharov, "Learning curves and impact of psychomotor training on performance in simulated colonoscopy: a randomized trial using a virtual reality endoscopy trainer," *Surg Endosc*, vol. 18, no. 10, pp. 1514–1518, Aug. 2004. [Online]. Available: <http://link.springer.com/article/10.1007/s00464-003-9264-9>
- [26] S. Sezek, B. Aksakal, and F. Karaca, "Influence of drill parameters on bone temperature and necrosis: A FEM modelling and in vitro experiments," *Computational Materials Science*, vol. 60, pp. 13–18, Jul. 2012. [Online]. Available: <http://www.sciencedirect.com/science/article/pii/S0927025612001498>
- [27] B. Allotta, G. Giacalone, and L. Rinaldi, "A hand-held drilling tool for orthopedic surgery," *IEEE/ASME Transactions on Mechatronics*, vol. 2, no. 4, pp. 218–229, Dec. 1997.
- [28] J. S. T.H. Massie, "The phantom haptic interface: A device for probing virtual objects, proc." in *ASME Dyn. Syst. Contr. Div.*, 1994, pp. 295–299.
- [29] E. F. B. R. R.Q. van der Linde, P. Lammerste, "The hapticmaster, a new high-performance haptic interface, proc." in *AEurohaptics Conf.*, 2002, pp. 1–5.

- [30] B. Siciliano and O. Khatib, Eds., *Springer Handbook of Robotics*. Berlin, Heidelberg: Springer Berlin Heidelberg, 2008. [Online]. Available: <http://link.springer.com/10.1007/978-3-540-30301-5>
- [31] N. Steyn, Y. Hamam, E. Monacelli, and K. Djouani, "Modelling and design of an augmented reality differential drive mobility aid in an enabled environment," *Simulation Modelling Practice and Theory*, vol. 51, pp. 115–134, Feb. 2015. [Online]. Available: <http://www.sciencedirect.com/science/article/pii/S1569190X14001865>
- [32] Y. Maddahi, K. Zareinia, and N. Sepehri, "An augmented virtual fixture to improve task performance in robot-assisted live-line maintenance," *Computers & Electrical Engineering*, vol. 43, pp. 292–305, Apr. 2015. [Online]. Available: <http://www.sciencedirect.com/science/article/pii/S0045790614001840>
- [33] J. Hallet, L. Soler, M. Diana, D. Mutter, T. F. Baumert, F. Habersetzer, J. Marescaux, and P. Pessaux, "Trans-Thoracic Minimally Invasive Liver Resection Guided by Augmented Reality," *Journal of the American College of Surgeons*, vol. 220, no. 5, pp. e55–e60, May 2015. [Online]. Available: <http://www.sciencedirect.com/science/article/pii/S1072751515000563>
- [34] R. W. Barnes, "Surgical handicraft: Teaching and learning surgical skills," *The American Journal of Surgery*, vol. 153, no. 5, pp. 422–427, May 1987. [Online]. Available: <http://www.sciencedirect.com/science/article/pii/0002961087907835>
- [35] N. Sugano, "Computer-assisted orthopedic surgery," *J Orthop Sci*, vol. 8, no. 3, pp. 442–448, May 2003. [Online]. Available: <http://link.springer.com/article/10.1007/s10776-002-0623-6>
- [36] V. Vitiello, K. W. Kwok, and G. Z. Yang, "1 - Introduction to robot-assisted minimally invasive surgery (MIS)," in *Medical Robotics*, ser. Woodhead Publishing Series in Biomaterials, P. Gomes, Ed. Woodhead Publishing, 2012, pp. 1–P1. [Online]. Available: <http://www.sciencedirect.com/science/article/pii/B9780857091307500016>
- [37] J. Lee, B. A. Gozen, and O. B. Ozdoganlar, "Modeling and experimentation of bone drilling forces," *Journal of Biomechanics*, vol. 45, no. 6, pp. 1076–1083, Apr. 2012. [Online]. Available: <http://www.sciencedirect.com/science/article/pii/S0021929011007809>
- [38] J. Rho, L. Kuhn, and P. Zioups, "Mechanical properties and the hierarchical structure of bone," in *Mechanical Engineering & Physics*, December 920102 1997.
- [39] J. Lee, B. A. Gozen, and O. B. Ozdoganlar, "Modeling and experimentation of bone drilling forces," *Journal of Biomechanics*, vol. 45, no. 6, pp. 1076 – 1083, 2012. [Online]. Available: <http://www.sciencedirect.com/science/article/pii/S0021929011007809>

- [40] N. Bertollo and W. R. Walsh, "Drilling of bone: Practicality, limitations and complications associated with surgical drill-bits," *Biomechanics in Applications*, pp. 53–64, 2011.
- [41] B. Zhu and L. Gu, "A hybrid deformable model for real-time surgical simulation," *Computerized Medical Imaging and Graphics*, vol. 36, no. 5, pp. 356–365, Jul. 2012. [Online]. Available: <http://www.sciencedirect.com/science/article/pii/S089561111200047X>
- [42] Y. Lin, X. Wang, F. Wu, X. Chen, C. Wang, and G. Shen, "Development and validation of a surgical training simulator with haptic feedback for learning bone-sawing skill," *Journal of Biomedical Informatics*, vol. 48, pp. 122–129, Apr. 2014. [Online]. Available: <http://www.sciencedirect.com/science/article/pii/S1532046413002013>
- [43] M.-D. Tsai, M.-S. Hsieh, and C.-H. Tsai, "Bone drilling haptic interaction for orthopedic surgical simulator," *Computers in Biology and Medicine*, vol. 37, no. 12, pp. 1709–1718, Dec. 2007. [Online]. Available: <http://www.sciencedirect.com/science/article/pii/S001048250700087X>
- [44] M. Vankipuram, K. Kahol, A. McLaren, and S. Panchanathan, "A virtual reality simulator for orthopedic basic skills: A design and validation study," *Journal of Biomedical Informatics*, vol. 43, no. 5, pp. 661–668, Oct. 2010. [Online]. Available: <http://www.sciencedirect.com/science/article/pii/S1532046410000857>
- [45] R. K. Pandey and S. S. Panda, "Evaluation of delamination in drilling of bone," *Medical Engineering & Physics*. [Online]. Available: <http://www.sciencedirect.com/science/article/pii/S1350453315001034>
- [46] P. Wang, A. A. Becker, I. A. Jones, A. T. Glover, S. D. Benford, C. M. Greenhalgh, and M. Vloeberghs, "A virtual reality surgery simulation of cutting and retraction in neurosurgery with force-feedback," *Computer Methods and Programs in Biomedicine*, vol. 84, no. 1, pp. 11–18, Oct. 2006. [Online]. Available: <http://www.sciencedirect.com/science/article/pii/S0169260706001647>
- [47] C. Paloc, R. I. Kitney, F. Bello, and A. Darzi, "Virtual reality surgical training and assessment system," *International Congress Series*, vol. 1230, pp. 210–217, Jun. 2001. [Online]. Available: <http://www.sciencedirect.com/science/article/pii/S0531513101000383>
- [48] V. N. Palter and T. P. Grantcharov, "Virtual Reality in Surgical Skills Training," *Surgical Clinics of North America*, vol. 90, no. 3, pp. 605–617, Jun. 2010. [Online]. Available: <http://www.sciencedirect.com/science/article/pii/S0039610910000101>

- [49] G. Bianchi, B. Knoerlein, G. Szekely, and M. Harders, "High precision augmented reality haptics," <http://citeseerx.ist.psu.edu/viewdoc/download?doi=10.1.1.61.6436&rep=rep1&type=pdf> 2001, [Online; accessed Jan-26-2015].
- [50] B. Bayart, J.-Y. Didier, and A. Kheddar, "Force feedback virtual painting on real objects: A paradigm of augmented reality haptics," in *Haptics: Perception, Devices and Scenarios*, ser. Lecture Notes in Computer Science, M. Ferre, Ed. Springer Berlin Heidelberg, 2008, vol. 5024, pp. 776–785.
- [51] Y. Kurita, A. Ikeda, T. Tamaki, T. Ogasawara, and K. Nagata, "Haptic augmented reality interface using the real force response of an object," in *Proceedings of the 16th ACM Symposium on Virtual Reality Software and Technology*, ser. VRST '09. New York, NY, USA: ACM, 2009, pp. 83–86. [Online]. Available: <http://doi.acm.org/10.1145/1643928.1643948>
- [52] F. Zheng, W. F. Lu, Y. S. Wong, and K. W. C. Foong, "An analytical drilling force model and gpu-accelerated haptics-based simulation framework of the pilot drilling procedure for micro-implants surgery training," *Computer Methods and Programs in Biomedicine*, vol. 108, no. 3, pp. 1170 – 1184, 2012. [Online]. Available: <http://www.sciencedirect.com/science/article/pii/S016926071200154X>
- [53] R. K. Pandey and S. Panda, "Drilling of bone: A comprehensive review," *Journal of Clinical Orthopaedics and Trauma*, vol. 4, no. 1, pp. 15 – 30, 2013. [Online]. Available: <http://www.sciencedirect.com/science/article/pii/S0976566213000039>
- [54] S. Jeon, B. Knoerlein, M. Harders, and S. Choi, "Haptic simulation of breast cancer palpation: A case study of haptic augmented reality," in *Mixed and Augmented Reality (ISMAR), 2010 9th IEEE International Symposium on*, Oct 2010, pp. 237–238.
- [55] Y. Lin, X. Wang, F. Wu, X. Chen, C. Wang, and G. Shen, "Development and validation of a surgical training simulator with haptic feedback for learning bone-sawing skill," *Journal of Biomedical Informatics*, vol. 48, no. 0, pp. 122 – 129, 2014. [Online]. Available: <http://www.sciencedirect.com/science/article/pii/S1532046413002013>
- [56] M. D. Karam, B. A. A. D. D. Westerlind, and M. J. Lawrence, "Development of an orthopaedic surgical skills curriculum for post-graduate year one resident learners - the university of iowa experience," *Iowa Orthop J*, vol. 33, pp. 178–184, JUNE 2013. [Online]. Available: <http://www.ncbi.nlm.nih.gov/pmc/articles/PMC3748876/>
- [57] M. Vankipuram, K. Kahol, A. McLaren, and S. Panchanathan, "A virtual reality simulator for orthopedic basic skills: A design and validation study," *Journal of Biomedical Informatics*,

- vol. 43, no. 5, pp. 661 – 668, 2010. [Online]. Available: <http://www.sciencedirect.com/science/article/pii/S1532046410000857>
- [58] S. Jeon and S. Choi, “Stiffness modulation for haptic augmented reality: Extension to 3d interaction,” in *Haptics Symposium, 2010 IEEE*. IEEE, March 2010, pp. 273–280.
- [59] L. Birglen, “Haptic devices based on parallel mechanisms. state of the art,” <http://www.parallemic.org/Reviews/Review003.html>, 2001, [Online; accessed Jan-26-2015].
- [60] T. R. Coles, N. W. John, D. A. Gould, and D. G. Caldwell, “Integrating haptics with augmented reality in a femoral palpation and needle insertion training simulation.” *IEEE TRANSACTION ON HAPTICS*, vol. 4, no. 3, pp. 199–209, JULY 2011.
- [61] P. Blyth, I. A. Anderson, and N. S. Stott, “Virtual reality simulators in orthopedic surgery: What do the surgeons think?” *Journal of Surgical Research*, vol. 131, no. 1, pp. 133 – 139, 2006. [Online]. Available: <http://www.sciencedirect.com/science/article/pii/S0022480405004634>
- [62] J. M. Albani and D. I. Lee, “Virtual reality-assisted robotic surgery simulation,” *J. Endourol.*, vol. 21, no. 3, pp. 285–287, Mar. 2007.
- [63] M.-D. Tsai, M.-S. Hsieh, and C.-H. Tsai, “Bone drilling haptic interaction for orthopedic surgical simulator,” *Computers in Biology and Medicine*, vol. 37, no. 12, pp. 1709 – 1718, 2007. [Online]. Available: <http://www.sciencedirect.com/science/article/pii/S001048250700087X>
- [64] T.-Y. Fang, P.-C. Wang, C.-H. Liu, M.-C. Su, and S.-C. Yeh, “Evaluation of a haptics-based virtual reality temporal bone simulator for anatomy and surgery training,” *Computer Methods and Programs in Biomedicine*, vol. 113, no. 2, pp. 674 – 681, 2014. [Online]. Available: <http://www.sciencedirect.com/science/article/pii/S0169260713003775>
- [65] K. Kuchenbecker, J. Fiene, and G. Niemeyer, “Event-based haptics and acceleration matching: portraying and assessing the realism of contact,” in *Eurohaptics Conference, 2005 and Symposium on Haptic Interfaces for Virtual Environment and Teleoperator Systems, 2005. World Haptics 2005. First Joint*, March 2005, pp. 381–387.
- [66] M.-D. Tsai, M.-S. Hsieh, and S.-B. Jou, “Virtual reality orthopedic surgery simulator,” *Computers in Biology and Medicine*, vol. 31, no. 5, pp. 333 – 351, 2001. [Online]. Available: <http://www.sciencedirect.com/science/article/pii/S0010482501000142>
- [67] S. L. MEGLAN DWIGHT, “Segrical burr hole drilling simulator,” USA Patent 44 402 840, 2010.

- [68] M. W. Spong and M. Vidyasagar, *Robot dynamics and control*. John Wiley & Sons, 2008.
- [69] K. Kotobi, P. B. Mainwaring, C. S. Tucker, and S. G. Biln, "Data-throughput enhancement using data mining-informed cognitive radio," *Electronics*, vol. 4, no. 2, p. 221, 2015. [Online]. Available: <http://www.mdpi.com/2079-9292/4/2/221>

Robotic Tools for Improving the Quality of Bone Drilling

by

Ashkan Pourkand

Permission to make digital or hard copies of all or part of this work for personal or classroom use is granted without fee provided that copies are not made or distributed for profit or commercial advantage and that copies bear this notice and the full citation on the last page. To copy otherwise, to republish, to post on servers or to redistribute to lists, requires prior specific permission and may require a fee.